LUTEAL AND FOLLICULAR COUNT IN BITCHES: ASSESSMENT BY MEANS OF MAGNETIC RESONANCE IMAGING

KURT GUIDO MIREILLE DE CRAMER

LUTEAL AND FOLLICULAR COUNT IN BITCHES: ASSESSMENT BY MEANS OF MAGNETIC RESONANCE IMAGING

KURT GUIDO MIREILLE DE CRAMER

Submitted in partial fulfilment of the requirements for the

degree MMedVet (Reproduction)

in the Faculty of Veterinary Science

University of Pretoria

Promoter: Prof. J.O. Nöthling

Co-promoter: Dr. V.R. Kammer

Pretoria

JUNE 2005

This work I dedicate to all our veterinary colleagues and their patients.

The fruits of this work I owe to my wife Zelda and children, Kyle and Mira.

TABLE OF CONTENTS

LIST OF TABLES

LIST OF FIGURES

ABBREVIATIONS USED IN TEXT

®	Registered trade mark
^{0}K	Degree Kelvin
^{12}C	Carbon
^{16}0	Oxygen
^{23}Na	Sodium
3−D	Three-dimensional
^{31}P	Phosphorus
^{39}K	Potassium
^{40}Ca	Calcium
ad lib	Ad Libitum
ANOVA	Analysis of Variance
ATP	Adenosine triphosphate
B_0	Strength of the external magnetic field
B_1	Second magnetic field applied to excite aligned nuclei
CL	Corpus luteum or corpora lutea
CNS	Central nervous system
CSF	Cerebrospinal fluid
CT	Computed tomography or (x-ray computed tomography)
CV	Coefficient of variation
d	Day or days
D1	Day one of cytological dioestrus
DTPA	Gadolinium-diethylenetriamine penta-acetic acid
ELISA	Enzyme-linked immunosorbent assay
et al.	And others
FISP	Fast imaging with steady state precession
Gd-DTPA	Gadolinium diethylenetriamine penta-acetic acid
GI	Gastro-intestinal
GRE	Gradient recalled echo

H	Hydrogen
HCL	Hydrochloric acid
Hz	Hertz
i.m.	Intramuscular
i.v.	Intravenous
KeV	Kilo electron volt
LH	Luteinising hormone
M	Net magnetization vector
mg kg^{-1}	Milligram per kilogram
MHz	Megahertz
Mmol	millimole
MPR NS	Multiplanar reconstruction non-selective excitation
MR	Magnetic resonance
MRB	Magnetiese resonasie beelding/beeld/e (Afrikaans for MRI)
MRI	Magnetic resonance imaging or magnetic resonance image/s
MRS	Magnetic Resonance Spectroscopy
Msec	millisecond
n	number
N	Proton spin density
$nmolL^{-1}$	nannomole per litre
NMR	Nuclear Magnetic Resonance
OVH	Ovariohysterectomy
Pet	Positron emission tomography
pg kg^{-1}	Picogram per kilogram
P^{i}	Inorganic phosphorus
PPC	Plasma progesterone concentration
PSIF	Time reversed FISP
R1	Relaxation rate
RF	Radio-frequency waves

RF coil	Radio frequency coil
RIA	Radioimmunoassay
ROI	Region of interest
S/N	Signal-to-noise ratio
SD	Standard deviation
SE	Spin echo
SEM	Standard error of the mean
SI	Signal intensity
T	Tesla, unit of measure of magnetic field strength
t	time
T_1	Time constant one
T_2	Time constant two
T_2*	T2 star
TE	Echo time
TI	Inversion time
TR	Repetition time or time between radio frequency pulses
VOI	Volume of interest
W_o	Frequency of precession
γ	Gyro magnetic ratio

DEFINITIONS, AND TERMINOLOGY USED IN TEXT:

Anechoic	Absence of echoes, appearing black on ultrasound scan.
B-mode ultrasonography	Multiple beams of ultrasound are used, and the echoes from each beam are analysed.
Chelation	Binding a paramagnetic substance to DTPA.
Complex fluid	Term used in MRI to describe proteinaceous fluid that probably contains cellular material, which ultimately leads the fluid to behave more like tissue in MRI rather than fluid. An example is pus.
Contrast enhancement	Increasing the difference in signal intensity (contrast).
Dioestrus	The phase of the oestrous cycle of the bitch that follows oestrus and is dominated by progesterone from corpora lutea.
Echo-values	The value with which the resulting signal is reflected back.
Fatsat	Fat Saturation sequence is a MRI technique used to decrease the Fat signal in the image in an effort to accentuate surrounding tissues.
Fertilization rate	The ratio between the number of fertilised oocytes and the number of ovulated oocytes.
Gantry	Space in the MRI apparatus into which the patient or specimen is placed in order to be examined.
Ghost images	Images that are partial copies of the parent image at a different location.
Homozygotic twinning	Twin offspring formed from the splitting of an embryo.
Hypoechoic	Sparse echoes, appearing dark grey on ultrasound scans.
Image contrast (in MRI)	The difference in signal intensity between two tissues.
Implantation rate	The ratio between the number of ovulated oocytes and implanted conceptuses (the number of ovulated oocytes are sometimes approximated by the number of corpora lutea on the ovaries during dioestrus).
Isotropic	A volume of tissue being imaged by means of MRI and of which the dimensions are all the same.
Larmor equation	Frequency of precession of the nuclear magnetic moment proportional to the external magnetic field.
Lattice	Non-proton environment

Localizer	Initial image to orient the examiner and to identify the region to be imaged.
Multiparous	An animal is multiparous if it has produced offspring more than once
Non-complex fluid	Term used in MRI to describe fluid that probably contains very little protein and cellular material, which ultimately leads to this fluid behaving more like water in MRI. An example is urine.
Nulliparous	An animal is nulliparous if it has never produced offspring.
Nutation/Nutate	Alteration of the biological field of the animal to prevent interference from the external field.
Ovulation rate	The number of ovulations per oestrous period.
Paramagnetic	Substances with magnetic properties that are used as contrast medium.
Polyovular follicles	Follicles that ovulate more than one oocyte each.
Polytocous	An animal is polytocous if it produces a litter consisting of more than one offspring.
Precess	Movement of a particle around the external magnetic field.
Pulse sequence	A series of radio-frequency pulses that tilt the magnetization vector.
Relaxation	Following cessation of the magnetic pulse, the excited nuclei return to equilibrium.
Relaxivity	A slope of the linear relationship between the relaxation rate of the protons and concentration of the paramagnetic contrast agent.
Reproductive efficiency	Due to lack of a better term this term has been defined for the purpose of this thesis. The reproductive efficiency of an inseminated bitch is the ratio between the number of offspring at the time of counting and the number of oocytes ovulated during the preceding oestrus period. Reproductive efficiency will reach a maximum value of one when each ovulated oocyte manifests as an offspring at the time of counting. Some pertinent times for offspring counting may be weaning, birth, after implantation or prior to implantation.
Resonance	Rapid nuclear oscillations.
Scout image	Synonym for localiser image
Specialist radiologist	Radiologist registered as a specialist with the Medical council.

Spinners	excited protons.
Stroma	Tissue bed that provides the framework for part of, or an entire organ
T_1	Time constant defining the time required for nuclei excited by a 90^0 pulse to return to 63.2% of the original value of M.
T_2	Time constant defining the time during which 63.2% of M is lost due to loss of phase coherence.
Voxels	volume elements.
Whelping rate	The ratio between the number of bitches bred and the number of bitches that whelped

CHAPTER 1 INTRODUCTION

Imagery in veterinary reproductive diagnostics and research has classically included direct visual inspection via a laparotomy incision, using endoscopic equipment and ultrasonography. More recently, Magnetic resonance imaging (MRI) has proven to be of value in diagnostic imagery of soft tissues particularly in the field of neurodiagnostics (Shores, 1993). MRI is a non-invasive technique that provides accurate and detailed anatomic images, which may provide a sensitive diagnostic tool in canine reproduction. The value of MRI in canine reproduction has not been researched to date.

1.1 A need to investigate the ovarian structures in the bitch

The number of ovulations per oestrous period (ovulation rate) differs among bitches, even when they are of the same breed and age (Nöthling and Volkmann, 1993; Nöthling *et al*., 2000). Studies that report serial observations on ovulation rates in the same bitch over oestrous cycles are lacking, as there is no reliable way to determine ovulation rate without destroying the ovaries. Ovulation rate may be approximated by litter size under conditions of optimal fertility. Johnston *et al*. (2001) speculate that the number of corpora lutea should be equal to the number of foetuses, assuming that conception was normal, foetal loss did not occur and splitting of the embryo (thus homozygotic twinning) did not occur. They further speculate that the total number of corpora lutea is normally less in breeds of dogs that produce smaller litters than those with larger litters. Tedor and Reif (1978) studied the natal patterns of dogs and found that litter size in their study, varied primarily with breed and followed to speculate that litter size is genetically based.

Mandigers *et al*. (1994) found a positive effect on litter size of maternal parity in a population of Dutch Kooiker dogs. Litter size however decreases with age beginning at 4-8 years in the beagle (Andersen and Simpson, 1973, cited by Johnston *et al*., 2001). From this it can be assumed that the litter sizes (under optimal fertile conditions) and thus ovulation rates of bitches depends primarily on breed, parity and age and that it cannot be assumed that the ovulation rate in the same bitch will not vary significantly over oestrous cycles. Currently the ovaries of a bitch have to be removed before the corpora lutea can be counted accurately. This results in spoiling the opportunity to use the same animal in future fertility trials. A follicle may ovulate more than one oocyte each (poliovular follicles) therefore, ovulation rate can only be approximated by the number of follicles on the ovary during the follicular phase or the number of corpora lutea during the luteal phase. Nöthling (1995) analysed data presented by Andersen and Simpson (1973) and showed that, in spite of a very high fertility rate in a group of bitches that produced 22 litters with a total of 117 conceptuses while the bitches had a total of 117 corpora lutea on their ovaries, the number of conceptuses exceeded the number of corpora lutea in 6 litters (by one conceptus in each case) only. The maximum litter size that

a bitch may have is dependent on her ovulation rate. It is, therefore, more sensitive to measure fertility in terms of the ratio between litter size and ovulation rate, rather than merely the litter size. In order to measure fertility in terms of the ratio between the number of conceptuses and the number of corpora lutea during an insemination trial, a bitch can be inseminated during one oestrous period only and cannot be used during a subsequent oestrus period in order to serve as her own control because her ovaries have to be removed in order to determine the ratio. If a non-invasive method can be found by which the ovulation rate of a bitch can be determined, artificial insemination trials, or any fertility trial can be made more sensitive because a bitch can receive two or more different treatments during subsequent oestrous periods, thereby serving as her own control, and also allowing the researcher to use statistical methods designed for meaningfully paired data, which are much more sensitive than other methods (Steel and Torrie, 1980). This increased sensitivity of a trial may result in smaller samples that are required to obtain meaningful results. A non-invasive, repeatable method of monitoring follicular development and counting follicles in the bitch will also allow the practitioner to select the bitch with the most follicles for the use of valuable semen.

1.2 Limitations of the current methods to investigate the ovarian structures of the bitch

Section 1.1 suggests that there is a need for a non-invasive, repeatable method to count the number of follicles or the number of corpora lutea on the ovaries of bitches. The extent to which currently existing diagnostic modalities fulfil this requirement is evaluated below.

1.2.1 Ultrasonography

Ultrasonography and MRI have the distinct advantage of being non-invasive and thus being suitable to serial examination of events. When compared to MRI, ultrasonography has the following shortcomings, which may be important with respect to imaging the ovaries of bitches:

- Imaging is severely affected by depth scanned
- Overlying tissues or organs that contain gas may make imaging impossible
- Acquisition of a real-time, large field image of an organ is not possible
- With conventional ultrasound apparatus, digital 3-D reconstruction is not possible

Ultrasonography may be used to measure the size of follicles and with more difficulty the thickness and echo-values of the follicular walls in the bovine follicle (Martinuk *et al*., (1992). The ovaries of the bitch are difficult, and sometimes impossible, to observe by means of conventional ultrasound because they are small, difficult to resolve from surrounding tissues and are often obscured by intra-intestinal gas (Yeager and Concannon, 1990). Therefore, ultrasound is not a useful means of counting the number of corpora lutea on the ovaries of a

bitch. The use of 3−D ultrasonographic examination has however not been employed for this purpose. Finding the ovaries reliably in the bitch and identifying structures on the ovaries is at best difficult (England and Yeager, 1993). Embryonic vesicles that are substantially larger and easier to echo-locate than ovaries could also not be accurately counted by (England and Allen, 1990) using B-Mode ultrasonography. Wallace *et al*. (1992) monitored the ovaries using a 7.5-Mhz transducer with a built-in standoff pad, from the onset of pro-oestrus until the onset of dioestrus. These authors monitored ovarian size, shape, location, echogenicity, follicular development, and apparent ovulation. Initially, the ovaries were uniform and had an echogenicity that was equal to or slightly greater than that of the renal cortex. Follicles appeared as focal hypoechoic to anechoic rounded structures. Ovaries were easier to identify as follicular development progressed. Ovarian size increased with time. Apparent ovulation was characterised by a decrease in number of follicles seen from one day to the next, but one or more follicles remained in at least one ovary of seven of 10 bitches. The ovaries had an oval shape that became rounded after ovulation. At some time after ovulation, all bitches had anechoic structures indistinguishable from follicles. These structures increased in echogenicity, decreased in size with time, and may have been follicles that did not ovulate, corpora haemorrhagica, fluid-filled corpora lutea (cavitated corpora lutea), or cystic luteinised follicles. Boyd *et al.* (1993) used real-time B-mode ultrasound on 40 fresh bitch cadavers to identify the presence of ovaries and significant ovarian structures. His results indicated that accurate identification of the ovaries depended on the presence of significant follicles or corpora lutea (CL). Hayer *et al*. (1993) monitored follicular development, ovulation, and the early luteal phase in 15 oestrous cycles of 13 individual bitches daily by ultrasonography using a 7.5 MHz sector scanner transducer. They identified follicles as early as day 1 of pro-oestrus in two cases and on days 3-4 in 13 cases. The average follicular size increased from 3.7 ± 0.6 mm to 6.9 ± 0.7 mm ($P < 0.001$) between day -5 and the LH surge (day 0). The anechoic structures then increased in size to 7.5 ± 0.7 mm ($P < 0.05$) until day 2 after the LH surge; their diameters continued to increase during corpus luteum development, up to 8.1 ± 0.6 mm ($P < 0.001$) on the first day of dioestrus. The average number of follicles counted imaged on the day of the LH surge was 3.3 ± 0.4 on the left ovary and 3.7 ±0.7 on the right ovary. The rapid disappearance of the anechoic antrum, corresponding to ovulation, was detected in only two bitches. In the remaining cases, follicular rupture was not detected. None of the above researchers attempted to verify their ultrasonography counts of the ovarian structures by means of direct inspection and dissection of the ovaries. It has to be taken into account that there has been considerable technological progress made in the ultrasound equipment, which may improve our ability to both locate the ovary and identify structures on it. More recently 3-D ultrasonography has become available and no literature on its application in canine ovarian imagery has been published.

Tissue harmonic imaging is a new greyscale imaging technique. It creates images that are derived solely from the higher frequency, second harmonic sound produced when the ultrasound pulse passes through tissue within the body. Tissue harmonics uses various techniques to eliminate the echoes arising from the main transmitted ultrasound beam ("the fundamental frequencies"), (Averkiou and Hamilton, 1995). Tissue harmonic imaging offers several advantages over conventional pulse-echo imaging, including improved contrast resolution, reduced noise and clutter, improved lateral resolution, reduced slice thickness, reduced artefacts (side lobes, reverberations) and, in many instances, improved signal-to-noise ratio (Hann *et al*., 1999). The major benefit of tissue harmonic imaging is artefact reduction. Tissue harmonic imaging reduces artefact by decreasing scatter from the body wall; reducing artefacts from weak echoes such as side lobes, scatter, and grating lobes and creates less near field haze from body wall reverberations (Hann *et al*., 1999). Preliminary studies suggest that tissue harmonic resolution improves clinical imaging in several applications (Shapiro *et al*., 1998). It is not known whether tissue harmonic imaging will improve ovarian imaging. Tissue harmonic imaging may display pathology and normal structures with greater clarity than fundamental imaging. With tissue harmonic imaging good images are often obtained with less effort. Hohl *et al*. (2004) found phase inversion tissue harmonic imaging 10 % more sensitive in detecting pancreatic lesions in the human patient than conventional B-mode ultrasonography. The eventual impact of tissue harmonic imaging, however, is not yet clear. Only when tissue harmonic techniques are technologically mature and more widely distributed will we know the ultimate clinical usefulness (Desser *et al*., 1999). Tissue harmonic imaging can however not overcome the impediment of gas-filled structures overlying the canine ovary.

From the above it appears that ultrasound currently has severe limitations with respect to counting follicles or corpora lutea in the ovaries of bitches.

1.2.2 Laparoscopy

Wildt *et al*. (1978) reported ovulation rates calculated from serial laparoscopic examination of the ovaries during pro-oestrus and oestrus. Laparoscopic examination of the ovary in the bitch requires anaesthesia, is invasive, and requires removal of the ovarian bursa for proper inspection of the ovarian structures, which may interfere with bitches' future reproductive performance.

1.2.3 Laparotomy

Tsutsui (1989) performed laparotomies to determine ovulation times relative to onset of behavioural oestrus and inspection of reproductive organs in his study required sterilization and dissection of the respective organs.

1.2.4 Magnetic resonance imaging

No literature exists on the use of magnetic resonance imaging (MRI) to examine bitches' ovaries. The corpus luteum can be seen by means of MRI in the ovary of the human and the cow (Ayida *et al*., 1997; Takahashi *et al*., 1998 and Sarty *et al*., 2000).

1.3 Research question

In Section 1.2 it was demonstrated that currently there exists no non-invasive, repeatable method by which to count the number of follicles or corpora lutea in the bitch. In contrast, MRI, with or without contrast enhancement may prove useful in this respect. The aim of this study was to determine if MRI could aid in our efforts to accurately count the number of follicles or corpora lutea in the ovary of the bitch, with or without the use of paramagnetic contrast enhancement. The hypothesis for Experiment 1, which was done on ovaries removed by ovariectomy, was that each of three veterinarians could correctly derive the number of corpora lutea or follicles on MR images for at least 80% of bitches and, where the count was wrong, that it would be wrong by only one structure per ovary. The first hypothesis for Experiment 2, which was done on live bitches, was that each of three veterinarians could correctly derive the numbers of corpora lutea or follicles on MR images of the ovaries scanned *in situ* of at least 80% of bitches and, where the count was wrong, that it would be wrong by only one structure per ovary. In addition, it was postulated for Experiment 2 that gadolinium would enhance the contrast between follicles or corpora lutea and the surrounding ovarian tissue.

CHAPTER 2 LITERATURE REVIEW

2.1 Vaginal cytology

Vaginal cytology may be employed in conjunction with vaginoscopy in order to determine the stage of the oestrus cycle of the experimental bitches and thereafter assign them to the luteal or follicular experimental groups. Per definition vaginal cytology is the only way to determine the onset of cytological dioestrus (D1), which needs to be determined in order to assign the bitches to the early luteal group or late luteal experimental group.

The vaginal epithelium and morphology of the cells of the adluminal layers of the vaginal epithelium, changes during the oestrous cycle (Schutte, 1967). Vaginal cells may be obtained by passing a cotton-tipped swab moistened with sterile saline into the vaginal canal. The vestibule and clitoral fossa should be avoided during the procedure as superficial cells from these areas could alter the cytological interpretation. Vaginal smears may be stained with a trichrome stain (Schutte, 1967), Wright's Giemsa stain (Holst and Phemister, 1974), a rapid modified Wright's Giemsa stain (Olson *et al*., 1984). Keratinized cells stain orange with the trichrome stains in contrast to non-keratinized cells that stain blue and the percentage of orange stained cells resembles the eosinophilic index (Schutte, 1967). Even though all cell types described by Schutte (1967) and Christie *et al*. (1972) as well as the onset of cytologic dioestrus can be identified on smears stained with Giemsa or modified Giemsa (Holst and Phemister, 1974 and Olson *et al*., 1984), the modified Giemsa stain is the preferred method because of its ease of use and reliability. (Olson *et al*., 1984).

In 2 separate studies, Schutte used nuclear size to classify the vaginal epithelial cells as superficial, intermediate or anuclear whereas Christie *et al*. included nuclear pycnosis as a criterion to classify an epithelial cell as superficial (Schutte, 1967 and Christie *et al*., 1972). The classification by Holst and Phemister (1974) compared the incidence of anuclear and superficial cells combined, with the incidence of parabasal cells and small intermediate cells combined. Their method is the more practical one. They used the Giemsa stain and defined the onset of cytologic dioestrus (D1) as that day on which the anuclear and superficial cells combined, decreased by at least 20% and the small intermediate cells and parabasal cells combined, increased to at least 10%. Since the pioneering study of Concannon *et al*. (1977) others have studied the temporal relationship between the LH surge and ovulation (Wildt *et al*., 1978), PPC (Concannon *et al*., 1977 and Renton *et al*., 1991), and vaginal cytology (Concannon *et al*., 1977, Lindsay *et al*., 1988 and Wright, 1991). Holst and Phemister (1975) found that the mean interval between the LH peak and D1 for 11 bitches was 8.0 d (SEM 0.3 d), showing that there is relatively little variation in this interval. Since D1 is easier to determine than the time of the LH peak, D1 may be used instead of the time of the LH peak as a chronological landmark by which to identify the stage of the oestrus cycle a bitch is in.

2.2 Evaluation of the macroscopic appearance of the vaginal mucous membrane (vaginoscopy)

Lindsay (1983) described the macroscopic changes that occur in the vaginal mucous membrane of the bitch throughout the oestrous cycle. Using a 4.7 mm diameter, rigid, paediatric telescope she examined the luminal surface of the paracervix. Anoestrus was characterised by low, simple, rounded vaginal folds with a pink or red colour. Pro-oestrus was initially characterised by increasing oedema, and later by decreasing oedema of the folds resulting in a concertina-like appearance of the folds. During pro-oestrus all profiles of folds remained rounded. During oestrus, the vaginal folds became pale and dry with profiles that became increasingly more angular. During early dioestrus, there was a rapid lowering and rounding of the profiles of all vaginal folds. The vagina also becomes pinker during early dioestrus.

Lindsay *et al*. (1988) and Jeffcoate and Lindsay (1989) found that the first sign of angularity of the vaginal folds occurred 2-4 days after the LH peak, thus coinciding with the time of ovulation. Vaginoscopy may therefore be useful in selecting bitches for pre-ovulatory and post-ovulatory experimental groups.

2.3 Significance of number of corpora lutea or follicles in the bitch

The fertility of a bitch may be measured in various ways. One way is to measure it categorically, by merely determining whether she is pregnant or not, or whether she produced a litter or not. Obviously, such categorical methods are not very sensitive and therefore not very useful measurements of fertility because two bitches, one that produced a litter of one pup and another that produced a very large litter will both provide the same categorical measurement of fertility. Better ways of measuring fertility will therefore be measurements such as litter size, number of pups weaned per breeding attempt, number of conceptuses counted during pregnancy diagnosis, etc. Two bitches, each having produced a litter of, for example six pups, may differ vastly in their fertility if the one provided six oocytes during ovulation and the other 12. Obviously, measurements of fertility that relate the number of pups or conceptuses to the number of available oocytes are even better measurements of fertility as they provide measurements of reproductive efficiency.

An accurate measurement of reproductive efficiency in the bitch may be used for the comparison of insemination methods, or assessing the effects of drugs or procedures on fertility.

2.3.1 Categorical measurement of the fertility of bitches

Farstad and Andersen Berg (1989) used the term conception rate, whereas Linde-Forsberg and Forsberg (1989) used the terms pregnancy rate or whelping rate as categorical measurements

of fertility in bitches. These measurements do not reflect differences in reproductive efficiency as these measurements neither account for differences in the number of offspring nor differences in ovulation rate.

2.3.2 Measurement of the number of offspring

Lyngset and Lyngset (1970) measured fertility in the bitch by counting the litter size at birth while others, as shown below, counted the number of conceptuses at various stages of gestation or counting number of oocytes or pre-implantation embryos. Implantation in the bitch occurs approximately 16 -20 d after the onset of behavioural oestrus or 11 d after the onset of cytologic dioestrus at which stage the blastocysts large enough to accurately count by direct visual inspection (Holst and Phemister, 1971). Andersen and Simpson (1973), cited by Nöthling (1995), counted conceptuses at various stages throughout the post-implantation period by means of direct inspection of the uterus. Tsutsui *et al*. (1988), Tsutsui *et al*. (1989a) and Tsutsui *et al*. (1989b) counted the number of post-implantation conceptuses by direct inspection of the uterus at 29-35 d after the onset of behavioural oestrus (approximately 9-19 d after implantation, or 20-30 d after the onset of cytologic dioestrus). England and Allen (1990) used B-mode ultrasonography to determine the number of post-implantation conceptuses 20-24 d after the onset of cytologic dioestrus but they were only accurate in 5 of 16 litters. The canine embryo enters the uterus 4 -5 d after the onset of cytologic dioestrus (Holst and Phemister, 1971). Pre-implantation embryos may be dissected (Holst and Phemister, 1971) or flushed from the uterus (Kraemer *et al*., 1979; Kraemer *et al*., 1980 and Ferguson *et al*., 1989). Doak *et al*. (1967), Holst and Phemister (1971) and Tsutsui (1975) flushed embryos from the uterine tubes. The number of pups born (litter size) to a bitch is obtained by subtracting from the number of oocytes that were fertilized the number of embryos that died (Tsutsui, 1975, and Ferguson *et al*., 1989) and the number of foetuses that died (Holst and Phemister, 1974 and Ferguson *et al*., 1989). Andersen and Simpson 1973 cited by Nöthling, 1995, reported a foetal death rate of 11% for 22 beagle litters. Using the number of post-implantation conceptuses in the measurement of reproductive efficiency provides a better estimate of fertilisation rate than using litter size because the number of post-implantation conceptuses only depends on the number of oocytes that were fertilized and the number of embryos that died and not also the number of foetuses that died after implantation. Flushing embryos and oocytes may allow one to differentiate between fertilization failure and embryonal death as causes of lowered reproductive efficiency (Tsutsui, 1975). Canine embryo flushing methods however have the serious impediment of unknown or poor embryo or oocyte recovery rates. Doak *et al*. (1967) were only able to recover 16 embryos of 4 bitches that had a total of 27 corpora lutea (recovery rate of 59%). Holst and Phemister (1971), Kraemer *et al*. (1979), Kraemer *et al*. (1980) and Ferguson *et al*. (1989) described methods to remove embryos from the uterus but did not critically evaluate their embryo recovery rate by

comparing them to the number of corpora lutea. Theoretically, the ratio of embryos flushed from the uterine tubes or uterus to corpora lutea will be excellent measurements of fertilization rate. The methods of flushing embryos from the uterine tubes have been validated in the bitch by Tsutsui *et al*., 2001). They found that the embryo recovery rate was high (mean 95.7%) by means of salpingectomy but poor by means of tubal flushing (mean 31.1%).

2.3.3 Estimation of ovulation rate

More accurate measurements of fertility than merely counting offspring could be made by also taking into account the numbers of ovulated oocytes in order to derive a measurement of reproductive efficiency. The numbers of ovulated oocytes are related to the numbers of follicles or corpora lutea.

The number of follicles will overestimate the number of ovulations by the number of follicles that do not ovulate. Anovulatory cycles, in which the serum progesterone concentration fails to rise above 11 nmol L^{-1} are rare and were reported in only 11 of 1152 bitches (Arbeiter, 1993). The incidence of partial anovulation, where individual anovulatory follicles in the bitch that otherwise has an apparent normal ovulatory cycle with ovulated follicles in the same or contra-lateral ovary is unknown. The number of corpora lutea depends on number of follicles that matured, ovulated and luteinised. In contrast to using the number of follicles as an estimate of the number of oocytes that will be ovulated, using the number of corpora lutea as an estimate of the number of ovulated oocytes removes the effect of anovulatory follicles or non-luteinised follicles on reproductive efficiency.

In their study, Nöthling and Volkmann (1993) assumed that each corpus luteum stems from the ovulation of a single oocyte and thus defined ovulation rate as the number of corpora lutea on both ovaries. This assumption seems a justifiable approximation because Andersen and Simpson (1973, cited by Nöthling, 1995) reported an implantation rate of 100% in 22 litters that consisted of 117 conceptuses at various times after implantation. The number of conceptuses exceeded the number of corpora lutea by one in 6 litters whereas, in another three litters, the corpora lutea exceeded the number of conceptuses by 1, 2 and 3, respectively.

Normally, each ovulatory follicle releases one oocyte at ovulation and the number of ovulatory follicles or corpora lutea will equal the ovulation rate. The number of conceptuses will overestimate the number of follicles or corpora lutea only if polyovular follicles were present. One percent of late pre-antral follicles in the ovaries of young (1 to 2 y old) bitches in anoestrus contain more than one oocyte whereas the corresponding figure for old (7 to 11 y) bitches is zero (Telfer and Gosden, 1987). Assuming that late pre-antral follicles remain randomly available for ovulation, the incidence of polyovular follicles has a negligible effect on the accuracy of using the number of preovulatory follicles or corpora lutea as a measurement of ovulation rate.

Ovulation rate increases with the size of bitches (Miramontes-Vidal, 1987) and varies within breeds (Tsutsui *et al*., 1988 and Tsutsui *et al*., 1989a).The ovulation rate of 22 beagles varied from 3 to 9 (mean 5.3,SD 1.5, CV 28.1%) (Andersen and Simpson, 1973 cited by Nöthling, 1995). Due to the variability in ovulation rate, the relationship between the number of offspring and ovulation rate is a better measurement of fertility than the mere number of offspring.

2.3.4 Measurement of reproductive efficiency in terms of the relationship between the number of offspring and ovulation rate

Differences in ovulation rate have been compensated for by determining the ratio between the numbers pups born or post-implantation conceptuses and the numbers of corpora lutea (Holst and Phemister, 1974; Tsutsui *et al*., 1988, 1989a and 1989b). The ratio of pups born to corpora lutea, however, depends on the fertilization rate, embryonal death rate, and foetal death rate, whereas implantation rate is affected only by fertilization rate and embryonal death rate. Andersen and Simpson (1973), cited by Nöthling (1995) reported an implantation rate of 100% in 22 litters that consisted of 117 conceptuses at various times after implantation. Tsutsui *et al*. (1988) showed that the mean implantation rate of 18 bitches that conceived after having been mated at the optimal time to proven sires was 90.7%. The 9.3% corpora lutea, for which no conceptuses were found, accounted for fertilization failure and embryonal death. Tsutsui (1975) found five degenerate ova amongst 101 oocytes and embryos and Kraemer *et al*. (1979) found that 95.7% of 46 oocytes or embryos flushed from the uteri of 11 bitches were fertilized. From these findings, one must assume that the mean implantation rate will be 0-9.3% lower than the mean fertilization rate and, according to the data of Tsutsui (1975) and Kraemer *et al*. (1979), usually about 5% lower.

From the above it appears that some measurement of the number of oocytes that were available for fertilisation during a breeding attempt is essential for the measurement of reproductive efficiency and that the number of follicles and, more so, the number of corpora lutea provide useful approximations of ovulation rate and are therefore useful divisors in the determination of reproductive efficiency.

2.4 Development of follicles and corpora lutea

Ovarian follicles are imbedded in the stroma of the cortex of the ovary. Three types can be distinguished, namely primordial follicles, growing follicles, and mature Graafian follicles. Primordial follicles and early growing follicles are too small to see with the naked eye. Follicular growth involves mainly the follicular cells but also the primary oocyte and surrounding stroma. The most mature stage includes follicles having a focal area of a marked thinning along a portion of the ovarian surface (Phemister *et al* 1973). No literature could be found on the comparative sizes of the canine follicle in different breeds but logic would

dictate that large breeds with larger ovaries would have larger-sized follicles and corpora lutea than smaller breeds.

In the dog, slightly before ovulation, the granulosa cells and those of the theca interna form a temporary endocrine gland called the corpus luteum (yellow body). Lipochrome is the fat-soluble pigment that gives rise to the yellow colour of the CL and is contained within the cytoplasm of the lutein cells. Luteinization occurs from the periphery inwards, leading to a CL that is initially cavitated but later solid. The mature CL in humans is named the *corpus luteum verum*. Following spontaneous luteolysis, the site occupied by the CL in the cow and human is replaced by dense connective tissue forming a corpus albicans (Adams, E.C. and Hertig, A.T. 1969). The canine corpus albicans has been described by Dore, (1989). In the cyclic bitch, small remnants of corpora lutea 1-2 mm in diameter can be seen in the ovarian stroma at 3-8 months after last cycle (Dore, 1989). These are presumably remnants of corpora lutea of the previous cycle that are degenerate.

2.5 Method of counting corpora lutea or follicles by dissection

The canine corpus luteum is pale to bright salmon pink, distorted in shape due to compression by neighbouring corpora lutea, 4 -7 mm in diameter, and bulging slightly above the ovarian surface (Andersen and Simpson, 1973 cited by Nöthling, 1995). From the data of Andersen and Simpson it appears that the canine corpus luteum is large enough and has such a distinctive colour that it should be easily identifiable macroscopically. Nöthling and Volkmann, (1993) dissected the ovaries of bitches to count the corpora lutea in order to calculate the mean ratio of conceptuses to corpora lutea (conception rate) as a measurement of fertility in a study on artificial insemination. Tsutsui *et al*, (1989b) and Fuji *et al*, (2000) dissected the ovaries of bitches only to recover oocytes from them.

2.6 Ovarian structures that could be mistaken for follicles or corpora lutea

For the purposes of this study, it is imperative that structures on or within the ovaries other than follicles or corpora lutea be identified during dissection so that they would not be erroneously counted. Correctly, identifying these other structures and noting their anatomic position within or on the ovary may also be helpful in the recognition of these structures on MRI.

Many cystic ovarian structures have been described in the bitch. They include follicular cysts (Dow, 1960 and Fayrer-Hosken *et al.,* 1992). Luteal cysts, germinal cysts, cystic corpora lutea, cystic *rete ovarii*, cystic atretic follicles, cystic granulosa cell tumours and parovarian cysts (Dow, 1960; McEntee, 1990; Rowley, 1980 and Nemzek *et al.,* 1992). Clinical signs of cystic ovarian follicular disease in dogs are attributed to increased serum oestrogen

concentrations and the presenting complaint is usually prolonged pro-oestrus or oestrus (McEntee, 1990; Fayrer-Hosken *et al*., 1992; Rowley, 1980; Poffenbarger and Feeney, 1986 and Miller *et al.,* 1983). Ultrasonography may allow visualization of cystic structures caudal to the kidney and therefore presumably within the ovary. The cysts appear as hypoechoic to anechoic structures and small cysts are difficult to see (Poffenbarger and Feeney., 1986). Ultrasonography did not always rule out cystic ovarian disease (Poffenbarger and Feeney, 1986). Normal mature follicles in the dog average 5-8 mm in diameter (Concannon *et al.,* 1977). Even though the size of the structure, its cross sectional appearance and its location within the ovary may aid in a macroscopic diagnosis of the ovarian structure, definitive diagnosis of a cystic structure on the dog ovary rests upon histologic examination (Poffenbarger and Feeney, 1986).

2.6.1 Follicular cysts

Concannon and co-workers measured normal follicles in various bitches at 5-8 mm and suggested that ovarian follicular structures larger than 8 mm in diameter present within the stroma bulging from the ovarian surface during any stage of the cycle are defined as follicular cysts (Concannon *et al.*, 1977). Andersen and Simpson (1973), cited by McEntee (1990) reported a prevalence of 3 % of follicular cysts in an aging beagle population.

2.6.2 Luteal cysts

Luteal cysts, also called luteinised follicles, are luteinised anovulatory follicles. Luteal cysts vary in diameter from 1.5 to 5 cm (McEntee, 1990). The cyst wall is thicker and more opaque than that of a follicular cyst, but radiographic and ultrasonographic appearance are similar (Poffenbarger and Feeney, 1986).

2.6.3 Germinal cysts

Germinal cysts are also called cysts of sub-surface epithelial structures (McEntee, 1990). These form as infoldings of the continuously growing peritoneal covering of the ovary and are usually only visible with a microscope. These cysts are uncommon in young bitches but occur with increasing frequency in the aging bitch. They are small cysts, seldom larger than 5 mm (McEntee, 1990).

2.6.4 Cystic corpora lutea

Cystic corpora lutea are reported to occur rarely in the dog and are characterised by normal luteal tissue mass filled with a viscous fluid and are 1,5 cm in diameter or larger (Miller *et al*.,

1983).Their size distinguishes them from a normal very much smaller cavitated early corpus luteum.

2.6.5 Rete cysts

Cystic *rete ovarii*, or rete cysts, are small structures (size not reported) of irregular, anastomosing tubules with cystic changes in the hilar region of the ovary (Dow, 1960). They are reported to occur in 9 to 35 per cent of dogs with cystic ovarian disease (Dow, 1960). Although they do not cause clinical disease, they may replace the surrounding normal ovarian tissue (McEntee, 1990).

2.6.6 Parovarian cysts

Parovarian cysts are cystic structures in remnants of the mesonephric and paramesonephric tubules surrounding the ovary (McEntee, 1990). Parovarian cysts may be single or multiple and are greater than 1 cm in diameter. They are not reported to impair ovarian function (McEntee, 1990).

From the above it is evident that cysts may be recognized at least by direct inspection during dissection on their relative position within the ovary as well as their sizes.

2.7 Signal intensity and changes in vasculature and temperature

MRI is a sensitive diagnostic tool and even subtle changes of the tissues under examination may bring about changes that are visible on MRI. For example, Inoue-Minakuchi *et al*. (2002) illustrated that MRI was sufficiently sensitive to detect intramuscular haemodynamic changes caused by cold pressor stimulation.

2.7.1 MRI of small structures

Llabres-Diaz and Dennis (2003) illustrated that MRI could be used in imaging minute fractions like the adrenal gland in the dog. They used ultra fast spin echo sequences to study forty-three dogs without evidence of endocrine disease that underwent spinal or abdominal MRI for clinical reasons. These authors suggested that because the procedures were not optimised for inclusion of the adrenal glands, they were not always visible in all planes. Eighty-five of the 86 adrenal glands were seen and only the left gland in a 6-month-old Irish wolfhound could not be found. In many dogs, the whole adrenal gland was difficult to visualize clearly, and this hindered the measuring process. It is important to note that the adrenals are more fixed to the abdominal wall and are less likely to be affected by breathing movement artefact than are the free moving ovaries of the bitch.

2.8 Contrast enhancement in MRI using intravenous paramagnetic contrast media

Many MRI studies are performed with the use of contrast enhancement via intravenous injection of paramagnetic gadolinium-containing contrast media. Kuriashkin and Losonsky (2000) described the use, safety, and value of MRI contrast media in humans. Image contrast is the difference in signal intensity between two tissues, and contrast enhancement is the process of emphasizing this difference. It is not yet known whether contrast enhancement in MRI has any role to play in the imaging of the reproductive tract of the bitch.

2.9 Safety aspects of magnetic resonance imaging and associated procedures

Considering MRI as a method of counting ovarian structures of bitches without impeding their fertility requires that the bitch be sedated or anaesthetised, exposed to a very strong magnetic field, radio-frequency waves and possibly also to magnetic-enhancing contrast agents, and that these procedures be safe to the bitch and her fertility. Safety aspects in theriogenology of man and animal are a difficult topic to research or review in the literature. A substance or procedure may have "effects" on many different levels. The "effect" may be directly on the dam and its foetus, which is the simplest form of interference. In the reproductively active female, it may also affect:

- Endocrinological events and thus follicular development
- Oocyte maturation and survival
- Ovulation
- Development of corpus luteum and progesterone production
- Fertilization
- Ovum transport and survival
- Embryonal development
- Implantation
- Foetal development , growth and survival
- Maintenance of pregnancy
- Partus
- Effect on lactation
- Infant survival

The effect in one species is not a reliable indicator of what the effect may, or may not be in another. Antivivisection regulations are getting stricter by the day. Liability is also a growing concern for researchers and pharmaceutical companies alike. Given all these difficulties, pharmaceutical companies will continue to report, "Safety during pregnancy has not been established." The net result is that our knowledge on the safety of drugs and procedures on reproductively active animals will remain scant.

2.9.1 Safety of tranquillisation or anaesthetic agents required to minimise movement in the gantry

The subject to be imaged needs to be stationary for several minutes whilst the MRI is in progress. Adult humans can cooperate by lying still and even holding their breath for 10 to 20 seconds at a time. Animals and small children require intervention to ensure a sufficient stationary status for at least several minutes.

Studies on laboratory animals showed no teratogenic effects due to halothane; ethrane; isofluorane; ketamine or thiopental. No deleterious effects have been reported when these drugs were used on pregnant women (Davis, L. E.: Veterinary Clinical Pharmacology. Philadelphia, W. B. Saunders Co.)

Tsutsui (1989) used 1% halothane in oxygen around the time of ovulation to perform laparotomies and inspect the ovaries of bitches that had been mated and 91 % of the bitches in his study conceived. This compares well to the 94.5% conception rate achieved by Holst and Phemister (1974) of bitches that were mated under optimal conditions.

Santiago-Moreno *et al,* 2001 noticed no deleterious effect on the results of embryo transfer in merino sheep when using the alpha 2-agonist medetomidine ("Dormitor," Novartis AH).

Sakamoto *et al.* 1997 investigated the effects of medetomidine on late pregnant goats. Medetomidine induced changes in maternal or foetal circulation and acid-base balance, as well as changes in intrauterine pressure and uterine blood flow. These observations in late pregnant goats suggested that medetomidine induced a decrease in maternal cardiac output and medetomidine can have a suppressive effect on the foetus. It did not however influence outcome of pregnancy or neonatal survival.

Wildt *et al*. (1977) anaesthetized 9 bitches with ketamine (11 mg kg^{-1}) and xylazine (2.2 mg kg^{-1}) and performed laparoscopic examinations on them every 2-5 d during pro-oestrus and every 1-2 d during oestrus. This treatment did not prevent development and maturation of follicles, ovulation, luteal development or did not alter the LH surge of bitches. Unfortunately, he did not breed these bitches and therefore no fertility results could be reported

Rosenblatt *et al.* 1997 found that propofol had no negative impact on oocytes, embryonal development, implantation, or clinical pregnancy in women. Christiaens *et al*. (1998) found no difference in implantation rates in women undergoing in vitro fertilization assistance when anaesthetized with propofol or local blocks.

Sia Kho *et al. (1993)* used propofol and midazolam combination and found no effect on follicular development in women.

2.9.2 Treatments that proved harmful to fertilization

The data by Scudamore *et al*. (1991) suggests that ewes sedated with acetylpromazine (5 mg i.m. per ewe) before laparoscopic insemination significantly reduces the pregnancy rate. The data from Howard *et al*. (1992) suggest that pre-ovulatory anaesthesia induced by ketamine HCL (20 mg kg^{-1}, i.m.) and acetylpromazine (0.18 mg kg^{-1}, i.m.) and maintained with halothane gas in the cat, significantly affects various aspects of fertility.

2.9.3 Safety of MRI techniques

Although MRI is often used in pregnant patients for neurologic examinations, and no detrimental effect has ever been documented on pregnancy, routine MRI examinations cannot be recommended until safety studies in pregnant human patients have been completed. Porat *et al*. (2002) used MRI as prenatal and gestational imaging modality in man with no deleterious effects to the foetus or mother. MRI proved harmless in a study by Hubbard (2001) using MRI to detect foetal abnormalities. Baker *et al.* (1994) concluded in his study that MRI has no known biologic effects in women of reproductive age.

A real hazard arises from loose, iron-containing objects in the area of the magnet, as these can be accelerated to potentially lethal velocities (Valk *et al.*, 1985). Any anaesthetic and handling materials must be composed of nonferrous materials such as plastic or aluminium and, if patient-monitoring equipment is used, it should be MRI compatible. Dog and cat collars need to be removed before scanning, as pieces of metal affect the magnetic field and result in distorted images. Microchips in the neck produce small areas of signal void (black areas on the image) but are usually distant from the tissues being examined and are themselves unaffected by the magnetic field. People and pets with pacemakers should not enter the scanning area and watches, credit cards, and computer discs should be left outside the room. Aside from the potential hazard posed by metallic objects, safety is not a serious issue with veterinary MRI. The National Radiological Protection Board issues guidelines for human MRI, which in practical terms is believed to be entirely safe for veterinary patients and handlers. The main risk lies in anaesthetising patients with possible raised intracranial pressure caused by trauma or disease, although with expert anaesthesia /sedation this is minimal. (Chanalet *et al.,* 1995).

2.9.4 Safety of contrast media

Runge and Wells (1995) reported very rare anaphylactoid reactions in humans following contrast media and reported its routine use to be very safe with few adverse reactions. Tresley *et al*. (1997) evaluated the safety of Gd administered at 0.1 mmol kg^{-1} for serial monthly MRI evaluations for up to 4 years. Chanalet *et al.* (1995) reported the safety of MRI in neurological

cases in humans. Marti-Bonmati *et al.* (2000) established the safety of "omniscan" in infants ingesting contrast enhancement via lactogenic routes in the human.

2.10 Magnetic resonance imaging

2.10.1 MRI with special reference to gynaecological/ reproductive research

MRI has proven to be a valuable diagnostic technique for the clinical assessment of soft tissue morphology and pathology in a wide range of applications (Margulis and Fisher, (1985), Dennis, (1995). Robert *et al (2002)* reviewed MRI in Human gynaecology and considered it to be a complementary imaging tool particularly in endometriosis and neoplasia of the pelvic organs. Kuroiwa *et al.* (2004) established that MRI was a more reliable diagnostic modality than ultrasound to diagnose neonatal ovarian cysts in humans. Kunz *et al*. (2000) used MRI to monitor the serial progression of endometriosis in women. Gianfelice *et al.* (2003) found MRI a reliable non-invasive method for assessing mammary tumours left behind following ultrasound-guided surgery.

MRI is non-invasive, does not use ionizing radiation, and is considered safe when used for serial measurements over a period. MRI, being non-invasive, allows quantitative, three-dimensional serial measurements and is thus ideally suited for measurements of the progression of disease. MRI holds obvious benefits for veterinary research. It has had a major impact in the diagnosis of disease. Waterton *et al.* (1992) and MacKenzie and Casey (1975) used MRI as means to diagnose and monitor serial progression of endometriosis in Macaca and Rhesus monkeys. Endometriosis has been described in old world monkeys, and indeed is not uncommon in captive populations. Human endometriosis is common, and endometriosis in rhesus monkeys provides a valuable animal model for the human disease. The clinical assessment of endometriosis in monkeys is done by abdominal palpation, rectal palpation and by radiographic evidence of abdominal soft tissue masses, or by laparotomy (MacKenzie and Casey 1975). The non-invasive character of MRI is particularly valuable where variable pathology is present since each animal can act as its own control.

In a pilot study conducted by Nöthling, De Cramer, and Gerber (unpublished data) using MRI without contrast enhancement and coils, it proved impossible to accurately count the number of corpora lutea on the ovaries of the bitch embedded in a phantom.

Kähn *et al*. (1989) used three-dimensional 3-D MRI and computer software generated high-resolution medical animations to examine the uteri of heifers on day 26, 28, 32 and 55 of pregnancy, respectively. The 3-D imaging of these uteri demonstrated the presence of crescent-shaped folds usually at right angles to the long axis of the uterine horn. Using this 3-D modality in MRI, it is now possible to display soft tissue structures, such as muscle and tendon surrounding a joint, in 360^0 rotation around the structure (Shores, 1993). This process

provides the diagnostician with an invaluable perspective of the structures involved in the disease process. This technique may be useful in examination of the uterus and ovaries of the bitch.

2.11 Use of a phantom

A phantom has the advantage that it does not move inside the gantry, does not require dedicated experimental animals, and allows imaging without interference of surrounding structures. It is particularly useful in experimental settings where it is anticipated that the techniques, whilst under investigation, might take a very long time. Research on a phantom is also less expensive than working with live animals. A cadaver has similar advantages but the operators in the human MRI unit found the concept objectionable. A phantom has the added advantage in that numerous organs may be scanned simultaneously. The main disadvantage of a phantom is that the tissues to be scanned are subjected to changes during the collection, storage, and mounting in a phantom. These changes may be reflected in the images obtained (unpublished data De Cramer and Nöthling). Another disadvantage of a phantom is that the tissues imaged are no longer subject to haemoperfusion.

Frye *et al.* (2000) used a phantom to develop and refine a pulse sequence and protocol for MR-hysterosalpingography to evaluate fallopian tube patency.

Blechinger *et al.* (1988) described the preparation of tissue-mimicking gelatine agar gels for use in MRI phantoms. They developed a phantom gel consisting of 17 % glycerol and animal hide gelatine that has characteristics of smooth muscle tissue. The exact characteristics of the phantom gel are not too important as long as it is homogenous and its image characteristics differ somewhat from the tissues imaged in order to provide some contrast.

CHAPTER 3 A BRIEF OVERVIEW OF SOME TECHNICAL ASPECTS OF MRI AND OTHER NEW IMAGING TECHNIQUES

Bloch and Purcell (Bloch *et al*,. 1946 and Purcell *et al*,. 1946) first discovered the basic concept of Nuclear magnetic resonance (NMR) or magnetic resonance imaging (MRI) in 1946. It involves the interaction of atomic nuclei having magnetic properties with electromagnetic radiation (radio frequency) and magnetic fields, causing the nuclei to absorb and release detectable levels of energy (NMR). This energy is then used to create an image through a computer-assisted technique (MRI). Jackson was the first to apply MRI in live animals (General Electric,. 1967). Since the initial clinical experiences of Holland *et al*. (1980), MRI has become an important diagnostic method in humans. In recent decades human health care, and following suit, veterinary health care, has undergone major technical advances, especially in the area of diagnostic imaging. The advent of advanced imaging techniques in veterinary medicine has broadened the scope of our diagnostic imaging capabilities. MRI in veterinary medicine will always lag behind its human counterpart. Advances in MRI as a diagnostic modality is increasing at a rapid pace, and especially researchers are realizing its benefits. MRI is a non-invasive technique that provides accurate, detailed, anatomic images and has had a major impact in the diagnosis of disease (Kornegay, 1990).

3.1 Properties of atomic nuclei

Any living organism consists of atoms. The nuclei of these atoms are electrically charged and consist of particles called protons and neutrons. These structures are in constant motion, spinning about the internal axis of the atom, giving the particles angular momentum as well as creating the magnetic field of the nuclei (Pykett *et al*., 1982). When the nucleus of an atom is evenly paired (same number of each particle type), the spin of a particle is opposite to that of its paired particle, in which case the nucleus has a net angular momentum of zero, and the atom does not posses spin. When the total particle number is unpaired, the unpaired particle yields the net angular momentum for the nucleus, and the atom possesses spin. Spinning nuclei act like small magnetic dipoles or bar magnets. In the absence of any orienting force, these dipoles are randomly arranged. When placed in a static external magnetic field (B_0), a slight majority of dipoles align with B_0 into a parallel or low energy state. The remainder of the dipoles become aligned in antiparallel fashion, and in high-energy state (Villafana, 1988). The magnetic field acts on the dipoles; causing them to precess (rotate or “wobble”) at an angle k around the vertical lines of induction of B_0. This type of movement is called precession. The summed magnetic force exerted by the dipoles is known as the net magnetization vector (M), (Villafana, 1988 and Kean and Smith, 1986) and consists of a

longitudinal and transverse magnetization. As a vector, M has magnitude and direction. When under the influence of B_0, M lies parallel to this magnetic field (Thomson *et al*., 1993).

3.2 Resonance

Application of radio frequency (RF) pulses perpendicular to B_0 causes the aligned nuclei to undergo rapid nuclear oscillation (resonance) between different energy states. If the RF pulse frequency is similar to precessing nuclei within the magnetic field, some of the previously aligned nuclei will be excited into a higher energy, antiparallel state. This phenomenon is called resonance (Friedman *et al*., 1989). The resonance phenomenon holds that a system's response to an external cyclic force applied at the system's natural frequency of cyclic motion will be larger than for any other frequency of an external cyclic force (Friedman *et al*., 1989). This additional magnetic field (magnetic pulse sequence) is applied as a cyclic force consisting of radio frequency pulses at the natural frequency of the animal's nuclear field (spin) and perpendicular to the external magnetic field. The effect is a "tipping" or nutating of the animal's nuclear magnetic field. The degree of nutating is governed by the strength and duration of the magnetic pulse (Friedman *et al*., 1989). Application of a magnetic pulse sequence imparts minute amounts of energy to atomic nuclei. If the particle possesses spin, it moves (precession) around the external field, in a manner similar to that of a gyroscope (Shores, 1993). Particles without spin simply fall back to the external field with each cessation of the magnetic pulse. The rate of precession for a particle is termed the Larmor frequency and is determined by the gyroscopic properties of the atomic nuclei and the strength of the external field, (Shores, 1993). (The Larmor equation-frequency of precession of the nuclear magnetic moment is proportional to the external magnetic field: $w_o = \gamma B_o$, where w_o is the frequency of precession, which is measured in Hz or MHz. γ is the gyro magnetic ratio, and B_0 is the strength of the external magnetic field, which is measured in Tesla (T) (Shores, 1993).

3.3 Relaxation

Following cessation of the RF pulse, the excited nuclei return to equilibrium. During this process known as relaxation, they give up their energy to the environment. Since the net magnetization vector consisted of a longitudinal and transverse magnetization (see 3.1), relaxation also has longitudinal and transverse components. Longitudinal relaxation involves an energy exchange between excited protons (spinners) and the surrounding non-proton environment (lattice). Longitudinal relaxation is therefore also called spin-lattice relaxation (Kean and Smith, 1986, as well as Pavlicek *et al*., 1984) and are denoted T_1. Transverse relaxation involves an energy exchange between excited protons and other protons. It is therefore called spin-spin relaxation and are denoted T_2 (Villafana, 1988). In spin-spin relaxation there is an interaction between different nuclei. However, each of the nuclei has

their own minute magnetic fields that interfere with each other. When the transfer of energy between the nuclei takes place, the precessional frequencies of some are delayed and others are accelerated. Hence, phase coherence is lost (Thomson *et al*., 1993). Loss of phase coherence results in a decrease in the transverse magnetization and the signal is lost. What is more this interaction with other nuclei must occur within the static magnetic field (B_0). T_2 relaxation is therefore also influenced by inhomogeneities in the static magnetic field. Taking all these influences into account gives the effective transverse relaxation time, termed T_2* or T_2 star. (Note some references refer to the effect of B_0 heterogeneity alone as T_2* (Villafana, 1988).

3.4 Pulse sequences

A single NMR signal is based mainly on proton density and has poor contrast. Generation of multiple signals using different sequences exploits the relaxation characteristics of different tissues enhancing image contrast (Kean and Smith, 1986). The pulse sequence that is selected determines the image that we receive from the tissue. The image we receive can either be T_1 or T_2 weighted. In a T_1 weighted picture the difference of signal intensity between tissues in that picture, the tissue contrast, is mainly due to their difference in T_1. Differences in proton contrast create T_2 weighted pictures. Pulse sequences are designed by the various manufacturers of MRI who then give them specific names. Another manufacturer may have an entirely different name for a sequence with very similar or identical parameters. Pulse sequences are frequently tailor designed to suit imaging of a particular area or pathological condition. Generally, the smaller the VOI, the more information is required to ensure good detail when enlarged and the longer the acquisition time is.

Three particular pulse sequences are discussed here.

3.4.1 Saturation recovery

This is the simplest sequence of pulses used to increase the contrast of a NMR image. It is done by applying successive 90^0 pulses (a RF pulse which tilts the magnetization 90^0 is called a 90^0 pulse) separated by a constant TR (time to repeat) interval (Thomson, 1993). The TR interval is long. The protons have relaxed and are thus saturated, consequently the images are T_1 weighted. Fat has a short T_1 and, therefore, appears white; white and grey matter have intermediate T_1 values and appear as various shades of grey, whereas fluid such as CSF appears black because of its extremely long T_1 value (Kean and Smith, 1986). Relaxation occurs through a plane of only 90^0, so minimal distinction between different tissues can be made. Accordingly, the saturation-recovery sequence is rarely used.

3.4.2 Spin echo

As mentioned in 3.3, T_2 is affected not only by spin-spin interaction between different nuclei, but also by inevitable inhomogeneities in the applied magnetic field. Therefore, local fluctuations in the strength of B_0 induce different rates of precession of the individual dipole magnetization vectors. This causes the individual dipole vectors to lose phase coherence, thereby shortening the T_2 value. In an effort to remove the effect of magnetic field inhomogeneities on the signal, a spin-echo pulse sequence is applied. A spin-echo pulse sequence consists of a series of 90^0 and 180^0 pulses, separated by time (Thomson *et al*., 1993). A RF pulse is applied and this rotates the nuclear vector by 90^0. After the first 90^0 pulse, the free induction signal (it is free because it occurs in the absence of the RF field) that is obtained is large, but it then decreases over time because of spin-spin interaction and magnetic field inhomogeneities, causing loss of coherence. The decrease of the free induction signal over time is known as free induction decay (Kean and Smith,. 1986). After a specific time a second pulse is applied. This pulse causes an 180^0 rotation at time t_2. Because the effects of B_0 inhomogeneity are constant, coherence is regained at time t_2; causing the free induction signal to increase and a second signal peak is reached. The 180^0 pulse refocuses the dephasing protons, which result in a stronger signal. The signal is echoed back by the 180^0 pulse. Hence the name spin echo. This second free induction signal peak, however, is not as large as the original because of T_2 relaxation. A succession of spin echoes of decreasing size will be obtained as T_2 relaxation continues. The time between the beginning of the 90^0 pulse and the peak of the echo is referred to as the echo time (TE) (Pavlicek *et al*., 1984). The TE value at which maximum signal is obtained is defined as 0; with increasing TE values, signal is exponentially lost. If the 180^0 pulse were not used, the signal intensity would decay much faster. Spin echo is the most common pulse sequence used in clinical MRI. (Aisen, 1990 and Friedman *et al*., 1989). By varying TE and the TR, the spin-echo sequence can be used to produce T_1 -weighted, T_2 -weighted or proton density weighted images. Short TR's ($\leq$500 msec) and very short TE intervals ($\leq$40 msec) produce T_1- weighted images and signal intensity is a factor of intrinsic properties of a given tissue. Tissue with shorter T_1 times is brighter (hyper-intense) and tissue with longer T_1 times is darker (hypo-intense). Short TR's and very short TE intervals also produce proton density weighting. Long TR's ($\geq$2000 msec) and short TE's highlight proton density only, whereas relatively long TR's and TE's ($\geq$100msec) accentuate T_2 differences (Kuriashkin, 2000). Images that are T_2-weighted are equated with longer TE times, and signal intensity is a factor of intrinsic properties of a given tissue. Tissue with longer T_2 times is brighter (hyperintense or more intense), and tissue with shorter T_2 times is darker (hypointense or less intense) (Friedman *et al*., 1989).

3.4.3 Inversion-recovery

In this pulse sequence, an 180^0 or inversion pulse is applied first, followed after a period of time TI (inversion time), by a 90^0 pulse and then an 180^0 rephasing pulse. That is, a spin echo sequence is used in signal collection, and the sequence is sometimes referred to as an inversion recovery spin-echo sequence (Hendrick, 1988) The time between the 90^0 pulse and the centre of the echo peak is TE. Traditionally, inversion recovery spin-echo sequences have been used for T_1-weighted imaging. These are preferred to saturation recovery sequences because they offer a greater range of contrast thus allowing discrimination of tissues with similar T_1 values. However, inversion recovery spin-echo images have limited clinical usefulness, as signal differences from tissues are best discriminated using T_2 relaxation characteristics rather than T_1 or proton density (Kean and Smith, 1986 as well as Foster, 1984).

3.5 Fundamentals of image acquisition.

The MRI system includes the magnet, RF coil, and computer station. The magnet is housed in a metal casing, filled with liquid helium. The magnet surrounds the gantry (opening where the patient or specimen to be examined is placed). It is important that the magnetic coils be super cooled to decrease the electrical current resistance and minimize heat production. Inside the gantry, a copper coil is placed parallel to the external magnetic field. The region to be imaged is surrounded by the copper coil and acts as a radio frequency signal receiver. The computer station allows the programmer to set parameters for the image study, formulates and transmits instruction for the production of a radio frequency pulse sequence directed at the region of interest (ROI), and analyzes the sampled data to produce the image 3-D (Aisen, 1990 and Friedman *et al*., 1989). The patient or specimen possesses a magnetic field and images are created when radiofrequency waves interact with the hydrogen ions of tissue inside this magnetic field. These magnetic fields also posses spin (a form of angular momentum created by spinning about an axis), at a frequency that is specific for that magnetic field. Tissue components with spin can be measured with MRI, those without spin cannot (Shores, 1993). Atoms with uneven numbers of protons and neutrons in their nuclei, numbers, such as Sodium (^{23}Na), phosphorus (^{31}P) and hydrogen (^{1}H), posses spin and can therefore be imaged. Hydrogen is abundant in biologic tissue e.g. water and fat and is therefore most important for MRI in biological systems. Other possibly important nuclei for MRI of biological substances are ^{23}Na, ^{31}P, and ^{39}K. Although these nuclei have a lower physiologic concentration and MRI sensitivity, they may be used in future as tracers when introduced into the body (Foster, 1984). Isotopes with even atomic numbers like; carbon (^{12}C), oxygen (^{16}0), and calcium (^{40}Ca) are common components of bone and air these atoms and do not posses spin because they have equal numbers of protons and neutrons in their nuclei and, therefore, appear void when imaged (Shores, 1993).

When an animal is placed in the gantry, the external magnetic field within the bore of the magnet is considerably stronger than the biologic field. This causes the biologic field to align and reach a state of equilibrium with the external field, within the bore of the magnet. In order to measure the animal's magnetic field and avoid interference from the external field, it is necessary to disturb the biologic field (Shores, 1993). This alteration of the biologic field is accomplished using a specified sequence of electromagnetic radio frequency pulses and taking advantage of the resonance phenomenon (Friedman *et al*, 1989).

In MRI, RF pulse sequences are applied perpendicular to the external magnetic field and at the Larmor frequency, which is 42.58 MHz/T for (^{1}H) hydrogen (Shores, 1993). As a result, the patient's (biologic) magnetic field undergoes two simultaneous Larmor precessions: one around the external magnetic field and one around the rotating (cyclic) magnetic field applied in the pulse sequence. This allows the steady tipping or nutation of the biologic field. If a different frequency is applied, nutation does not occur. (Friedman *et al*., 1989).

After nutating the biologic field to the desired degree or angle, the magnetic pulse is discontinued, and the biologic field realigns with the external field. Application of specific strengths and durations of the magnetic pulse results in the production of measurable radio-frequency waves created by realignment of the nuclear field. Only the tissue components with the same natural cyclic motion (spin) frequency as the applied magnetic pulse (cyclic force) create these measurable radio frequency (RF) waves. A coil, with its diameter placed parallel to the external magnetic field, detects the radio frequency waves, which are transmitted to a computer station. The computer analyses the data received, using Fourier transformation, to construct the resultant image (Friedman, *et al*., 1989).

3.6 Spatial characteristics and construction of the MR image

The actual MR image is composed of an array of pixels (picture elements) that correspond to volumes of tissue termed "voxels" (volume elements). Brightness of the individual pixel varies with the excitatory properties of the tissue in the corresponding voxel. The use of large voxels gives a high signal-to-noise ratio. Increasing voxel size reduces spatial resolution and may limit image quality (Thomson *et al*., 1993). Spatial orientation in an MR image is accomplished, in part, through a process that involves the application of magnetic gradients across the imaging volume. The homogeneity of B_0 is predictably disturbed through a system of three pairs of gradient coils positioned in the x, y, and z planes. These coils produce magnetic fields that, while being considerably weaker than B_0 itself, create differences, i.e., gradients, in the magnetic field strength applied through the imaging volume (Thomson *et al*., 1993). Because of this variation in magnetic field strength, protons at different levels of the imaging volume precess at different rates. Only protons in a slice with a particular resonant frequency rate will be excited when the corresponding radio frequency is applied. If the gradient of magnetic fields applied across the imaging volume is steep, the slices of tissue that

can be distinguished will be thin (1-2 mm) (Thomson *et al.*, 1993). Application of a radio frequency pulse with a narrow wave band has a similar effect. The orientation of the slice can be in any plane, depending on which combination of coils is activated. Selective activation of the x and y gradients within each transverse slice yields information on individual voxels of the imaging volume. Hence, the signal from individual voxels within a thin slice of tissue can be collected and converted to an actual anatomic image, using computer-assisted reconstruction based on Fourier techniques (Foster, 1984). Using Fourier transformation the computer can analyze how much signal of a specific frequency and phase is emitted. As these signals can be assigned to a certain location in the slice, the image can be reconstructed.

3.7 Contrast

Image contrast is enhanced by using different pulse sequences and exploiting the relaxation characteristics to create either T_1-weighted or T_2-weighted pictures. Signals contributing to the image may be acquired at varying times that emphasize those generated from one type of relaxation more than the other. Tissues with shorter T_1 or longer T_2 values are associated with NMR signals of relatively higher intensity (whiteness) on the MR image (Foster, 1984). Because cerebrospinal fluid (CSF) has a markedly longer T_2, relaxation time than brain tissue, it appears dark on a T_1-weighted image (General Electric 1984). In contrast, CSF appears white on a T_2-weighted image. Depending upon the degree of T_1, or T_2 weighting, grey matter appears darker than white matter with T_1 weighting due to its longer relaxation time, and vice versa for T_2 weighting. This difference has been attributed to the lower water content of white versus grey matter (Wehrli, 1986).

As a general rule, the greater the intracellular water to protein ratio, or the greater the ratio between extracellular and intracellular water, the greater is the T_2 value and the more intense the signal. Urine and very glandular tissues such as the endometrium, thus give rise to higher signal intensity than skeletal muscle or connective tissue (Dennis, 1998). In certain circumstances, such as haemorrhage, the water T_2 value can be greatly reduced in the vicinity of high concentrations of molecules carrying unpaired electrons, such as deoxyhaemoglobin. Deoxyhaemoglobin is the break down product of haemoglobin and acts as paramagnetic substance. Paramagnetic substances have small local magnetic fields, which causes a shortening of the relaxation times of the surrounding protons. Another paramagnetic substance is methaemoglobin, which is found in haematomas.

3.7.1 Contrast enhancement in MRI using intravenous paramagnetic contrast media

Paramagnetic substances can be used as contrast media due to their magnetic properties. The contrast media increase the visibility of certain tissue and lesions, when injected into the bloodstream. The paramagnetic substance that is commonly used is the rare earth Gadolinium. Gadolinium is toxic in its free state but not when bound by chelation as Gadolinium-

diethylenetriamine penta-acetic acid (DTPA). Chelated gadolinium products include gadopentate, gadoteridol and gadodiamide (Chanalet *et al.,* 1995). Forming a chelated product not only removes the toxicity but also makes the product more water-soluble. The molecules of chelated gadolinium are too large to penetrate the normal intact blood-brain barrier. However, if the barrier is damaged by neoplasia or inflammatory disease, contrast medium enters the affected tissues and temporarily alters their magnetic properties so that they appear brighter on subsequent T_1-weighted images but this effect is not as pronounced on T_2-weighted images. In fact, T_2-weighted acquisitions are seldomly generated of patients that received contrast enhancement. The process is known as contrast enhancement (Dennis, 1998). With contrast enhancement, the image contrast can be enhanced by increasing the signal intensity of one tissue relative to another. The use of contrast media may provide more sensitive detection of various lesions, especially in the central nervous system, better defines margins of the lesions and allows more accurate differentiation of lesions. In this way, many brain tumours can be outlined precisely, allowing for more accurate treatment by surgery or radiotherapy. In other parts of the body, contrast enhancement is a reflection of the vascularity of the tissues and can be useful in outlining avascular areas, such as abscesses and foreign bodies (Dennis, 1998).

Contrast-enhancing media have been used in magnetic resonance imaging since the earliest stages of the development of this imaging modality (Swanson, 1990). This relates to experimental, as well as clinical (human) applications and veterinary medicine (Moss, 1983). A wide range of chemical compounds have been tested in vitro and in vivo with varying success, but obviously not every agent was consequently developed into a medically useful product (Duroux, 1995). Clinical applications are restricted to those agents that underwent extensive chemical, biological, and clinical testing and have been approved by proper agencies for medical use according to the current regulations governed in each country. For veterinary clinical applications, water-soluble contrast media designed for intravenous (i.v.) administration and targeted primarily at central nervous system (CNS) lesions are available. These agents are Magnevist®, ProHance®, and Omniscan®. Although the chemical structure of MR contrast media differs, all contain the paramagnetic element Gadolinium (Gd), and their mechanism of action is based on the same physical principle. Contrast media used in MR and x-ray computed tomography (CT) operate by entirely different mechanisms. CT contrast media are visualized directly as they accumulate in the tissue by their ability to absorb x-ray photons. MR contrast media, on the other hand, function indirectly through their alteration of the local magnetic environment (Kuriashkin, 2000).

3.7.2 Mechanism of action of intravenous contrast media for MRI

There are three main parameters determining signal intensity and contrast in the MR image: proton spin density (N), spin-lattice relaxation time, also known as longitudinal relaxation

time, (T_1) and spin-spin relaxation time (T_2), which are specific for every tissue. Gd is a rare earth element that has seven unpaired electrons (more than any other element) in ionic (Gd^{+3}) form and produces a significant magnetic moment (Brasch, 1993). The magnetic moment of the unpaired electron is much stronger (nearly 700 times) than the one of the proton, and due to dipole-dipole interaction it causes the proton to relax faster, shortening its relaxation time. This effect is called proton relaxation enhancement (Brasch, 1993) and results in image contrast enhancement. Signal intensity is directly proportional to relaxation rate R_1, ($1/T_1$,). Areas where concentration of contrast media is higher, therefore, are more signal intense than surrounding tissue. The effectiveness of a specific paramagnetic medium for proton relaxation enhancement is often expressed as its' relaxivity and generally measured experimentally in water at 1 mmol concentration. Relaxivity is actually a slope of the linear relationship between the relaxation rate of the protons and concentration of the paramagnetic contrast agent. Of all known elements, Gd produces the largest T_1, relaxation enhancement effect, which makes it the substance of choice for MR contrast media (Kuriashkin, 2000).

3.7.3 Biological safety of intravenous contrast media

Forming a metal chelate complex reduces toxicity of Gd-based contrast media, as well as increased water solubility. In addition, it defines its biodistribution in extracellular spaces due to the large molecular weight (over 500 Daltons) and allows renal filtration and urinary excretion, not reducing its paramagnetic properties. Their high safety index is an indication of high pharmacologic safety and effectiveness of gadolinium chelates as contrast-enhancing agents (Runge, 2001). Most commercially available contrast media have very similar relaxation effects on T_1, and T_2, toxicity and effectiveness (Stark, 1992). Caution should be exercised in patients with renal insufficiency. There are no known contraindications for the Gd-chelate based contrast media (Kuriashkin, 2000).

3.7.4 Lack of enhancement with intravenous contrast media in MRI

An important concept is that lack of enhancement does not necessarily indicate the absence of a particular lesion or tumor (Atlas, 1991). One of the reasons could be improper administration of contrast medium. In order to verify successful administration of contrast media, certain characteristic indicators on the MR image can be used, such as mild enhancement of some normal tissues following contrast medium administration (Moore *et al.*, 1996). Those tissues and anatomic areas include endoturbinates and mucosa of the nasal cavity, hard and soft palate, oral mucosa, base of the tongue, pituitary gland, and zygomatic, parotid, and mandibular salivary glands. Mild focal enhancement can also be noticed in the

lateral, 3rd, and 4th ventricles of the brain, as well as venous sinuses of the cranial dura mater. Normal lymph nodes do not enhance. On routine T_1-weighted lumbosacral spine images, where contrast enhancement was used, gadolinium is excreted into the urine and the bladder is thus seen as a high-signal structure in the pelvis, (Kuriashkin, 2000). It is important to stress that a waiting period of 10 - 12 minutes post-contrast medium administration be allowed prior to image acquisition. Unless the contrast medium is used for magnetic resonance angiography, it cannot produce tissue enhancement while in the blood pool. Not allowing sufficient time for the contrast medium to accumulate in tissues can result in poor tissue enhancement. This is especially important for agents with a slower plasma clearance rate, like ProHance® Based on biodistribution and elimination rate of Gd-chelate containing contrast media, optimal time to detect contrast enhancement is between 10 to 75 min. after intravenous administration (Chang, 1994).

3.8 Motion artefacts

Motion artefact on images involving the chest cavity or abdomen may be considerable, but new gating techniques and averaging techniques may improve the ability to image these regions (Dennis, 1995). Motion can lead to blurring and ghost images, the latter which are partial copies of the parent image at a different location. Fast spin echo pulse sequences decrease the imaging time to a number of minutes and help reduce the overall time for imaging and to improve image quality. (Miyabayashi *et al.*, 2000), but are not yet fast enough to eliminate the motion artefacts created by breathing movements. Breath withholding for a few seconds during image acquisition in adult human patients is a distinct advantage lost in animal MRI protocols. There is generally an inverse relationship between the VOI and motion artefact (Dennis,. 1995). So for example, during a fast imaging with steady state precession FISP sequence, with an acquisition time of 20 to 30 seconds and slice thickness of 5 mm, which is commonly used for imaging the abdominal aorta,, it is practical for the average human patient to achieve breath withholding for the entire acquisition. However, a time reversed FISP (PSIF) sequence capable of a slice thickness of 1 mm, may take 5 to 7 minutes, making it impossible to withhold breath for the entire duration of the scan.

3.9 Patient preparation

The scanning procedure requires the animal to be immobilized for the entire duration of image acquisition. With less advanced MR equipment, this may take 20-30 minutes or longer during the initial stages of the experiments while suitable pulse sequences for the purpose are found. Once ideal pulse sequences are found, and scout images have been produced, the scanning can be performed in less than 15 minutes using high field strength (1,5 Tesla) scanners. Animals with pre-existing or coexisting major organ disease may require special considerations in the choice of anaesthetic agents. Propofol (“Diprivan,” Zeneca) is often used as an intravenous

anaesthetic agent (Vincent *et al*., 1995). It offers the advantages of a short duration of its effects, administration by bolus or continuous intravenous infusion, and safety for animals with intracranial disease. Medetomidine ("Dormitor," Novartis AH) may provide safe and adequate sedation for short procedures such as MRI of abdomen (Sakamoto *et al*, 1997). The dogs may be immobilized using intravenous medetomidine at the dose of 40-80 pg kg^{-1} bw. The sedation may be prolonged after 30 to 45 minutes with repeated intravenous injections of medetomidine 10-20 pg kg^{-1}, if necessary. At the end of the examination, an intramuscular injection of a medetomidine antagonist atipamezole ("Antisedan," Novartis AH) at the dose 200-320 mg kg^{-1} may be given (Sakamoto *et al*, 1997). Shores (1993) described the use of Propofol induction and maintenance with gas inhalation anaesthesia during an MRI examination. It is important to note that gas inhalation anaesthesia requires special equipment with non-ferrous materials and long pipes and anaesthetic monitoring devices outside the MRI room. This makes gas inhalation anaesthesia in MRI impractical.

The animal is routinely positioned in ventral recumbency, with the head entering the gantry first. Consistent positioning for all imaging procedures facilitates image interpretation and identification of right and left sides (Dennis, 1998). Near perfect symmetrical positioning, aids in the ability to correctly interpret the images. If one side of the head is rotated more rostrally than the other, for example, many structures (e.g., lateral ventricles) will appear asymmetrical on the scans, and this could lead to an erroneous diagnosis. A scout film also called a localiser is initially made to determine patient position in the gantry and to identify the ROI to be imaged. Slice thickness and the number of scans necessary for the study are determined before continuing the procedure. This ensures that the area of interest is contained in the completed study.

3.10 The MR examination

The MR examination usually consists of acquisition of T_1-weighted and T_2-weighted images of an anatomic region (e.g., brain) in one or more planes. Images may be oriented in sagital, transverse (axial), or dorsal (coronal) planes. MRI acquisition can be oriented in any plane, regardless of patient orientation inside the magnet. This property of MRI does not require computer generated reformatting of data obtained in one plane and can therefore be performed without sacrifice of image quality (Shores, 1993). Transverse plane images are considered standard in veterinary imaging. (Friedman, *et al* 1989). In addition to T_1- and T_2-weighted images, and depending on the purpose of the examination, the T_1 study may be repeated with the addition of gadolinium DTPA for contrast enhancement. On T_1 studies, the images of tissues containing the contrast agent appear more hyperintense. The resultant effect is much the same as for iodinated contrast agents used in computed tomography imaging studies (Aisen, 1990)

3.10.1 Data acquisition

A multisided acquisition technique is usually used, allowing simultaneous acquisition of image data from several tissue slices within the chosen field of view. Slice thickness is chosen based on the purpose of the examination and the area being imaged, the size of the organ and the capability of the MR apparatus. Generally thinner slices offer better resolution, but image quality suffers because the signal produced is related to the volume of tissue being pulsed (signal-to-noise ratio). Volume coverage also is reduced (Friedman *et al*, 1989 and Aisen, 1990).

Field of view and matrix size are additional parameters to be addressed. Smaller fields of view may increase the spatial resolution, but at the expense of signal-to-noise ratio. An increase in matrix size will also increase spatial resolution, but with loss of signal-to-noise ratio. Most scans are performed using a 256 X 256-matrix size (Aisen, 1990). All these parameters need to be adjusted to create the best image.

3.10.2 Low and high field-strength magnetic resonance imaging

Magnetic field strength commonly referred to as field strength has a considerable bearing on several aspects of MRI. MRI has its widest application in human and veterinary neurodiagnostics and, therefore, the effects of low- and high field-strengths of the MRI scanner have been compared in this field. The signal intensity in MRI depends, in part, on the magnetic field strength of the scanner and can vary from 0.02 to 2T (and up to 8 T in research laboratories). There is currently no uniform agreement on classification of field strengths. Kärkkäinen (1995) classified devices <0.1 T as ultralow-field, 0.1 - 0.3 T as low-field, 0.35 - 0.6 T as mid-field and 1-2 T as high-field. Sepponen *et al*. (1985) reported that low-field systems were able to produce images in the human brain characterised by high T_1 contrast. The poor spatial resolution associated with ultra low and low-field devices was expected to improve with the development of improved radio frequency and surface coils. Subsequent human studies confirmed this hypothesis (Agartz *et al*., 1987). Since high-field scanners are sometimes prohibitively expensive or unavailable, there is interest in using modern low field-strength MR scanners in veterinary neurological diagnosis if the quality of the images is suitable for clinical use in veterinary medicine (Kärkkäinen, 1995). However, since amplification of field strength linearly increases the signal-to-noise ratio (S/N) (Rinck, 1993), the image quality is better in high-field MRI than in low-field MRI due to the presence of a better S/N.

The S/N can also be improved by means of using better transmitter and receiving coils, decreasing the bandwidth of RF pulses, decreasing the distance from ROI to either the receiver or transmitter or both, by using RF coils or increasing scan time by either increasing the number of acquisitions per image or by increasing the number of phase-encoding steps

(this progress is in pace with faster computer processors). RF coils may be receiver coils, transmitter coils or both and are then named transceiver coils.

Kärkkäinen (1995) had to use all these methods to attain comparable images with low field strength as opposed to normal high field strength. Most low field-strength MRI studies were performed using gradient echo (GRE) techniques. At 0.1 T when the field strength is homogeneous, the S/N is better with GRE than with spin echo (SE) techniques (Virolainen, 1993). The use of the GRE sequences also enables three-dimensional imaging and manipulation of contrast with the flip angle. At low field strength, the disadvantages and artefact associated with GRE pulse sequences are not as disturbing as they are at high-field-strength imaging.

Disadvantages of low-field MRI compared to high-field MRI are poorer resolution and longer acquisition times.

Low field-strength MRI holds several advantages of importance to veterinary use, such as substantially lower initial and maintenance costs, easy fitting in average laboratory rooms without need of special shielding, and no danger of cryogen accidents. Low field-strength MRI is more silent than high field-strength MRI because it creates less noise when switching gradients, which may be more convenient for the patients and the veterinarians observing them.

3.10.3 Image characteristics and principles of interpretation

Unlike conventional radiological and computed tomography techniques, which are almost completely dependent on differences in electron density of tissue, MRI reflects complex interactions of the T_1 and T_2 times and proton density. Both CT and MR images are representations of each voxel, constructed from an array of numbers representing computer data, and displayed as two-dimensional structures termed pixels (see 3.6). A fundamental difference exists, however, in the pixels in CT and pixels in MRI. CT scanners are calibrated so that pure water has a value (CT number or Hounsfield units) of zero and air has a value of 1000 (Shores, 1993). Other structures have values based on these calibration units as determined by their relative electron density. With MRI, pixel values have no absolute values, and the same structure imaged on different scanners or on the same scanner on two separate occasions may have very different signal intensities, even if the TR, TE and other parameters remain the same. Relative differences in tissue density (for instance, Cerebrospinal fluid CSF versus white matter) will remain constant. Patient positioning within the coil, how the scanner is tuned, and other factors are often responsible for the differences in the signal intensity (Aisen, 1990).

Rapid flow of blood or CSF creates a signal void. This is because the hydrogen containing components of the fluid, present at the time of the radio-frequency pulse in the slice being

imaged, do not remain within the voxel long enough to encounter both the 90^0 and 180^0 pulses and therefore do not produce a signal (Shores, 1993). Fluid that moves much slower can produce the opposite effect and appear bright. This occurs because the slower-moving fluid is less saturated with signal than are adjacent structures. The MR image is derived from the signal produced from multiple radio-frequency pulses, and all tissues lose some signal from this process. The slower-moving fluid encounters fewer total radio frequency pulses, lose far less signal from saturation, and produce higher signal intensity.

3.11 New and future advanced magnetic resonance techniques

3.11.1 Three-dimensional magnetic resonance imaging

MRI has expanded to include three-dimensional (3-D) reconstruction, which is undergoing continued development. Using this modality, the brain is imaged so the imaging voxel is the same size in all dimensions (isotropic), usually less than 1 mm on each side. The data collected mathematically represents the entire head and can be reconstructed into a 3-D representation. With available computer software, cutaway views can be created that allow one to view surface details and internal structures in 3-D representation. Each layer of tissue can be dissected on-screen to mimic a surgical approach to, for instance, a brain lesion (Waluch and Dyck, 1990).

3.11.2 Positron emission tomography (pet scans)

The use of positron emission tomography (PET) scans in human imaging studies is expanding as more PET scan units become available. PET scans are performed following injection of a radioisotope-labelled substance, usually 18-2-fluorodeoxyglucose and the resultant colour image identifies regions of increased metabolic activity. One study determined a correlation in the metabolic activity of meningiomas and the aggressiveness of the tumour and its propensity for recurrence (De Michele, 1991). PET scans are also used to measure cerebral blood flow, and current research includes studies in cognitive function of the brain and the development of radiopharmaceuticals, which are tumour receptor ligands tagged with positron emitters (De Michele, 1991).

3.11.3 Computer software generated high resolution medical animations

Using a specialized software package, a method of reconstructing computed tomography or MRI data into three-dimensional videotape animations has recently become available. The method employs imaging data saved on magnetic tape, a computer workstation for transformation of image data, and laser disks for storage and display of video images. This highly technical procedure is relatively inexpensive and allows displays of cerebral angiograms from intravenous contrast administration during the imaging procedure

(Harbaugh, 1992). Of interest with MRI is the ability of the techniques to display soft-tissue structures, such as muscle and tendon surrounding a joint, in 360^0 rotation around the structure. This process provides the diagnostician with an invaluable perspective of the structures involved in the disease process (Shores, 1993).

3.11.4 Goals for the future development of diagnostic imaging

Undoubtedly, our ability to image internal structures will continue to increase. Goals for the future are focused on the ability to image not only structure, but also function and cellular characteristics (Shores, 1993). Future diagnostic imaging developments also will concentrate on limiting patient risk and invasiveness of the procedure. Integration of computer programs and current diagnostic imaging techniques allow pinpoint accuracy in localisation of lesions. Allied imaging techniques, such as MRS. are generating considerable interest in the establishment of diagnostic criteria based on imaging characteristics. Earlier detection of disease and elimination of the need for most biopsy procedures is certainly in the minds of the developers of future diagnostic imaging techniques (Shores, 1993).

CHAPTER 4 MATERIALS AND METHODS

4.1 Bitches

Eighteen German shepherd bitches, varying in age between one and nine years, were used (Table 1). None of the bitches had histories of, or any clinical signs indicative of, disease or malfunctioning of the reproductive system. Both nulliparous bitches and multiparous bitches were used.

4.2 Management of bitches

Each bitch was individually identifiable by means of a tattoo to the right ear and or a name. Bitches were kept individually in kennels with cement floors and small grass runs and no artificial lighting. They were fed *ad lib* with self-feeders using a balanced, pelleted commercial dog ration. They had free access to clean drinking water at all times. The bitches were routinely exercised on weekdays once a day by taking them for a walk on a lead. The kennel veterinary nurse and her staff performed the vaccination, deworming and dipping as routine.

4.3 Experimental groups

4.3.1 Experiment 1 (phantom study)

Fifteen bitches were used in Experiment 1.They were divided into 3 groups: Six were in the follicular phase; three in the early luteal phase (1-5 weeks into dioestrus) and six in the late luteal phase (5-8 weeks into dioestrus), see Table 1. A bitch was estimated to have been in the follicular phase if she either had large, round, edematous vaginal folds or if there were signs that the edema has decreased sufficiently to result in large, rounded folds but with distinct secondary folds, which were also round in shape. The bitch was estimated to have ovulated and to have entered the luteal phase if the edema has sufficiently decreased to render the folds angular in shape. For bitches in the luteal phase the duration of the luteal phase was measured relative to D1 as established by vaginal cytology. In one of the late luteal group bitches named (Zaro), D1 was not known, but she was known to have been in late dioestrus as the ovariohysterectomy was done at the time of a full-term caesarean section.

One additional bitch (Mira) that was in anoestrus was included in this experiment because she became available and there was space left in the phantom.

The ovaries of these 16 bitches were collected in three groups and embedded in gelatine in three phantoms and imaged in three planes, using a slice thickness and a slice interval of 1mm each. Three operators independently determined the number of follicles or corpora lutea in

each ovary on all the planes of imaging. The accuracy of their counts was determined by counting the structures during dissection of the ovaries.

Table 1
Details of experimental bitches and the groups they were assigned to

[a] Refers to the last heat before the onset of the study

Name	Age	Parity	Interval since previous heat (months)[a]	Phase of oestrous cycle	Phantom no.
Experiment 1					
Brogen	14 m	0	7	Follicular	1
Minnie	10 m	0	n/a	Follicular	1
Zaro	5 y	3	7	Late luteal	1
Rita	2 y	1	6	Late luteal	1
Zeal	9 y	5	9	Late luteal	1
Betsie	3 y	1	5	Follicular	2
Sabrina	3 y	0	7	Follicular	2
Ellie	6 y	2	7	Late luteal	2
Dusty	8 y	3	Unknown	Late luteal	2
Kia	Unknown	Unknown	Unknown-	Late luteal	2
Xala	2 y	0	7	Follicular	3
Bibi	3 y	0	6	Follicular	3
Kori	5 y	0	9	Early luteal	3
Velvet	3 y	0	7	Early luteal	3
Sara	4 y	?	8	Early luteal	3
Mira	2 y	0	4	Anoestrus	3
Experiment 2					
Charisma	3½ y	1	Unknown	Follicular	
Amigo	14 m	0	8	Follicular	

4.3.2 Experiment 2 (in vivo study)

Ten bitches were allocated for this experiment. The ovaries of 10 live bitches would have been imaged twice, once before administration of gadolinium and again there after, where after the bitches would have been spayed. T_1- and T_2-weighted images would have been collected. Five bitches would have been in the follicular phase and 5 in the luteal phase. Experiment 2 was abolished after all attempts at obtaining images of the ovaries in the first

two live dogs failed. Using numerous echo-spin sequences, the images were not clear enough to identify the ovaries due to motion artefacts.

4.4 Monitoring of oestrous cycles

The bitches were observed daily for signs of pro-oestrus at the kennels. Once pro-oestrus had been observed by the kennel nurse, the cycle was monitored by vaginoscopy (Jeffcoate and Lindsay, 1989) and vaginal cytology. The vaginoscopes consisted of pieces of perspex tubing, 220 mm long, 15 mm outer diameter and 11 mm inner diameter. All vaginoscopes were disinfected with Hibitane-alcohol before use. The vaginoscope was passed into the vagina of the bitch and light from a cold light source was shone through it to illuminate the vaginal mucous membrane cranial to the scope. The appearance of the folds of the vaginal mucous membrane was described as being oedematous, shrinking rounded (still large, but shrinking with rounded profiles), shrunken with angular folds, or small and rounded (indicating that the bitch was in dioestrus or anoestrus (Jeffcoate and Lindsay, 1989).

Vaginal cytology smears were obtained by means of cotton-tipped swabs, which were moistened with saline. The swab was passed into the caudal vagina, taking care to avoid the clitoral fossa and vestibulum and vulvar skin (Olson *et al.*, 1984 and Cowell *et al*, 1989). Cells were then rolled onto a marked glass slide, dried and stained with CAM'S Quick-stain (C.A. Milsch (Pty) Ltd., Krugersdorp, RSA) (Olson *et al.*, 1984). The first vaginal smear was made either on the day that the bitch was exhibiting signs of pro-oestrus or within 48 hours thereafter. In bitches destined for the follicular phase group, vaginal cytology and vaginoscopy was performed until the bitch was in late oestrus but not yet in dioestrus. On bitches destined for the early or late luteal groups, vaginoscopy was performed daily from first signs of pro-oestrus and vaginal smears made daily from when the vaginoscopy indicated that the bitch was in late oestrus until dioestrus was confirmed. Vaginal epithelial samples were collected immediately prior to the vaginoscopic examination. Cytology was thus only used to confirm the onset of dioestrus as defined by Holst and Phemister (1974) in the luteal groups. One bitch named Zaro was not monitored as a full term caesarean section and an ovariohysterectomy (OVH) was performed. This automatically qualified her for inclusion within the late luteal group. Another bitch named Mira was found to be in anoestrus at the time that a phantom had to be prepared and her ovaries were included to "fill the space" in the phantom.

4.5 Plasma progesterone concentrations (PPC)

PPC is low during most of the follicular phase, starts rising distinctly during the late follicular phase and reach highest levels during the early luteal phase, whereafter it remains elevated but somewhat lower during the late luteal phase before declining to basal levels during anoestrus (Concannon *et al*., 1975 and 1977). Accordingly, a heparinised blood sample was collected

from each bitch on the day of OVH in order to measure PPC at the time of harvesting the ovaries in order to confirm the stage of the oestrous cycle. The blood sample of Velvet was lost.

The PPC was assayed by means of a radio-immuno assay method (Coat A Count, Diagnostic Products, Randburg, Gauteng). All samples were assayed as a single batch.

4.6 Collection of the ovaries

In both experiments, the ovaries were collected by means of routine OVH at the Rant en Dal Animal Hospital. The bitches were premedicated using medetomidine HCL 1mg ml^{-1} ("Dormitor", Novartis Animal Health, Isando, Gauteng) at the dose of 0.05-0.08 ml kg^{-1} i.v. prior to induction using sodium thiopentone ("Intraval", Merial Randburg, Gauteng) for induction and intubation and halothane gas inhalation was used for maintenance of anaesthesia. The bitch was then shaved and the skin aseptically prepared for surgery. Pulse oximetry was used to monitor anaesthesia. During surgery, care was taken not to damage the ovaries or the structures they contained by crushing or pinching them with instruments or rough handling. Particular care was taken in bitches in the follicular phase not to rupture follicles during removal of the ovaries by only handling the vascular appendage cranial to the ovary. Each ovary was immediately placed into a separate container filled with normal saline, which was identified with the name of the bitch and whether it contained a left or right ovary.

4.7 Preparation of the phantom

The ovaries were kept in a fridge until placed into the phantom, which usually occurred within 24 h and occasionally up to 48 h after collection. The phantom was usually imaged on the same day it was prepared but never more than 12 h after preparation. The total time from collection of the ovaries until imaging never exceeded 48 h. The basic concept of the phantom preparation was adopted from the method described by Blechinger *et al*. (1988), but no preservative was added to our gelatine. Previous experience with preservation of the ovaries in either 50% glycerol-saline or 10% formalin had altered the macroscopic appearance of the ovaries and is believed to have altered the ovary sufficiently to alter its appearance on MRI, presumably because both preservatives are hygroscopic, which may have altered the water content of the ovaries. On the day of phantom preparation, the ovaries were removed from the saline and their bursae removed. Ordinary commercial gelatine (Royal, Chloorkop, Gauteng) as used for cooking purposes was then prepared by dissolving the gelatine powder in very hot but not boiling water and stirred very gently. Care was taken not to agitate the mixture in order to avoid the formation of gas bubbles. The amount of gelatine powder added to the water varies in cooking whether you require a soft set or firm set. For the purposes of the phantom, a firm set was considered desirable because it made the phantom more robust. A Vitamin E gel capsule was placed inside the phantom (Figure 1) to orient the phantom

rostrally (or head first as with the human). A schematic drawing was made of the phantom with the rostral, left, and right positions, as well as the position of each ovary marked on the figure that allowed tracing an image to an ovary, to its side (left or right), and to the bitch from which it came.

Only half the amount of required water was used to dissolve the gelatine. The other half was added cold as soon as all the gelatine powder was properly dissolved. This was done to speed up the setting of the gelatine and to ensure that there would be no heat-induced damage to the ovaries whilst cooling down. The phantom had to be made in two stages. In the first stage, the first layer (2 to 3cm) of gelatine was prepared and allowed to set in a flat Tupperware container. This was done so that the ovaries would not sink to the bottom of the container and so that they could be suspended and totally surrounded by a homogenous mass within the phantom. As soon as the first layer was firmly set, the ovaries were placed on this gelatine layer and the container was marked rostral, left, and right on its sides to positively identify the ovaries within the container (Figure 1). The second layer of gelatine was then prepared as above and slowly decanted into the container without flushing the ovaries away or swirling them around. Although extreme care was taken in order to prevent gas bubble formation in the preparation of the phantom, which would result in signal voids on MRI, there remained a small number of bubbles on the surface, which were gently teased away towards the sides of the container where they disintegrated as the mixture set. The gelatine was then allowed to cool and the phantom placed in the refrigerator until it was firmly set and ready for scanning. Figure 2 shows an MR image of a section through the phantom and the two layers of gelatine, with an ovary lying on the lower layer.

4.8 Imaging ovarian structures in the phantom (Experiment 1)

Once the gelatine had fully cooled down and set, the phantoms were placed inside the gantry of a 1,5 Tesla Siemens Magnetom Symphony scanner.

A circular polarized head array radio frequency receiver coil was used to surround the phantoms during image acquisitions, as it is standard to use RF coils to reduce S/N ratio where practically possible. It was the opinion of the radiologist that the images obtained whilst searching for the best pulse sequence obtainable with the machine, was better in most instances with the head coil. The choice of coil was limited to the size of the subject to be scanned. Theoretically, the smallest possible coil should be used to scan the subject. The size of the phantom was ideally suited to fit into the head coil.

For the purposes of this study, the relative size of structures was important. It was vital that the pulse sequence used in this study would both allow a slice thickness of 1 mm and a slice interval of 1 mm and that the subject be scanned in three planes. Not all pulse sequences meet

these requirements; neither can all apparatus perform any pulse sequence that a researcher might want to perform. One is limited to the capabilities of the MR apparatus at the disposal of the researcher. The best pulse sequences to be used for the imaging of the phantoms were eventually decided upon by an experienced specialist human radiologist. He made his decision by simply looking at images of the same structure imaged numerous times using different pulse sequences.

The canine follicle is a fluid-filled structure and the corpus luteum is a dense tissue mass and, considering that fluid generally looks markedly different from tissue on MRI, it was anticipated that follicles and corpora lutea would also look distinctly different on MRI. It was therefore crucial that we included an ovary with follicles and an ovary with corpora lutea in the pulse sequence seeking efforts in the first phantom. In order to identify the pulse sequence most suitable for counting the ovarian structures, various pulse sequences were used on the first phantom.

The gradient echo pulse sequence finally used for the T_1-weighted images was the multiplanar reconstruction non-selective excitation 3d sequence MPR NS and the T_2-weighted sequence was the PSIF (Time reversed fast imaging with steady state precession FISP). The image acquisition time was approximately 5-7 minutes each for both the T_1 and T_2-weighted images. This protocol appeared best for ovaries of bitches that were in the luteal phase as well as those that were in the follicular phase.

Once the best-suited pulse sequence had been selected, a standard commercial head coil was placed around the phantom, and it was established that images generated with the coil were marginally better than those with the surface gantry coil. Hence, all images thereafter were generated using the head coil.

Three sets of MR images with the planes of the images perpendicular to one another were obtained. Within sets, the planes of the images for each set were parallel to one another for each ovary within the phantom. The slices were contiguous with slice intervals and thicknesses of 1mm. For the first set of images, the planes were sagital and for the second, the planes were transverse and for the third dorsal or coronal. For the purposes of this study, the plane of imaging e.g. sagital, coronal or transverse is relative to the phantom and not the ovary. The images were exported to a dedicated workstation for further storage and processing and selected studies were printed onto laser film for later evaluation.

4.9 Imaging ovarian structures in the live dogs (Experiment 2)

The first live dog was tranquilised using medetomidine HCL 1mg ml^{-1} (Dormitor, Novartis Animal Health, Isando, Gauteng) at the dose of 0.05-0.08 ml kg^{-1} i.v. prior to positioning the

dog in dorsal recumbency on a sponge wedge and strapped to the MR table. The dog was lying perfectly still and did not move except for the normal breathing movements during the entire stay in the MRI gantry. Both the pulse sequences described above that produced the best images in the phantoms, were initially used on the live dogs. Thereafter, other pulse sequences and a Fatsaturation sequence with or without head coils were used but they all failed to improve the images. The images obtained could not be used for interpretation as the images were spoiled with motion artefact (Figure 3,Figure 4, Figure 5,Figure 6).Attempts to improve the images failed repeatedly using the same apparatus and methods. This process was repeated with a second live dog that was scanned using the same apparatus and methods. This again failed to produce images suitable

4.10 Dissection of ovaries and description of its structures

After the MR images had been collected, the ovaries were removed from the gelatine and their sizes recorded, where after each ovary was sliced with a scalpel in order to count the number of corpora lutea, follicular structures, or cystic structures by means of direct inspection. Elongated ovaries were dissected by slicing them along their long (sagital) axis, whereas round or lobulated ovaries were sliced along any convenient axis, using a sharp scalpel blade in each case. The slice thickness was approximately 1-2 mm. Extreme care was taken to assess whether any structure seen on the second and subsequent slices, formed part of a new structure or whether it was still part of one of the structures seen in previous slices. The dissections and counts of ovarian structures were done by two persons in phantom 1 and they agreed on each count. As there was consensus that dissection and counting the structures was straight forward, it was agreed that only one person would dissect and count the remainder of the ovaries in experiments 1 and 2.

The following was recorded with respect to each structure in each ovary:

- Whether the structure was considered a follicle, a corpus luteum, or a cyst
- The size of the structure
- If the structure was considered a cyst, then its position within the ovary was noted, e.g. cortical, hilar, immediately subsurface or parovarian
- The shape of structure
- The colour of structure
- Whether structure was solid, fluid filled or cavitated
- If the structure was cavitated, the thickness of the wall was noted
- Number of structures.

For each ovary, a record was made of its size and a subjective assessment on the ease or difficulty in counting or identifying the structures.

4.11 Evaluation of images

Hard copies of each set of images of each ovary within the phantom were made and used to count the structures on them. Each of three operators independently counted the number of ovarian structures on each of the three sets of MR images of all the ovaries and gave opinions whether the structures seen were corpora lutea, follicles, or cysts.

4.12 Data analysis

Data analysis was done by direct count. The number ovarian structures as determined from each set of MR images was compared to the actual number determined by dissection and the counts of each operator were compared to the actual number of ovarian structures.

In order to determine whether the accuracy of MRI differs between early and late luteal phases of the oestrous cycle, a factorial ANOVA was performed with the difference between the number of corpora lutea on MRI and the number on dissection as response variable, Operator (2 degrees of freedom) as a random factor, and Phase of cycle (one degree of freedom) and View (2 degrees of freedom) as fixed factors, and α set at 0.05. Bitches in the follicular phase of the cycle were omitted from this analysis.

After it was found that each operator mistook follicles for corpora lutea on MRI (Table 6), and because the dissection revealed that no bitch in the follicular phase had any corpora lutea, it was decided to add the number of follicles and the number of corpora lutea seen on each ovary of a bitch in the follicular phase and use the difference between this total and the number of follicles found on dissection as the error due to MRI. This manipulation seems justified if one assumes that a person knowing that a bitch is in pro-oestrus or early oestrus at the time of MRI would, in contrast to the three operators of the current study who did not know the stage of the oestrous cycle the bitches were in, expect to see follicles rather than corpora lutea on MRI and would therefore not make the same mistake but would correctly classify and count the structures as follicles. Given this assumption, a repeated-measures ANOVA with the difference between the sum of corpora lutea and follicles seen on MRI and their sum found on dissection as response variable, Ovary as subject (29 degrees of freedom) and Operator (2 degrees of freedom), View (2 degrees of freedom) and Phase of cycle (2 degrees of freedom) as within-group factors were done with α set at 0.05.

Pearson's correlation coefficient was determined between the number of physiological structures (follicles or corpora lutea) and the error in estimation by means of MRI.

Throughout the text, data are presented as actual counts or means with their standard deviations.

CHAPTER 5 RESULTS

5.1 Bitches

The bitches used in this study neither developed clinical signs of disease nor exhibited any signs of malfunctioning of the reproductive system for the duration of the trial and their respective oestrous cycles appeared to progress normally based on vaginoscopy and vaginal cytology. All the uteri collected by OVH appeared macroscopically normal. All bitches recovered uneventfully after OVH.

5.2 Monitoring of oestrous cycles

It is standard practice at many dog-breeding stations to daily check all bitches for signs of pro-oestrus. The kennel staff, dog handlers, and kennel cleaners are also instructed to alert the kennel nurse if there was any "spotting" (small spots of blood noticed on the cement floors of the kennels). A vasectomized male assisted the nurse in identifying bitches in pro-oestrus. All the bitches that entered the trial with the exception of Zaro (pregnant) and Mira (anoestrus) were accurately identified to be in pro-oestrus by the kennel nurse, as this was confirmed by vaginoscopy at the beginning of the trial. Vaginoscopy was performed with ease and considered a practical tool to differentiate between the various stages of the oestrous cycle and it acted as a guide in predicting the onset of dioestrus. Vaginal cytology proved useful in accurately determining the onset of cytological dioestrus. The presence of corpora lutea in all bitches established to be in the luteal phase confirmed that ovulation had indeed occurred in these bitches and that they were in dioestrus (Table 2).

5.3 Plasma progesterone concentrations

The plasma progesterone concentrations (PPC) in the bitches were mostly analogous with the phase of ovarian cycle (Table 2), except for Velvet, whose PPC was not available. The PPC for Sabrina suggests that she had probably ovulated a day or two prior to OVH, which automatically qualifies her for inclusion in the early luteal phase. In her case, the luteinising remnants of the follicles still contained substantial volumes of fluid, causing the structures to adopt a spherical, fluid-filled appearance. The structures on Sabrina's ovaries were anticipated to provide signal intensities more like those of follicles rather than those of corpora lutea and, for this reason, they were considered follicles for the purpose of this study. Sabrina was thus included in the follicular phase group.

Table 2
Summary of Plasma progesterone concentrations (PPC) and ovarian phase of the 18 bitches used in Experiments 1 and 2

Bitch	PPC (nmol L^{-1})	Phase
Xala	1.66	Follicular
Bibi	1.95	Follicular
Minnie	5.41	Follicular
Betsie	8.09	Follicular
Brogen	9.19	Follicular
Charisma	19.12	Follicular
Amigo	25.62	Follicular
Sabrina	52.28	Follicular
Kori	53.79	Early luteal
Sara	83.73	Early luteal
Velvet	not done	Early luteal
Dusty	71.52	Late luteal
Zeal	29.36	Late luteal
Zaro	10.55	Late luteal
Ellie	8.46	Late luteal
Kia	3.52	Late luteal
Rita	1.53	Late luteal
Mira	1.76	Anoestrus

5.4 Collections of the ovaries and preparation of the phantoms

The collection of the ovaries by means of OVH was uneventful. Dissection of the ovaries revealed that no follicles have ruptured.

Three phantoms, each of which contained five or six pairs of ovaries were prepared. The gel prepared easily, appeared clear, and homogenous to the naked eye.

Table 3
Numbers and types of structures found on the ovaries of bitches during dissection

			Numbers of follicles in the ovaries		Numbers of corpora lutea in the ovaries		Numbers of cysts in ovaries	
Name of bitch	Age	Phase of oestrus cycle	Left	Right	Left	Right	Left	Right
Experiment 1								
Minnie	10 m	Follicular	6	6	0	0	1 follicular	0
Brogen	14 m	Follicular	8	8	0	0	1 hilar	0
Xala	2 y	Follicular	6	11	0	0	0	0
Betsie	3 y	Follicular	9	9	0	0	2 para-ovarian	
Bibi	3 y	Follicular	4	7	0	0	0	0
Sabrina	3 y	Follicular	2	6	0	0	0	0
Kori	5 y	Early luteal	0	0	6 (one cavitated)	2	0	0
Sara	4 y	Early luteal	0	0	8	4 (one cavitated)	1 hilar	0
Velvet	3 y	Early luteal	0	0	7 (three cavitated)	4	0	0
Zaro	5 y	Late luteal	0	0	3	3	0	0
Rita	2 y	Late luteal	0	0	3	7	0	0
Zeal	9 y	Late luteal	0	0	3	3	0	3 hilar
Ellie	6 y	Late luteal	0	0	3	6	0	2 para-ovarian
Dusty	8 y	Late luteal	0	0	4	5	1 follicular; 1 hilar	1 hilar
Kia		Late luteal	0	0	5	3	0	2 follicular
Mira	2 y	Anoestrus	0	0	0	0	0	0
Experiment 2								
Charisma	3½ y	Follicular	0	0	3	5	0	1 hilar
Amigo	14 m	Follicular	0	0	3	4	0	0

5.5 Dissection of the ovaries and description of the number and types of structures

The ovaries appeared unaffected by their storage and appeared fresh, firm and without outward signs of autolysis. A slice thickness of approximately 1-2 mm could be achieved in each ovary during dissection. In case of the luteal-phase ovaries, dissections were easy and the corpora lutea in them could easily be recognised and counted (Figure 7). This was probably because the corpus luteum is a firm structure that does not collapse after it has been transected. In addition, the entire ovary could be sliced (and the slices kept in sequence) in very much the same fashion that a bread is sliced. The structures in each slice could then be serially examined carefully and the counting could be repeated if necessary. The dissection of the follicular phase ovaries was more difficult and required concentration. Due to the thin-walled, fluid-filled nature of normal follicles, they tended to collapse after they were transected (Figure 8). Follicles with thicker walls were easier to count (Figure 9). Follicles thus had to be counted as they were transected as it was difficult to repeat the counting process by working through all the collapsed, cavitated slices of ovarian tissue. Even though the count in follicular phase ovaries was more difficult and required more concentration and time, the counts were considered accurate. The cysts were considered easy to identify and classify on dissection. The uteri and ovaries of the bitches in Experiment 2 were intact and of normal size for breed. The structures on the ovaries in experiment 2 were counted as in Experiment 1.

The data regarding the number and type of structures are summarised in Table 3**.**

5.6 Evaluation of the images and counting of the structures on them

During routine MR examination in the human patient to detect pathology in a particular organ or region, the acquisition of both a T_1-weighted image and a T_2-weighted image is almost standard. This is done because some pathological conditions may be evident on the one but not on the other. In this study, however, T_1 images (MPR NS) were consistently poor and ovarian structures could not be clearly identified on them (see Figure 10 and Figure 11), hence, only one plane of the T_1.-weighted images was made and copied on laser film for record purposes.

The evaluation of the MR images proved exceedingly difficult and even impossible in some instances. On some images, no structures could be identified although significant structures were present (Figure 12). On some images, structures could be identified clearly, although, even on such images, the count in them still tended to be inaccurate, as was the opinion as to whether they represented follicles or corpora lutea, because corpora lutea and follicles appeared similar on the T_2-weigthed images (Figure 13 and Figure 14). Dissection revealed that some corpora lutea were cavitated (Table 3). Some of these corpora lutea had 2 to 3 mm thick walls and were fluid-filled. Likewise, some partially-luteinised follicles had thick walls,

which were clearly visible on dissection (Figure 9), but not on MRI. On MRI however, both the thick walled follicles and cavitated corpora lutea appeared homogenous and there was no indication that they were cavitated (fluid filled). In contrast, the ovarian cysts noticed on the ovaries were in most cases very clear by appearing more hyperintense on the images than follicles or corpora lutea.(see ovary 6 in Figure 15) This finding was unexpected, as one would expect that the follicular fluid and cystic fluid might have more properties in common than follicular fluid and luteal tissue. Yet, on MRI in this study, follicles, and early corpora lutea looked more similar than follicles and ovarian cysts (Figure 13 and Figure 14). The counts of structures on MR images are summarised in Table 4. Even without statistical analyses, casual inspection of the figures in Table 4 suggests inaccuracy of MRI as a method of counting follicles or corpora lutea when compared with the actual counts obtained during dissection of the ovaries. Table 4 suggests that follicles may have been confused with corpora lutea and that the number of corpora lutea was often underestimated. These impressions are confirmed by formal statistical analyses, as shown below.

Follicles and early corpora lutea, when imaged with the pulse sequence considered best for the capabilities of the apparatus used, did not appear different enough on the images to accurately distinguish between them (Figure 13 and Figure 14). The most common error, which was consistent among all three operators, was to count follicles as corpora lutea (Table 5, Table 6). Each of three operators mistook the mean of 6.8±2.4 follicles that occurred on the 12 ovaries from six bitches that were in the follicular phase for corpora lutea (Table 6), whereas none of the bitches actually had any corpora lutea. Less commonly, each operator counted corpora lutea as follicles: One operator stated that Sara had one (transverse and sagital views) or two (coronal view) follicles on one ovary, whereas the other two operators stated that Zeal had three follicles on one ovary (each view, except for one operator that counted no follicles on the coronal view).

Ovarian cysts were clearly seen by all operators because the cysts were generally significantly more hyperintense relative to the ovarian stroma (Figure 15). There were some ovaries however, in which follicles were recorded on MRI, which had no follicles but had cysts of 5 to 8 mm in diameter, suggesting that the operators confused cysts with follicles.

Table 4
Summary of counts of structures on MR images of ovaries in three planes by three operators

	View		
	Sagital	Coronal	Transverse
Follicular phase (6 bitches, 12 ovaries, 6.8±2.4 follicles and no corpora lutea per ovary on dissection)			
Number of follicles estimated by Operator 1	0.1±0.3	0±0	0.2±0.6
Number of follicles estimated by Operator 2	0±0	0±0	0±0
Number of follicles estimated by Operator 3	0±0	0±0	0±0
Number of corpora lutea estimated by Operator 1	7.0±3.7	6.4±3.2	5.4±2.7
Number of corpora lutea estimated by Operator 2	6.9±1.8	6.5±1.8	6.4±1.7
Number of corpora lutea estimated by Operator 3	5.6±1.6	5.8±1.7	5.3±1.6
Early luteal phase (3 bitches, 6 ovaries, 4.5±1.9 corpora lutea per ovary on dissection)			
Number of corpora lutea estimated by Operator 1	0.2±0.4	0.5±1.2	0±0
Number of corpora lutea estimated by Operator 2	3.7±1.2	3.2±1.0	3.3±0.5
Number of corpora lutea estimated by Operator 3	2.3±2.1	2.7±2.7	1.8±1.9
Late luteal phase (6 bitches, 12 ovaries, 4.3±1.8 corpora lutea per ovary on dissection)			
Number of corpora lutea estimated by Operator 1	2.3±2.6	1.4±2.5	0.9±1.9
Number of corpora lutea estimated by Operator 2	2.9±2.5	2.9±2.5	2.8±2.4
Number of corpora lutea estimated by Operator 3	2.5±2.0	2.5±2.1	2.5±2.1

None of the operators estimated the number of follicles or corpora lutea correctly in 80% or more of the bitches (Table 5). Operator 1 was not correct in any bitch, Operator 2 was correct in 2 of 15 bitches (13.3%) and Operator 3 was correct in one of 15 bitches (6.7%). The counts of Operators 1, 2 and 3 were out by one structure in one, two and four of 15 bitches (6.7%, 13.3% and 26.7%), respectively.

Table 5 suggests that all operators failed to recognise follicles on MRI, while Table 6 suggests that all operators often mistook follicles for corpora lutea on MRI.

When only bitches in the luteal phase were considered in the analysis, Operator ($P<0.01$) but not View ($P=0.14$) or Phase of cycle ($P=0.44$) had a significant effect on accuracy and there were no interactions among the factors. These results suggest that the accuracy of MRI in estimating the number of corpora lutea is similar for bitches evaluated during the early luteal phase compared to those examined during the late luteal phase.

When all phases of the oestrous cycle were included in the analysis and the difference between the sum of the number of corpora lutea and follicles on MRI and on dissection was used as indication of the accuracy of MRI, Subject (Ovary) and Operator but not View or Phase affected the accuracy of MRI, while Operator and Phase interacted with respect to accuracy. The nature of the interaction is mainly that the accuracy of Operator 1 was higher for bitches in the follicular phase compared to bitches in the luteal phase, whereas Operator 3 was more accurate with bitches in the luteal phase and the accuracy of Operator 2 appeared similar for the different phases of the oestrous cycle.

There was a weak but significant negative correlation between the numbers of follicles or corpora lutea on dissection and the error in the numbers estimated on MRI ($r=-0.19$, $P<0.01$, $n=270$ combinations among operator, plane of imaging and ovary). The numbers of follicles or corpora lutea were most often underestimated, resulting in negative errors, suggesting that the above-mentioned correlation indicates that MRI becomes less accurate as the numbers of follicles or corpora lutea on ovaries increase. This conclusion was supported by a weak but significant positive correlation between the absolute size of the error and the numbers of follicles or corpora lutea ($r=0.14$, $P<0.05$, $n=270$).

5.7 Imaging the ovarian structures in the live dogs (Experiment 2)

The sedation protocol of the live dogs using Medetomidine HCL 1mg/ml ("Dormitor", Novartis AH) at the dose of 0.05-0.08 ml kg^{-1} i.v. proved to adequately immobilise and keep the dogs perfectly still for the entire 20 minutes in the gantry.

No images suitable for evaluation could be generated in any of the two dogs scanned. The possible effects of contrast enhancement could therefore also not be evaluated. Figure 3 to Figure 6 show images obtained by a FISP T_2 sequence with an acquisition time of 20-25 seconds, which was used as a localiser of the abdomen in order to find the ovaries. This sequence has a slice thickness of 5 mm and illustrates the increase in artefacts (mainly ghost images and increased blurring caused, among others, by motion and zooming in on the ROI. These figures also illustrate that the 5-mm slice thickness does not contain enough information to provide detailed images when enlarged to view small structures.

Table 5
Each of three operators proved inaccurate in estimating the numbers of follicles or corpora lutea in the ovaries of bitches by means of magnetic resonance imaging

	Operator		
	1	2	3
Follicular phase (6 bitches, 12 ovaries, 6.8±2.4 follicles per ovary on dissection, MRI on each ovary done in 3 views)			
Number of views where MRI count was correct	0	0	0
Number of views where MRI count was out by one	0	0	0
Number of views where MRI count was out by 2 or more	36	36	36
Mean error in MRI count (n=36 views)	-6.8±2.4	-6.8±2.3	-6.8±2.3
Number of bitches in which count was correct	0	0	0
Number of bitches in which count in each ovary was out by one or less	0	0	0
Early luteal phase (3 bitches, 6 ovaries, 4.5±1.9 corpora lutea per ovary on dissection, MRI on each ovary done in 3 views)			
Number of views where MRI count was correct	0	4	1
Number of views where MRI count was out by one	0	4	4
Number of views where MRI count was out by 2 or more	18	10	13
Mean error in MRI count (n=18 views)	-4.3±1.6	-1.1±2.0	-2.2±2.0
Number of bitches in which count was correct	0	0	0
Number of bitches in which count on each ovary was out by one or less	0	0	1
Late luteal phase (6 bitches, 12 ovaries, 4.3±1.8 corpora lutea per ovary on dissection, MRI on each ovary done in 3 views)			
Number of views where MRI count was correct	0	6	5
Number of views where MRI count was out by one	8	10	15
Number of views where MRI count was out by 2 or more	28	20	16
Mean error in MRI count (n=36 views)	-2.8±2.5	-1.5±2.8	-1.8±2.0
Number of bitches in which count was correct	0	1[a]	1[a]
Number of bitches in which count in each ovary was out by one or less	0	1[b]	2[b]

[a] Bitch named Zeal assessed correctly by both operators

[b] Both operators underestimated the number or corpora lutea by one in the bitch named Dusty

Table 6
Each of three operators mistook the mean of 6.8±2.4 follicles that occurred on the 12 ovaries from 6 bitches that were in the follicular phase with corpora lutea

	Operator		
	1	2	3
Number of follicles estimated by means of MRI	0.1±0.5	0±0	0±0
Number of corpora lutea estimated by means of MRI	6.3±3.9	7.5±1.1	5.6±1.4
Number of views where number of corpora lutea on MRI count was the same as the number of follicles found on dissection[a]	3[b]	9	6
Number of views where number of corpora lutea on MRI count differed by one from the number of follicles found on dissection	11	15	12
Number of views where number of corpora lutea on MRI count differed by more than one from the number of follicles found on dissection	23	12	18
Number of bitches in which the number of corpora lutea counted on MRI was equal to the number of follicles on dissection	0	1	0
Number of bitches in which the number of corpora lutea counted on MRI differed by one from the number of follicles on dissection	1[c]	1	1[c]

[a] Three views, namely coronal, transverse and sagital, were obtained for each ovary, giving a total of 36 views

[b] For 2 views only corpora lutea and no follicles were counted whereas, for the third view, there were follicles and corpora lutea recognised and their sum was the same as the actual number of follicles on dissection

[c] Bitch named Brogen assessed correctly by both operators

CHAPTER 6 DISCUSSION

6.1 The answer to the research question

In this study, MRI did not aid in our efforts to accurately count the number of follicles or corpora lutea in the bitch. There is thus still no reliable non-invasive and repeatable method to accomplish this.

6.2 Monitoring of oestrous cycles

For the purposes of this study, it was important to collect ovaries at a specific stage in the oestrous cycle. On dissection of the ovaries, ovaries that were expected to have follicles on them did, as did the ovaries that were expected to have corpora lutea in them. Vaginoscopy and vaginal cytology was thus reliable in this study to distinguish follicular phase bitches from luteal phase bitches.

6.3 Plasma progesterone concentrations (PPC)

The PPC was used to aid in the determination of the stage of the cycle. The author speculated that an early corpus luteum and a late corpus luteum might appear different on MRI, and as a result, it might become evident that there is a correlation between the PPC and the signal intensity (SI) of the CL on MRI. Behavioural, clinical, hormonal, cytological, and physiological methods are used to classify the canine oestrous cycle into various stages (Johnston *et al.*, 2001). The physiological classification is the method used in this study. It refers to Graafian follicle development, ovulation and development of the corpora lutea. This method is analogous to structural (transition from follicle to corpus luteum) change within the ovary. It broadly divides the oestrous cycle into three stages, the follicular phase, the luteal phase, and the phase of ovarian quiescence. PPC remains at basal levels (below 1 to 2 $nmolL^{-1}$) during the early follicular phase until later on in the follicular phase when it begins to rise. This increase in PPC is related to preovulatory luteinization of follicles (Phemister *et al.*, 1973 and Concannon *et al.*, 1977). Strictly, the canine follicle is already a developing corpus luteum before ovulation. Ovulation or the approximation thereof, marks the transition from the follicular phase to luteal phase. There is no exact PPC that marks the time of ovulation and, hence, the transition from the follicular phase to luteal phase.

The PPC of the follicular phase bitches varied from 1.95 -19.12 $nmolL^{-1}$ in four of the bitches, and 52.28 nmolL-1 in Sabrina. It is not possible to state whether the structures in Sabrina's ovaries (fluid-filled developing corpora lutea shortly after ovulation) provided signal intensities more like those of follicles as anticipated or more like those of typical early-luteal-phase corpora lutea as the signal intensities of follicles and early corpora lutea were generally

very alike, rendering follicles and early corpora lutea impossible to distinguish on MRI. In the luteal phase, the PPC varied from 3.52 $nmolL^{-1}$ – 83.73 $nmolL^{-1}$. These values are analogous with the phase of the cycle.

The PPC of the luteal phase bitches confirmed the findings by Concannon *et al.* (1977) that the PPC tends to be higher in the early stages of dioestrus than in the later stages.

6.4 Collection and storage of the ovaries

It is possible to collect ovaries during OVH, leaving the structures on them intact for further examination and dissection. The ovaries were kept refrigerated at all times between collection and scanning, except when the phantoms were made. No preservatives were used as was done by Blechinger *et al.* (1988). During a previous study (Nöthling, De Cramer and Gerber, unpublished data), storage of ovaries in either glycerol or formalin discoloured and appeared to have caused shrinkage of the specimens. This shrinkage is believed to be attributable to dehydration due to the hygroscopic effects of the glycerol-saline. No macroscopically visible changes to the appearance of the ovaries were noted in the current study. As it was impossible to obtain images from the live dogs for comparison, it remains unknown whether the storage in first saline and later the phantom gel, altered their appearance on MRI. We however speculate, that an isotonic solution as normal saline would have had very little if any affect whatsoever, as the total water content of the tissue scanned is unlikely to have changed. From Figure 16 however, it is evident that a storage medium like formalin, which clearly alters the macroscopic appearance of tissues, also clearly altered the appearance on MRI and indeed for the better by making corpora lutea more hyperintense on T_1-weighted images than corpora lutea not preserved in formalin. Results from the study by Nöthling, De Cramer and Gerber (unpublished data) also indicated that storage of ovaries in glycerol may indeed have increased the SI of luteal tissue on MRI. No literature could be found on the storage of tissues for later MRI in a phantom. From the knowledge of principles of MRI, one may expect that preservation of tissue in a medium such as formalin or glycerol, which may alter the tissue's water content, might alter the magnetic properties of the tissue when scanned. One should therefore avoid storing specimens that have to undergo MRI in media that are likely to alter the water content of the specimens, but rather use an isotonic medium such as normal saline.

6.5 Preparation of the phantoms

In the current study, there were no controls to ascertain whether storage of the ovaries in the saline and phantom gel altered the properties (mainly water content) of tissues sufficiently to alter its appearance on MRI or not. This study was however not designed to elucidate potential effects of a phantom gel on MRI of tissues scanned, as these additional variables would necessitate the inclusion of much larger numbers of specimens and because Blechinger *et al.* (1988) reported no effects on either the macroscopic appearance of the tissues preserved

in his tissue-mimicking agar gel, or on the images produced by MR scanning of the same tissues. In the current study there were no macroscopically discernable signs of tissue decay, such as discolouration or shrinkage of the ovaries at the time of dissection. The specimens seemed as fresh as ovaries just harvested from a recently spayed bitch. The author speculates that lack of these changes might in part be attributable to the fact that gelatine sets quickly and therefore possibly entraps water molecules that would otherwise have moved along osmotic gradients. (The set gel is thought to have acted like a solid rather than a fluid). If the saline and or gelatine did affect the images in this study, it therefore seems reasonable to accept that it did so minimally.

Blechinger *et al.* (1988) added preservatives to his phantom gel albeit at low concentrations. In the current study, no preservatives were used as it was argued that the inclusion of another variable without control might complicate matters. Furthermore it seemed justified to assume that the lack of preservative would have had little effects on the tissues as the specimens remained refrigerated at all times except when handled. The author concludes that ordinary cooking gelatine, without any additives, works well as a phantom gel wherein tissues can be suspended for MRI.

6.6 Imaging ovarian structures in the phantoms

In this section, unless otherwise stated, all the references made to MRI, refer to T_2-weighted images.

Early on in this study, it became evident that the capabilities of the MRI technology were being strained. Indeed, the challenge appeared too great. This is so because evaluations of MRI of the first phantom firstly revealed inability to count ovarian structures and secondly revealed poor contrast between ovarian stroma and the structures in at least some ovaries (particularly late-luteal-phase corpora lutea).

In this study all the pulse sequences within the capabilities of the apparatus that met the requirements of slice intervals and slice thicknesses of 1 mm each were evaluated during the selection process. Theoretical knowledge of the principles of MRI led one to expect that the optimal pulse sequences for follicular-phase ovaries and luteal-phase ovaries would differ (T_2 versus T_1 sequence). Surprisingly, this was found not to be true. The pulse sequence that was selected as the best for the luteal-phase ovaries also happened to be the best for the follicular-phase ovaries.

Although good contrast between the ovarian stroma and both follicles and early corpora lutea was achieved on most images, the appearance of the luteal tissue in early corpora lutea and of follicular fluid, was too iso-intense (similar) on MRI to allow easy distinction between follicles and corpora lutea. The operators (all reproductive specialists and not radiologists) had, at the time of initial evaluation of the images, no sound reference as to what a typical

follicle, an early corpus luteum, or a late corpus luteum MRI should look like. The operators were at the time of evaluation also inexperienced at evaluating MRI and slow at distinguishing between T_1-and T_2-weighted images. The specialist radiologist, obviously was familiar with the different appearance of tissues and fluids on T_1- and T_2-weighted images, yet he also had difficulty in distinguishing between corpora lutea and follicles in most ovaries. Retrospectively, the operators realised that although the early corpora lutea were macroscopically identifiable as solid dense tissue masses at dissection, their appearance on MRI was similar to those of follicles, which all contained free fluid. The canine follicle starts luteinising before ovulation and the follicular fluid is replaced from the periphery inwards with luteal tissue, in the process possibly changing the free fluid from a non–complex fluid to a complex one. A complex fluid is one that is proteinaceous, possibly also containing cellular material, which leads the fluid to behave more like tissue in MRI rather than fluid. It may be that, as the follicle matures, it looses water while the protein and cellular content of the follicular fluid increases, leading to a gradual transition of the fluid from a hyperintense to a hypo intense appearance on MRI.

Although the fluid in cysts appeared physically similar to follicular fluid (on dissection), the fluid from cysts frequently but not always yielded much higher signal intensities than did follicular fluid, thereby providing images more typical of fluid-filled structures than were the images of follicles. Inspection of the results of evaluations of the MRI compared to the dissection results (Table 3) revealed that operators, in some ovaries at least, confused some of the cysts with follicles. Generally, the high SI of cysts gave them a distinctly different appearance to all surrounding structures, including follicles, corpora lutea and ovarian stroma. Not only do the cysts appear considerably more hyperintense on MRI but their borders and interface with the surrounding tissues were clear with good margin detail. Most cysts in this study were seen clearly on the images by all operators.

The contrast between the ovarian stroma and late corpora lutea, was consistently poor, which made it difficult to discern any structures at all in those ovaries. This lack of contrast was the main impediment to accurately counting late corpora lutea on MRI.

The evaluators (operators) of the images in the current study had not studied the dissection results prior to evaluating the MRI of the ovaries. This was purposely planned as prior knowledge of the numbers of structures on the ovaries may have led to operator bias.

The volume of the field of interest that is imaged has a significant bearing on the SI produced on images. From this it can be deduced that the size of the structures in this study was indeed of crucial importance. At first glance, one is led to believe that the relatively large sizes of the structures of interest in this study probably had little bearing on the poor results obtained, because the sizes of follicles and corpora lutea in this study were about 4 to 7 mm, which is

well within the resolution that the MR apparatus is capable of when using the selected pulse sequence, a 1-mm slice interval and a 1-mm slice thickness. In contrast, the ovarian stroma between the structures of interest was rarely thicker than the minimum required for resolution by the apparatus. It was paramount that the interface between structures and ovarian stroma be adequately visible on MRI, as such visibility is required before one can count the structures. The layer of ovarian stroma between neighbouring corpora lutea or neighbouring follicles was frequently thinner than 1 mm as judged with the naked eye during dissection (see Figure 7 and Figure 8). The layer of ovarian stroma between structures may often have been too thin to produce sufficient SI on MRI to allow for its proper identification. It is also possible that the volume imaged at the stromal interface might have included a part of the adjacent structure, leading to an artefact produced by partial volume averaging and further impeding the acquisition of an image with good margin contrast between the ovarian structure and stromal interface. This may seriously have hampered the differentiation of the various structures from ovarian stroma on MRI. In the cases where it was believed that a structure could be clearly seen on the images, the lack of sufficient stromal interface made it difficult to assess whether the operator counting the structures was repeatedly counting the same structure or a different structure when moving from one slice to the next. This uncertainty is thought to have been the main impediment in accurately counting the follicles and early corpora lutea, and maybe the other structure types as well.

A specialist radiologist subjectively judged that the use of a receiver coil improved the images obtained in this study. This is not unexpected, as it is in accordance with the principles of MRI. The coil brings the subject closer to the receiver and therefore likely to increase SI and reduce signal to noise ratio.

6.7 Imaging ovarian structures in the live dogs

The size of the structures under investigation necessitated the selection of a pulse sequence with the smallest possible slice interval and slice thickness that the apparatus allowed. As suggested under Section 6.6, even in a stationary phantom, the small size of the structures (particularly the layer of ovarian stroma between structures) was a serious impediment to obtaining adequate images for our purposes. Added to this in Experiment 2 was the impediment of a motion artefact brought about by the minimal breathing movements in the live dogs. The smaller the VOI, the larger the effect of movement and the more information per volume is required to obtain detailed images with clear margin definition of organs or structures.

Experiment 2 shows that using a 5-mm slice thickness, as was done when searching for the ovaries in the live dog, does not provide sufficient detail to allow resolution of the ovarian structures. In order to provide better detail, more information had to be collected by decreasing the slice interval to less than 5 mm. Pulse sequences with smaller slice thicknesses

required longer acquisition times of 5 to 7 minutes, which further increased the impact of motion artefact on the images. The net result is that images did not have enough detail to identify the ovaries or the structures in them.

The effect movement would have had in Experiment 2 was underestimated during the planning of the study. It was erroneously assumed that the ovaries would act similarly to the adrenals of dogs, which could at least be identified by Llabres-Diaz and Dennis (2003). This assumption seemed fair as the dogs would be in dorsal recumbency and not move except for normal breathing motions. Fact is that the adrenals are more fixed to the abdominal wall and are less likely to be affected by breathing movement artefact than are the more free-moving ovaries of the bitch in this study, effects of which were clearly illustrated by the exaggerated motion artefact encountered in our efforts to image the live dogs. Until it is possible to effectively negate the effect of motion, the use of MRI with very small volumes of interest to visualise small structures, such as ovaries and the structures they contain, in the abdomen of dogs will remain ineffective. A possible solution lies in the development of a gating method as is used in man for MRI of the heart, (Gladish, 2005) which is in constant motion. Gating in MRI involves the sequential and incremental acquisition of an image, taken at the same point in a cycle, e.g. breathing cycle in the case of the thorax and abdomen or heartbeat in case of cardiac examinations. In this study, the imaging time was 5-7 minutes. In future studies, ultra fast spin-echo pulse sequences may help reduce motion artefact by reducing imaging time to 3-4 minutes as it did in the study by U-King-Im *et al*, (2005).

The sedation protocol used in Experiment 2 ensured that neither of the two dogs made any movements other than the normal breathing movements. A surgical anaesthetic protocol would not have improved the results. It is concluded that medetomidine is a safe and adequate method of immobilising the dog for MRI. Medetomidine has the added advantage that it can be quickly and completely reversed using atipamizole HCL ("Antisedan," Novartis AH). This increases the safety of medetomidine as a choice of sedative. Immediately reversing medetomidine with its antagonist atipamizole, may also minimize any endocrinological effects medetomidine might have in the cyclic bitch.

6.8 Dissection of the ovaries

In Section 2.3 the significance of numbers of corpora lutea or follicles is explained. The dissection and determination of the numbers of corpora lutea in the ovaries of bitches in this study was considered easy and reliable, as it was in another (Nöthling and Volkmann, 1993). Although the follicular counts in this study are considered accurate, counting follicles was more difficult and required more concentration than counting corpora lutea. In experiments where the ovulation rates of bitches have to be determined, researchers might find it easier to use luteal counts rather than follicular counts. The identification and classification of cysts is considered easy on dissection.

6.9 Evaluation of the images and counting of the structures on them

For reasons explained in Section 6.6 none of three operators could accurately count the numbers of follicles or corpora lutea. They could also not differentiate corpora lutea from follicles on the images generated by means of MRI. Large cysts however, were easy to identify on the images.

6.10 Future research

Further studies are required to evaluate more advanced MRI techniques and apparatus. The ever increasing advances in technology will no doubt lead to the development of more advanced MRI and ultrasound equipment, and it may be of value to revisit these imaging techniques in future. In this study, it was attempted to count corpora lutea or follicles. With the exception of the effect of anovulatory follicles, the numbers of corpora lutea or follicles are equally sensitive in the measurement of bitch fertility. In future studies, more emphasis should be placed on counting the follicles as this has more prospective value.

6.11 Final conclusions

This study shows that it is not possible to accurately count the number of corpora lutea or follicles in the ovaries of the bitch using MRI techniques and apparatus commonly used in human MRI units. There still exists no reliable, non-invasive means by which the number of corpora lutea or follicles can be counted in the bitch.

CHAPTER 7 SUMMARY

LUTEAL AND FOLLICULAR COUNT IN BITCHES: ASSESSMENT BY MEANS OF MAGNETIC RESONANCE IMAGING

by

KURT GUIDO MIREILLE DE CRAMER

Promoter: Prof J O Nöthling

Section of Reproduction

Department of Production Animal Studies

Faculty of Veterinary Science

University of Pretoria

Co-promoter: Dr. V R Kammer

Radiology Department

Krugersdorp Private Hospital

Submitted in partial fulfilment of the requirements for the degree MMedVet (Reproduction)

Researchers require an accurate measurement of fertility in the bitch for the comparison of insemination methods, assessing the effects of procedures on fertility and assessing the effects of drugs on fertility. In clinical practice, a prospective measurement would enable the practitioner to select bitches with the largest numbers of follicles for breeding by artificial means or natural mating with valuable semen or studs. The ratio between the numbers of corpora lutea or follicles and litter size is a more sensitive measurement of fertility than is litter size, as the latter does not reflect the total number of oocytes that were available for fertilization. Magnetic resonance imaging (MRI) has proven to be of value in diagnostic imagery of particularly soft tissues. This is the first study that evaluated the use of MRI in canine reproduction and was done to determine whether the numbers of corpora lutea or follicles can be counted accurately by means of MRI.

The study was divided into two experiments. In Experiment 1, 16 bitches were used. Apart from one bitch that was in anoestrus, they were either in the follicular, early, or late luteal phase. Their ovaries were collected via ovariohysterectomy and placed into a phantom for MRI. The phantom was then scanned in three planes with a slice interval and slice thickness

of 1 mm, using a 1.5 Tesla SIEMENS Magnetom Symphony scanner. A circular polarized head array coil was also used around the phantom. The T_2-weigthed images were considered better than T_1-weighted images. This study showed that although the corpora lutea or follicles could be identified in most but not all images, it was not possible to accurately count the number of corpora lutea or follicles in the ovaries of bitches using MRI techniques and apparatus commonly used in human MRI units. Follicles were commonly confused with corpora lutea on the images. Although the study was not designed to detect ovarian pathology, MRI of the ovary in the phantom study, showed promise in detecting cystic ovarian disease.

In Experiment 2, it was attempted to find the ovaries, and count the structures in them, by doing MRI on two live, sedated bitches that were in the late follicular phase, whereafter the bitches were spayed and the ovarian structures counted. The effect of motion was so great that no image could be generated on which any ovary or its structures could be identified.

There still exists no reliable, non-invasive means by which the number corpora lutea or follicles can be counted in the bitch. Further studies are required to evaluate more advanced MRI techniques and apparatus.

CHAPTER 8 OPSOMMING

LUTEALE EN FOLLIKULÊRE TELLING IN TEWE: BEOORDELING DEUR MIDDEL VAN MAGNETIESE RESONANSIE BEELDING

deur

KURT GUIDO MIREILLE DE CRAMER

Promotor: Prof J O Nöthling

Afdeling Geslagskunde

Departement Produksiedierstudies

Fakulteit Veeartsenykunde

Universiteit van Pretoria

Mede-promotor: Dr. V R Kammer

Radiologie Departement

Krugersdorp Privaat Hospitaal

Voorgelê ter gedeeltelike vervulling van die vereistes vir die graad MMedvet (Reproduksie)

Navorsers benodig 'n akurate meting van vrugbaarheid in die teef vir die vergelyking van inseminasiemetodes en vir die beoordeling van die effekte van prosedures en middels op vrugbaarheid. In praktyk sou veral 'n prospektiewe meting van vrugbaarheid nuttig wees, omdat dit die klinikus in staat sal stel om daardie tewe met die grootste aantal follikels te selekteer vir teling in gevalle waar die koste van òf die semen òf dekking baie hoog is. Die verhouding tussen die aantal korpora lutea of follikels en werpselgrootte is 'n sensitiewer maatstaf van vrugbaarheid as werpselgrootte op sigself; omdat laasgenoemde nie die volledige aantal oösiete wat beskikbaar was vir bevrugting in bereken bring nie. Magnetiese resonansie beelding (MRB) is reeds bewys as 'n waardevolle tegniek vir die verkryging van diagnostiese beelde van veral sagte weefsels. Hierdie is die eerste studie wat die gebruik van MRB op die geslagstelsel van honde beoordeel en was spesifiek uitgevoer om vas te stel of die korpora lutea of follikels in die eierstokke van tewe d.m.v. MRB akkuraat getel kan word.

Die studie was verdeel in 2 eksperimente. In Eksperiment 1 was 16 tewe gebruik. Behalwe vir een teef wat in anestrus was, was hulle òf in die follikulêre fase, òf in die vroeë òf in die laat luteale fases. Hul eierstokke was versamel deur middel van ovariohistorektomie en in 'n fantoom geplaas vir MRB. Die fantoom was geskandeer in drie oriëntasies reghoekig tot mekaar, en 'n snitdikte en 'n snitinterval van 1mm is gebruik. Die MRB aparaat was 'n 1.5

Tesla SIEMENS Magnetom Symphony skandeerder. 'n Kopspoel was gebruik rondom die fantoom. Die T_2-gerigte beelde was beter as die T_1-gerigte beelde. Hierdie studie het getoon dat alhoewel die korpora lutea of follikels in die meeste beelde van die eierstokke geïdentifiseer kan word, dit nie moontlik is om hierdie strukture in die eierstokke van tewe te tel m.b.v. die apparaat wat oor die algemeen in die gemidelde privaathospitaal beskikbaar is nie. Dit was ook nie moontlik om altyd korpora lutea van follikels te onderskei nie. Alhoewel die studie nie ontwerp was om vir patologiese letsels op die eierstokke te soek nie, was die meeste ovariële siste duidelik sigbaar op die beelde in die fantoomstudie, wat daarop dui dat MRB in hierdie verband belowend mag wees.

In Eksperiment 2 is gepoog om die eierstokke in twee lewendige tewe wat laat in die follikulêre fase en onder berusting was, d.m.v. MRB op te spoor en die strukture daarin te tel, waarna 'n ovariohisterektomie op elke teef uitgevoer was en die strukture getel was. Die effek van beweging wat deur asemhaling teweeg gebring is was egter só groot dat daar geen beeld gegenereer kon word waarop 'n eierstok of sy strukture herken kon word nie.

Daar bestaan steeds geen betroubare manier, anders as disseksie van die eierstokke, om die follikels of korpora lutea indie eierstokke van tewe akkuraat te tel nie. Verdere navorsing is nodig om meer gevorderde MRB tegnieke en apparaat vir hierdie doel te evalueer.

REFERENCES

Adams, E.C. and Hertig, A.T. (1969) Studies on the human corpus luteum: Observations on the ultrastructure of development and regression of the luteal cells during the menstrual cycle. Journal of Cell Biology 41, 696-715.

Agartz, I., Saaf, I., Wahlund, L-O. and Wetterberg, L. (1987) Magnetic resonance imaging at 0.02 T in clinical practice and research. Magnetic Resonance Imaging 5, l79-187.

Aisen, A.M. (1990) Basics of MR image interpretation (prepared handout).Ann Arbor MI, University of Michigan School of Medicine.

Andersen, C.A. and Simpson, M.E. (1973) The ovary and reproductive cycle of the dog (beagle) Geron-X, INC., Los Altos, California, 290 pp. [cited by Nöthling, 1995 and Johnston et al., 2001].

Arbeiter, K. (1993) Anovulatory ovarian cycles in dogs. Journal of Reproduction and Fertility, Supplement 47, 453-456.

Atlas, S.W. (1991) Magnetic resonance imaging of the brain and spine. New York: Raven Press, 1137 pp.

Averkiou, M.A. and Hamilton, M. F. (1995) Measurements of harmonic generation in a focused finite-amplitude sound beam. Journal of the Acoustical Society of America 98 (6), 3439-3442.

Ayida, G., Chamberlain, P., Barlow, D., Koninckx, P., Golding, S. and Kennedy, S. (1997) Is routine diagnostic laparoscopy for infertility still justified? A pilot study assessing the use of hysterosalpingo-contrast sonography and magnetic resonance imaging. Human Reproduction 12 (7), 1436-1439.

Baker, P.N., Johnson, I.R., Harvey, P.R., Gowland, P.A. and Mansfield, P. (1994) A three year follow up of children imaged in utero with echo-planar magnetic resonance. American Journal of Obstetrics and Gynaecology 170, 32-33.

Blechinger, J.C., Madsen, E.L. and Frank, G.R. (1988) Tissue mimicking gelatine agar gells for use in magnetic resonance imaging phantoms. Medical Physiology 15, 629-636.

Bloch, F., Hansen, W.W. and Packard, M. (1946) The nuclear induction experiment. Physical Review 70 (7 and 8), 474-485.

Boyd, J.S., Renton, J.P., Harvey, M.J.A., Nickson, D.A., Eckersall, P.D. and Ferguson, J.M. (1993) Problems associated with ultrasonography of the canine ovary around the time of ovulation. Journal of Reproduction and Fertility, Supplement 47, 101-105.

Brasch, R.C. (1993) MRI contrast enhancement in the central nervous system: a case study approach. New York: Raven Press.

Chanalet, S., Masson, B., Boyer, L., Laffont, J. and Bruneton, J.N. (1995) Comparative studies of the tolerability of gadodiamide, dimeglumine gadopentetate and meglumine

gadoterate in MRI tests of the central nervous system. Journal de Radiologie 76(7), 4l7-421. (Abstract only).

Chang, W.P., Lang, P. and Gernant, H.K. (1994) MRI of the musculoskeletal system. Philadelphia: WB Saunders Company.

Christiaens, F., Janssenswillen, C., Van Steirteghem, A.C., Devroey, P., Verborgh, C. and Camu, F. (1998) Comparison of assisted reproductive technology performance after oocyte retrieval under general anaesthesia (propofol) versus paracervical local anaesthetic block: a case-controlled study. Human Reproduction 13(9), 2456-2460.

Christie, D.W., Bailey, J.B. and Bell, E.T. (1972) Classification of cell types in vaginal smears during the canine oestrous cycle. British Veterinary Journal 128(6), 301-310.

Concannon, P., Hansel, W. and McEntee, K. (1977) Changes in LH, progesterone and sexual behaviour associated with preovulatory luteinization in the bitch. Biology of Reproduction 17, 604-613.

Concannon, P.W., Hansel, W. and Visek, W.J. (1975) The ovarian cycle of the bitch: plasma estrogen, LH and progesterone. Biology of Reproduction 13, 112-121.

Cowell, R.L., Tyler, R.D. and Meinkoth, J.H. (1989) Diagnostic Cytology and hematology of the dog and cat. 21 American Veterinarian Publications, CA, New York, pp225-233.

Davis, L.E. Veterinary Clinical Pharmacology. Philadelphia, W. B. Saunders Co

De Michele, D.J., DiChiro, G. (1991) Grading meningiomas by positron emission tomography. In Meningiomas, p 243. Ed. Al-Mefty, New York, Raven.

Dennis, R. (1995) Magnetic Resonance Imaging: An overview of its current use in veterinary medicine. Veterinary International 7, 50-58.

Dennis, R. (1998) Magnetic resonance imaging and its applications in small animals. In Practice March, 117-124.

Desser, T.S., Jeffrey, R.B. (Jr)., Lane, M.J. and Ralls, P.W. (1999) Tissue harmonic imaging: utility in abdominal and pelvic sonography. Journal of Clinical Ultrasound 27 (3), 135-142.

Doak, R.L, Hall, A. and Dale, H.E. (1967) Longevity of spermatozoa in the reproductive tract of the bitch. Journal of Reproduction and Fertility 13, 51-58.

Dore, M.A.P. (1989) Structural aspects of luteal function and regression in the ovary of the domestic dog. Journal of Reproduction and Fertility, Supplement 39, 41-53.

Dow, C. (1960) Ovarian abnormalities in the bitch. Journal of Comparative Pathology 70, 59-69.

Duroux, M. (1995) Overview of MRI contrast agents. Radiologe 35, 247-248.

England, G.C.W. and Allen, W.E. (1990) Studies on canine pregnancy using B-mode ultrasound: Diagnosis of early pregnancy and the number of conceptuses. Journal of Small Animal Practice 31, 321-323.

England, G.C.W. and Yeager, A.E. (1993) Ultrasonographic appearance of the ovary and uterus of the bitch during oestrus, ovulation and early pregnancy. Journal of Reproduction and Fertility, Supplement 47, 107-117.

Farstad, W. and Andersen Berg, K. (1989) Factors influencing the success rate of artificial insemination with frozen semen in the dog. Journal of Reproduction and Fertility, Supplement 39, 289-292.

Fayrer-Hosken, R.A., Durham, D.H., Allen, S., Miller-Liebl, D.M. and Caudle, A B. (1992) Follicular cystic ovaries and cystic endometrial hyperplasia in a bitch. Journal of the American Veterinary Medical Association 201 (1), 107-108.

Ferguson, J.M., Renton, J.P., Farstad, W. and Douglas, T.A. (1989) Insemination of beagle bitches with frozen semen. Journal of Reproduction and Fertility, Supplement 39, 293-298.

Foster, M.A. (1984) Magnetic resonance in medicine and biology. Oxford: Pergamon Press. 1-27.

Friedman, B.R., Jones, J.P., Chaves-Munoz, G., Christoper, R. and Merritt, B. (1989) Principles of MRI. New York, McGraw-Hill, Incorporated.

Frye, R.E., Ascher, S.M. and Thomasson, D. (2000) MR Hysterosalpingography: protocol development and refinement for simulating normal and abnormal fallopian tube patency-feasibility study with a phantom. Radiology 214, 107-112.

Fujii, M., Otoi, T., Murakami, M., Tanaka, M., Une, S. and Suzuki, T. (2000) The quality and maturation of bitch oocytes recovered from ovaries by the slicing method. Journal Veterinary Medical Science 62(3), 305-307.

General Electric (1984) N.M.R:A Perspective on imaging. Milwaukee: General Electric Medical Company., Medical Systems Group.

Gianfelice, D., Khiat, A., Amara, M., Belblidia, A. and Boulanger, Y. (2003) MR imaging-guided focused ultrasound surgery of breast cancer: correlation of dynamic contrast-enhanced MRI with histopathologic findings. Breast Cancer Research and treatment 82(2), 93-101. (Abstract only).

Gladish, G.W., (2005) Advances in cardiac magnetic resonance imaging and computed tomography.Expert Review of Cardiovascular Therapy 3(2), 309-320.

Hann, L.E., Bach, A.M., Cramer, L.D., Siegel, D., Yoo, H. and Garcia, R. (1999) Hepatic sonography: comparison of tissue harmonic and standard sonography techniques. American Journal of Roentgenology 173(1), 201-206.

Harbaugh, R.E., Schlusselberg, D.S., Jeffery, R. Hayden, S., Laurence, D. Cromwell, M.D. and Pluta, D. (1992) Three-dimensional computerized tomography angiography in the diagnosis of cerebrovascular disease. Journal of Neurosurgery 76, 408-414.

Hayer, P., Günzel-Apel A.R., Lüerssen, D. and Hoppen, H.O. (1993) Ultrasonographic monitoring of follicular development, ovulation and the early luteal phase in the bitch. Journal of Reproduction and Fertility, Supplement 47, 93-l00.

Hendrick, R.E. (1988) Image contrast and noise. In Magnetic resonance imaging, pp66-83 Eds. Stark, D.D. and Bradley, W.G. St Louis: CV Mosby Company.

Hohl, C., Schmidt, T., Haage, P., Honnef, D., Blaum, M., Staatz, G. and Guenther, R.W. (2004) Phase-inversion tissue harmonic imaging compared with conventional B-mode ultrasound in the evaluation of pancreatic lesions. European Journal of Radiology 14, 1109-1117.

Holland, G.N., Hawkes, R.C. and Moore, W.S. (1980) Nuclear magnetic resonance (NMR) tomography of the brain: coronal and sagittal sections. Journal of Computer Assisted Tomography 4(4), 429-433.

Holst, P.A. and Phemister, R.D. (1971) The prenatal development of the dog: preimplantation events. Biology of Reproduction 5, 194-206.

Holst, P.A. and Phemister, R.D. (1974) Onset of diestrus in the beagle bitch: definition and significance. American Journal of Veterinary Research 35, 401-406.

Holst, P.A. and Phemister, R.D. (1975) Temporal Sequence of Events in the Estrous Cycle of the Bitch. American Journal of Veterinary Research 36, 705-706.

Howard, J.G., Barone, M.A., Donoghue, A.M. and Wildt, D.E. (1992) The effect of pre-ovulatory anaesthesia on ovulation in laparoscopically inseminated domestic cats. Journal of Reproduction and Fertility 96, 175-186.

Hubbard, A.M., States, L.J. (2001) Fetal magnetic resonance imaging. Topics in magnetic resonance imaging 12(2):93-103. (Abstract only).

Inoue-Minakuchi, M., Kuboki, T., Maekawa, K., Yanagi, Y., Inoue, E., Wakasa, T., Kishi, K., Yatani, H. and Clark, G.T. (2002) Signal intensity changes in T2-weighted MR image of the human trapezius muscle upon cold pressor stimulation. Dentomaxillofacial Radiology 31(6), 350-354. (Abstract only).

Jeffcoate, I.A. and Lindsay, F.E.F. (1989) Ovulation detection and timing of insemination based on hormone concentrations, vaginal cytology and the endoscopic appearance of the vagina in domestic bitches. Journal of Reproduction and Fertility, Supplement 39, 277-287.

Johnston, S.D., Root Kustritz, M.V. and Olson, P.N.S. (2001) Canine and Feline Theriogenology. W.B. Saunders Company Philadelphia, 592 pp.

Kähn, W. Leidl, W. and Rienmüller, R. (1989) Die kammerung des rinderuterus während der frühgravidität. Journal of the Veterinary Medical Association 36, 641-652. (Abstract only).

Kärkkäinen, M. (1995) Low- and high-field strength magnetic resonance imaging to evaluate the brain in one normal dog and two dogs with central nervous system disease. Veterinary Radiology & Ultrasound 36 (6), 528-532.

Kean, D. and Smith, M. (1986) Magnetic resonance imaging: principles and applications. Baltimore: Williams & Wilkins. .

Kornegay, J.N. (1990) Imaging brain neoplasms. Computed tomography and magnetic resonance imaging. Veterinary Medical Report 2, 372-390.

Kraemer, D.C., Flow, B.L., Schriver, M.D., Kinney, G.M. and Pennycook, J.W. (1979) Embryo transfer in the nonhuman primate, feline and canine. Theriogenology 11 (1), 51-62.

Kraemer, D.C., Kinney, G.M. and Schriver, M.D. (1980) Embryo transfer in the domestic canine and feline. Archives of Andrology 5, 111-113.

Kunz, G., Beil, D., Huppert, P. and Leyendecker, G. (2000) Structural abnormalities of the uterine wall in women with endometriosis and infertility visualized by vaginal sonography and magnetic resonance imaging. Human Reproduction 15(1), 76-82. (Abstract only).

Kuriashkin, I.V. and Losonsky, J.M. (2000) Contrast enhancement in magnetic resonance imaging using intravenous paramagnetic contrast media: a review. Veterinary Radiology & ultrasound 41(1), 4-7.

Kuroiwa, M., Hatakeyama, S.I., Suzuki, N., Murai, H., Toki, F. and Tsuchida, Y. (2004) Neonatal ovarian cysts: management with reference to magnetic resonance imaging. Asian Journal of Surgery 27(1), 43-48. (Abstract only).

Linde-Forsberg, C. and Forsberg, M. (1989) Fertility in dogs in relation to semen quality and the time and site of insemination with fresh and frozen semen. Journal of Reproduction and Fertility, Supplement 39, 299-310.

Lindsay, F.E.F. (1983) The normal endoscopic appearance of the caudal reproductive tract of the cyclic and non-cyclic bitch: post-uterine endoscopy. Journal of Small Animal Practice 24, 1-15.

Lindsay, F.E.F., Jeffcoate, I.A. and Concannon, P.W. (1988) Vaginoscopy and the fertile period in the bitch. 11th International Congress on Animal Reproduction an Artificial Insemination, Dublin 4, 565. [cited by Nöthling,1995].

Llabres-Diaz, F.J. and Dennis, R. (2003) Magnetic resonance imaging of the presumed normal canine adrenal glands. Veterinary Radiology & Ultrasound 44(1), 5-19. (Abstract only).

Lyngset, A. and Lyngset, 0. (1970) Kullstørrelse hos hund. Litter size in the dog. Nordisk Veterinaer Medicin 22, 186-191. [cited by Nöthling,1995].

MacKenzie, W.F. and Casey, H.W. (1975) Animal model: endometriosis in Rhesus monkeys. American Journal of Pathology 80 (2), 341-344.

Mandigers, P.J., Ubbink, G.J., Vanden Broek, J. and Bouw, J. (1994) Relationship between litter size and other reproductive traits in the Dutch Kooiker dog. Veterinary Quarterly 16(4), 229-232.

Margulis, A.R. and Fischer, M.R. (1985) Present clinical status of magnetic resonance imaging. Magnetic Resonance in Medicine 2, 309-327

Marti-Bonmati, L., Vega, T., Benito, C., Munoz, A., Niewel, M., Menor, F., Meurer, K. and Encina, J.L. (2000) Safety and efficacy of Omniscan (gadodiamide injection) at 0.1mmol/kg for MRI in infants younger than 6 months of age: phase 111 open multicenter study. Investigative radiology. 35(2), 141-147. (Abstract only).

Martinuk, S.D., Chizen, D.R. and Pierson, R.A. (1992) Ultrasonographic morphology of the human preovulatory follicle wall prior to ovulation. Clinical Anatomy 5, 1-14.

McEntee,K. (1990) Cysts in and around the ovary. In Reproductive Pathology of Domestic Mammals. San Diego, Academic Press, pp 52-68.

Miller, D.M., McCrory, J.S. and Anderson, W.I. (1983) Polycystic ovarian tissue in a spayed bitch. Modern veterinary practice 64, 749.

Miramontes-Vidal, A.C. (1987) Effect of season on the oestrous cycle in stray bitches in Mexico City. Veterinaria Mexico 18, 165. (Abstract only). [cited by Nöthling, 1995].

Miyabayashi, T., Smith, M. and Tsuruno, Y. (2000) Comparison of fast spin echo and conventional spin-echo magnetic resonance spinal imaging techniques in four normal dogs. Veterinary Radiology & Ultrasound 41(4), 308-312.

Moore, M.P., Bagley, R.S., Harrington, M.L. and Gavin, P.R. (l996) Intracranial tumours. Veterinary Clinics of North America: Small Animal Practice 26(4), 759-777.

Moss, A.A. (1983) NMR intervensional radiology and diagnostic imaging modalities, San Francisco: UCSF Printing Department.

Nemzek, J.A., Homco, L.D., Wheaton, LG. and German, G.L. (1992) Cystic ovaries and hyperestrogenism in a canine female pseudohermaphrodite. Journal of the American Animal Hospital Association 28, 402-406.

Nöthling, J.O. and Volkmann, D.H. (1993) Effect of addition of autologous prostatic fluid on the fertility of frozen-thawed dog semen after intravaginal insemination. Journal of Reproduction and Fertility, Supplement 47,329-333.

Nöthling, J.O. Gerber, D. and Shuttleworth, R. (2000) Effect of sperm number and addition of prostatic fluid on fertility results after vaginal insemination of frozen-thawed dog semen. Reproduction in Domestic Animals, Supplement 6, 71.

Nöthling, J.O. (1995) Effect of the addition of autologous prostatic fluid on the fertility of frozen-thawed dog semen after intravaginal insemination. MMedVet thesis, University of Pretoria RSA, 140 pp.

Olson, P.N., Thrall, M.A., Wykes, P.M., Husted, P.W., Nett, T.M. and Sawyer, H.R. (1984) Vaginal cytology. Part I. A useful tool for staging the canine oestrous cycle. The compendium of continuing education 6 (4), 288-297.

Pavlicek, W., Modic, M. and Weinstein, M. (1984) Pulse sequence and significance. RadioGraphics (Special Edition) 4, 49-65.

Phemister, R.D., Holst, P.A., Spáno, J.S. and Hopwood, M.L. (1973) Time of ovulation in the beagle bitch. Biology of Reproduction 8, 74-82.

Poffenbarger, E.M. and Feeney, D.A. (1986) Use of gray-scale ultrasonography in the diagnosis of reproductive disease in the bitch: 18 cases (1981-1984). Journal of the American Veterinary Medical Association 189 (1), 90-95.

Porat, S., Agid, R., Elchalal, U., Ezra, Y., Gomori, J.M. and Nadjari, M. (2002) Magnetic resonance imaging as a prenatal diagnostic tool supplementary to ultrasound in diagnosing fetal and gestational abnormalities. Harefuah 141(4), 329-334, 412, 411. (Abstract only).

Purcell, E.M., Torrey, H.C. and Pound, R.V. (1946) Resonance absorption by nuclear magnetic moments in a solid. Physical Review 69, 37-38.

Pykett, I.L., Newhouse, J.H., Buonanno, F.S., Brady, T.J., Goldman, M.R., Kistler, J.P. and Pohost, G.M. (1982) Principles of nuclear magnetic resonance imaging. Radiology 143, 157-168.

Renton, J.P., Boyd, J.S., Eckersall, P.D., Ferguson, J.M., Harvey, M.J.A., Mullaney, J. and Perry, B. (1991) Ovulation, fertilization and early embryonic development in the bitch (Canis familiaris). Journal of Reproduction and Fertility 93, 221-231.

Rinck, P.A. (1993) Magnetic resonance in medicine. The basic textbook of the European magnetic resonance forum. 3rd. edition, Oxford: Blackwell Scientific Publications, 241pp.

Robert, Y., Launay, S., Mestdagh, P., Moisan, S., Boyer, C., Rocourt, N. and Cosson, M. (2002) MRI in Gynaecology. Journal de gyécologie, obstétrique et biologie de la reproduction 31(5), 417-439. (Abstract only).

Rosenblatt, M.A., Bradford, C.N., Bodian, C.A. and Grunfeld, L. (1997) The effect of a propofol-based sedation technique on cumulative embryo scores, clinical pregnancy rates, and implantation rates in patients undergoing emryo transfers with donor oocytes. Journal of Clinical Anesthesia 9, 614-617.

Rowley, J. (1980) Cystic ovary in a dog: a case report. Veterinary Medicine / Small Animal Clinician 75, 1888.

Runge, V.M. and Wells, J.W. (l995) Update: safety, new applications, new MR agents. Topics in Magnetic Resonance Imaging 7(3), 18l-l95. (Abstract only).

Runge, V.M. (2001) Safety of magnetic resonance contrast media. Topics in Magnetic Resonance Imaging 12(4), 309-314. (Abstract only).

Sakamoto, H., Kirihara, H., Fujiki, M., Miura, N and Misumi, K. (1997) The effects of medetomidine on maternal and fetal cardiovascular and pulmonary function, intrauterine pressure and uterine blood flow in pregnant goats. Experimental Animals 46(1), 67-73. (Abstract only).

Santiago-Moreno, J., González-Bulnes, A., Gómez-Brunet, A., Cocero, M.J., del Campo, A., García-García, R. and López-Sebastián, A. (2001) Procedure for successful interspecific embryo transfer from mouflon (Ovis gmelini musimon) to Spanish Merino Sheep (Ovis aries). Journal of Zoo and Wildlife Medicine 32(3), 336-341.

Sarty, G.E., Adams, G.P. and Pierson, R.A. (2000) Three-dimensional magnetic resonance imaging for the study of ovarian function in a bovine in vitro model. Journal of Reproduction and Fertility 119, 69-75.

Schutte, A.P. (1967) Canine vaginal cytology − I Technique and cytological morphology. Journal of Small Animal Practice 8, 301-306.

Scudamore, C.L., Robinson, J.J. and Aitken, R.P. (1991) The effect of timing of laparoscopic insemination in superovulated ewes, with or without sedation, on the recovery of embryos, their stage of development and subsequent viability. Theriogenology 35 (5), 907-914.

Sepponen, R.E., Sipponen, J.T. and Sivula, A. (1985) Low field (0.02T) nuclear magnetic resonance imaging of the brain. Journal of Computer Assisted Tomography 9(2), 237-241.

Shapiro, R.S., Wagreich, J., Parsons, R.B., Stancato-Pasik, A., Yeh, H.G. and Lao, R. (1998) Tissue harmonic imaging sonography: evaluation of image quality compared with conventional sonography. AJR American Journal of Roentgenology 171(5), 19O3-1906.(Abstract only).

Shores, A. (1993) Magnetic resonance imaging. Veterinary Clinics of North America: Small animal practice 23(2), 437-460.

Sia Kho, E., Grifo, J., Liermann, A., Mills, A. and Rosenwaks, Z. (1993) Comparison of pregnancy rates between propofol and midazolam in IVF-vaginal retrieval of oocytes. Anesthesiology 79, Supplement 3A. (Abstract only).

Stark, D.D. and Bradley,W.G.(Jr) (1992) Magnetic resonance imaging. St Louis: Mosby year book 3 rd. edition, 2520 pp.

Steel, R.G.D. and Torrie, J.H. (1980) Principles and procedures of statistics. A biometrical approach. Second Edition. McGraw-Hill, Singapore, 633 pp.

Swanson, D.P. (1990) Pharmaceuticals in medical imaging. New York: Macmillan Publishing Company.

Takahashi, S.M. Murakami, T. Narumi, T. Kurachi, H. Tsuda, K. Kim, T. Tomoda, K. Nakamura, H. and Murata, Y. (1998) MRI appearance of ruptured corpus luteum. Radiation Medicine 16, 487-489.

Tedor, J.B. and Reif, J.S. (1978) Natal patterns among registered dogs in the United States. Journal of the American Veterinary Medical Association 172(10), 1179-1185.

Telfer, E. and Gosden, R.G. (1987) A quantitative cytological study of polyovular follicles in mammalian ovaries with particular reference to the domestic bitch (*Canis familiaris*). Journal of Reproduction and Fertility 81, 137-147.

Thomson, C.E., Kornegay, J.N., Burn, R.A., Drayer, B.P., Hadley, D.M., Levesque, D.C., Gainsburg, L.A., Lane, S.B., Sharp, N.J.H., and Wheeler, S.J. (1993) Magnetic resonance imaging −a general overview of principles and examples in veterinary neurodiagnosis. MRI − principles and neurodiagnosis 34(1), 2-17.

Tresley, R.M., Stone, L.A., Fields, N., Maloni, H., McFarland, H. and Frank, J.A. (1997) Clinical safety of serial monthly administrations of gadopentetate dimeglumine in patients with multiple sclerosis: implications for natural history and early-phase treatment trials. Neurology 48(4), 832-835.

Tsutsui, T. (1975) Studies on the physiology of reproduction in the dog. V. On cleavage and transport of fertilized ova in the oviduct. Japanese Journal of Animal Reproduction 21, 70-75 [cited by Tsutsui, 1989 and Nöthling, 1995].

Tsutsui, T. (1989) Gamete physiology and timing of ovulation and fertilization in dogs. Journal of Reproduction and Fertility, Supplement 39, 269-275.

Tsutsui, T., Hori, T. and Kawakami, E. (2001) Intratubal transplantation of early canine embryos. Journal of Reproduction and Fertility, Supplement 57, 309-314.

Tsutsui, T., Kawakami, E., Murao, I. and Ogasa, A. (1989b) Transport of spermatozoa in the reproductive tract of the bitch: observations through uterine fistula. Japanese Journal of Veterinary Science 51, 560-565.

Tsutsui, T., Shimizu, T., Ohara, N., Shiba, Y., Hironaka, T., Orima, H. and Ogasa, A. (1989a) Relationship between the number of sperms and the rate of implantation in bitches inseminated into unilateral uterine horn. Japanese Journal of Veterinary Science 51, 257-263.

Tsutsui, T., Tezuka, T., Shimizu, T., Murao, I., Kawakai, E. and Ogasa, A. (1988) Artificial insemination with Fresh Semen in Beagle Bitches. Japanese Journal of Veterinary Science 50(1), 193-198.

U-King-Im, J.M., Trivedi, R.A., Graves, M.J., Harkness, K., Eales, H., Joubert, I., Koo, B., Antoun, N., Warburton, E.A., Gillard, J.H. and Baron, J.C. (2005) Utility of an ultrafast magnetic resonance imaging protocol in recent and semi-recent strokes. Journal of Neurology, Neurosurgery, and Psychiatry 76(7), 1002-1005.

Valk, J., MacLean, C. and Algra, P.R. (l985) Basic Principles of Nuclear Magnetic Resonance Imaging. Amsterdam: Elsevier, 11-52.

Villafana, T. (1988) Fundamental physics of magnetic resonance imaging. Radiology Clinics of North America 26, 701-715. (Abstract only).

Vincent, R.D., Syrop, C.H., Van Voorhis, B.J., Chestnut, D.H., Sparks, A.E., McGrath,J.M., Choi, W.W., Bates, J.N. and Penning, D.H. (1995) An evaluation of the effect of anaesthetic technique on reproductive success after laparoscopic pronuclear stage transfer: Propofol/Nitrous Oxide versus Isoflurane/Nitrous Oxide. Anesthesiology 82(2), 352-358.

Virolainen, H., Visuri, T. and Kuusela,T. (1993) Acute dislocation of the patella: MR findings. Radiology 189, 243-246.

Wallace, S.S., Mahaffey, M.B., Miller, D.M., Thompson, F.N. and Chakraborty, P.K. (1992) Ultrasonographic appearance of the ovaries of dogs during the follicular and luteal phases of the estrous cycle. American Journal of Veterinary Research 53(2), 209-215.

Waluch,V and Dyck,P.(1990) Magnetic resonance imaging of posterior fossa masses. In Neurosurgery update1 pp.30-46. Ed Wilkins R.H. and Rengachary S.S. New York McGraw-Hill.

Waterton, J.C., Miller, D., Morrell, J.S.W., Dukes, M., West, C.D. and Wadsworth P.F. (1992) A case of endometriosis in the macaque diagnosed by nuclear magnetic resonance imaging. Laboratory Animals 26, 59-64.

Wehrli, F.W. (1986) Signal to noise and contrast in MR imaging. In NMR in medicine, the instrumentation and clinical applications. Eds Thomas, S.R. and Dixon, R.L. American Association of Physicists in Medicine. Medical Physics, Monograph 14.

Wildt, D.E., Chakraborty, P.K., Panko, W.B. and Seager, S.W.J. (1978) Relationship of reproductive behavior, serum luteinizing hormone and time of ovulation in the bitch. Biology of Reproduction 18, 561-570.

Wildt, D.E., Levinson, C.J. and Seager, S.W.J. (1977) Laparoscopic exposure and sequential observation of the ovary of the cycling bitch. Anatomical Record 189, 443-450.

Wright, P.J. (1991) Practical aspects of the estimation of the time of ovulation and of insemination in the bitch. Australian Veterinary Journal 68, 10-13. (Abstract only).

Yeager, A.E and Concannon, P.W. (1990) Association between the preovulatory luteinizing hormone surge and the early ultrasonographic detection of pregnancy and fetal heartbeats in beagle dogs. Theriogenology 34, 655-665.

APPENDIX

Figure 1: Two prepared phantoms showing ovaries imbedded in gelatine (the arrows indicate imbedded gelatine capsules used for orientation)

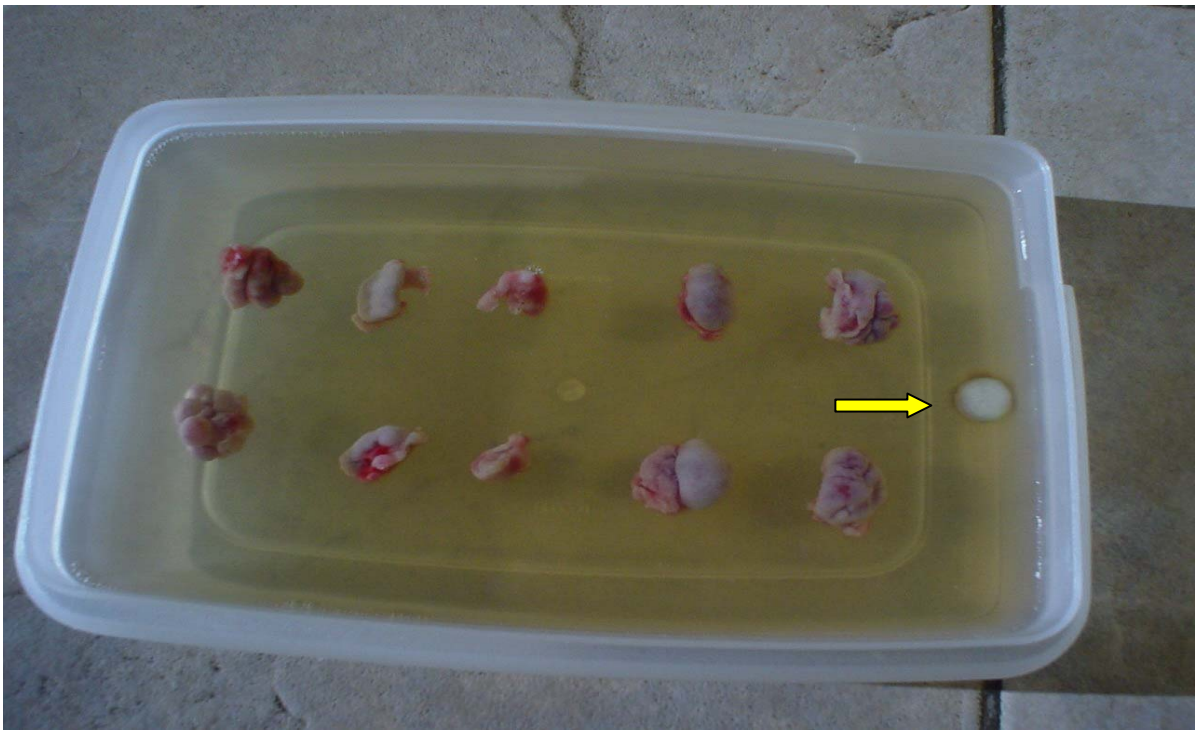

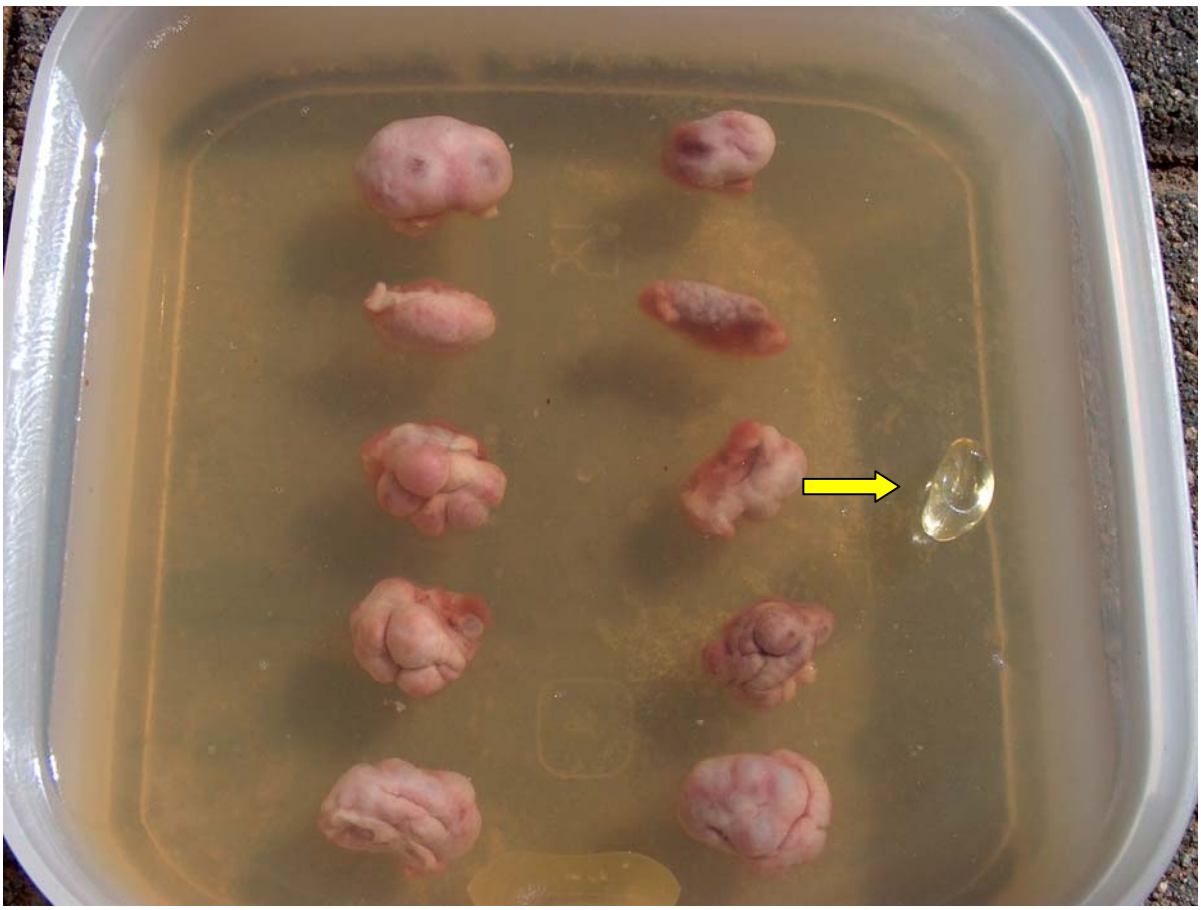

Figure 2: Magnetic resonance image of homogenous gel surrounding an ovary (the arrow points at the division line formed by the contact of the two layers of gel used during preparation)

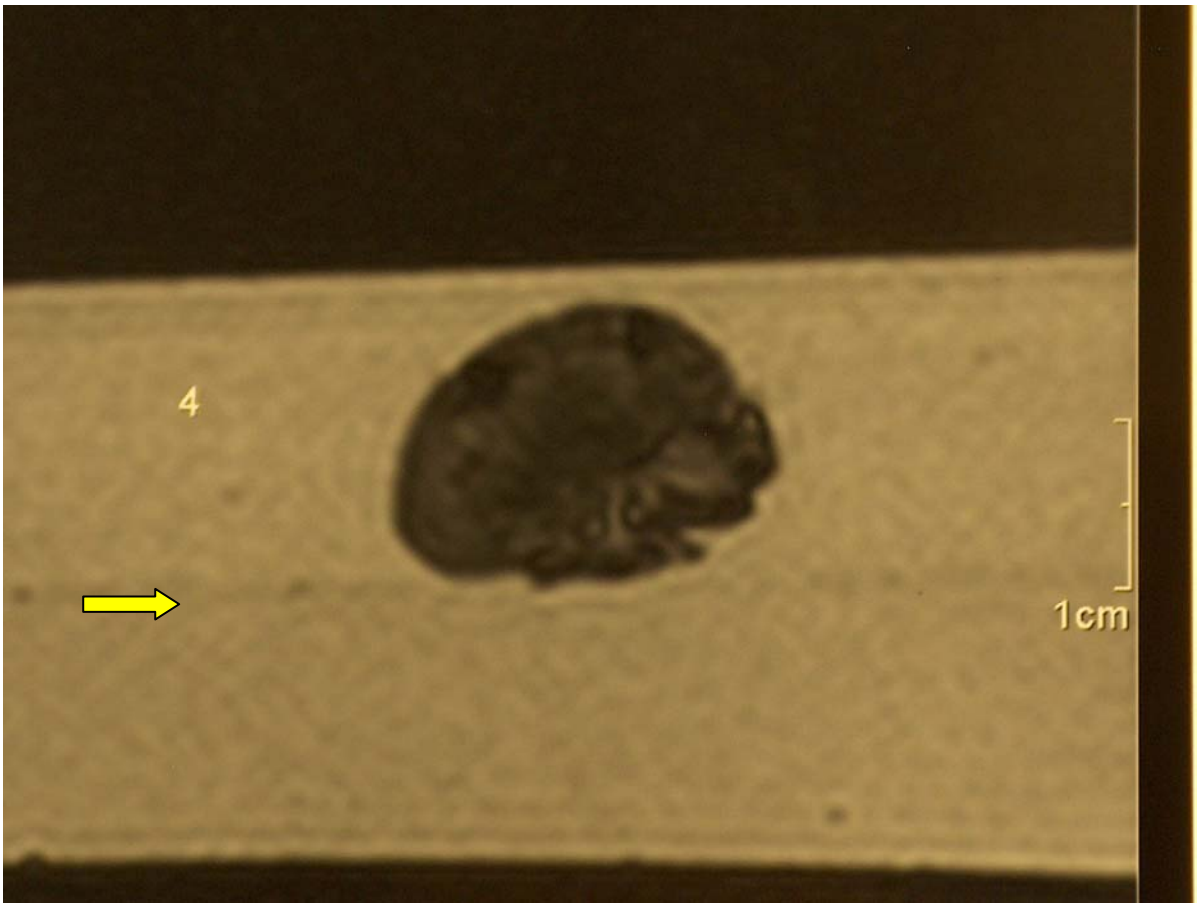

Figure 3: MR image obtained with the FISP localiser in a live dog: This low-zoom image clearly shows the kidneys. The yellow arrow clearly shows the cortico-medulary junction of the kidney. The white arrow indicates the transverse plane through which Figures 5 and 6 were obtained.

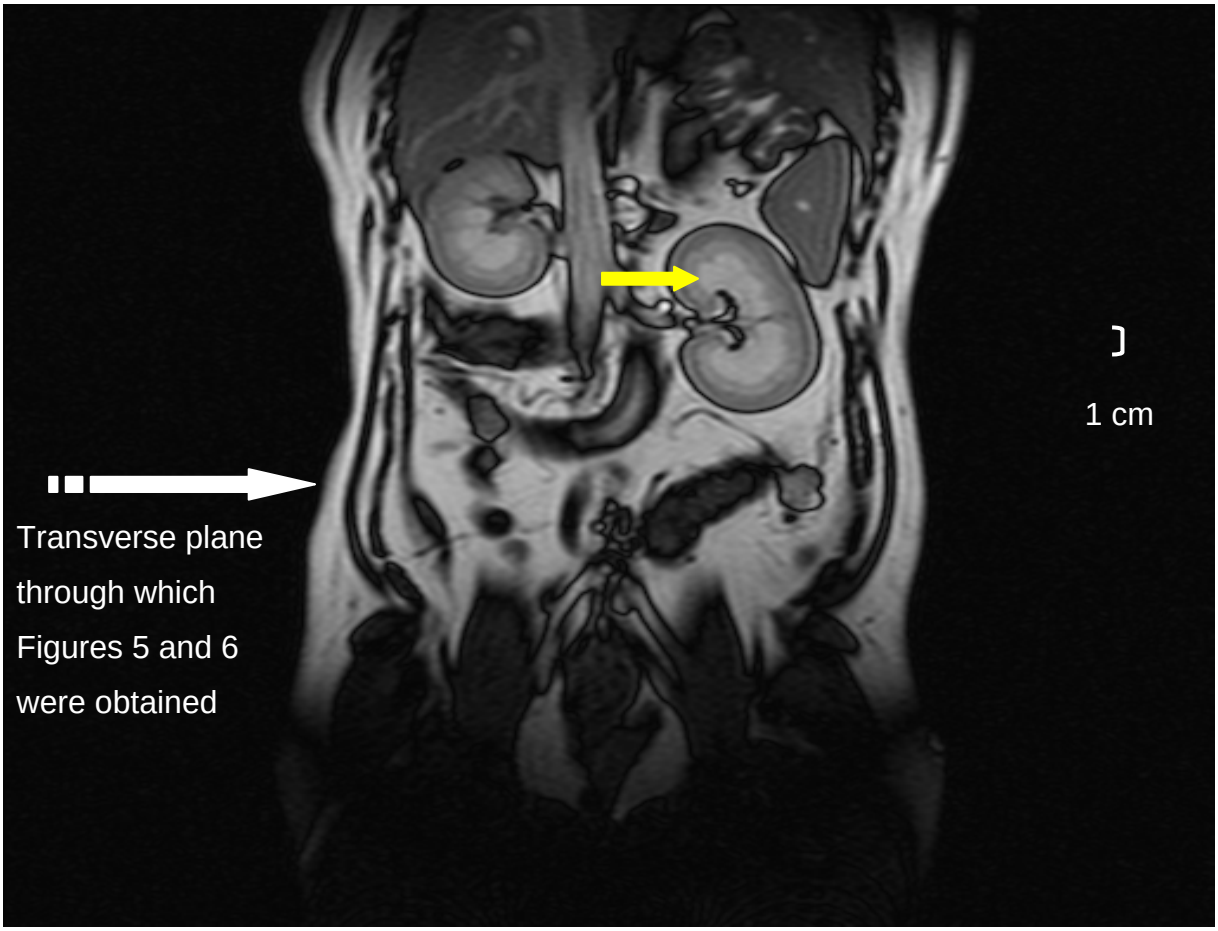

Figure 4: MRI image obtained in the same way Fig 3, but zoomed in. This image clearly shows loss of margin details (white arrows), if compared to Fig 3. The general loss of detail (blurring) is clearly seen in the kidney. In this image, the kidney appears more homogenous and the cortico-medulary junction is no longer discernable as it is in Fig 3.The yellow arrow points towards a structure caudal to the kidney, which is suspected to be the ovary.

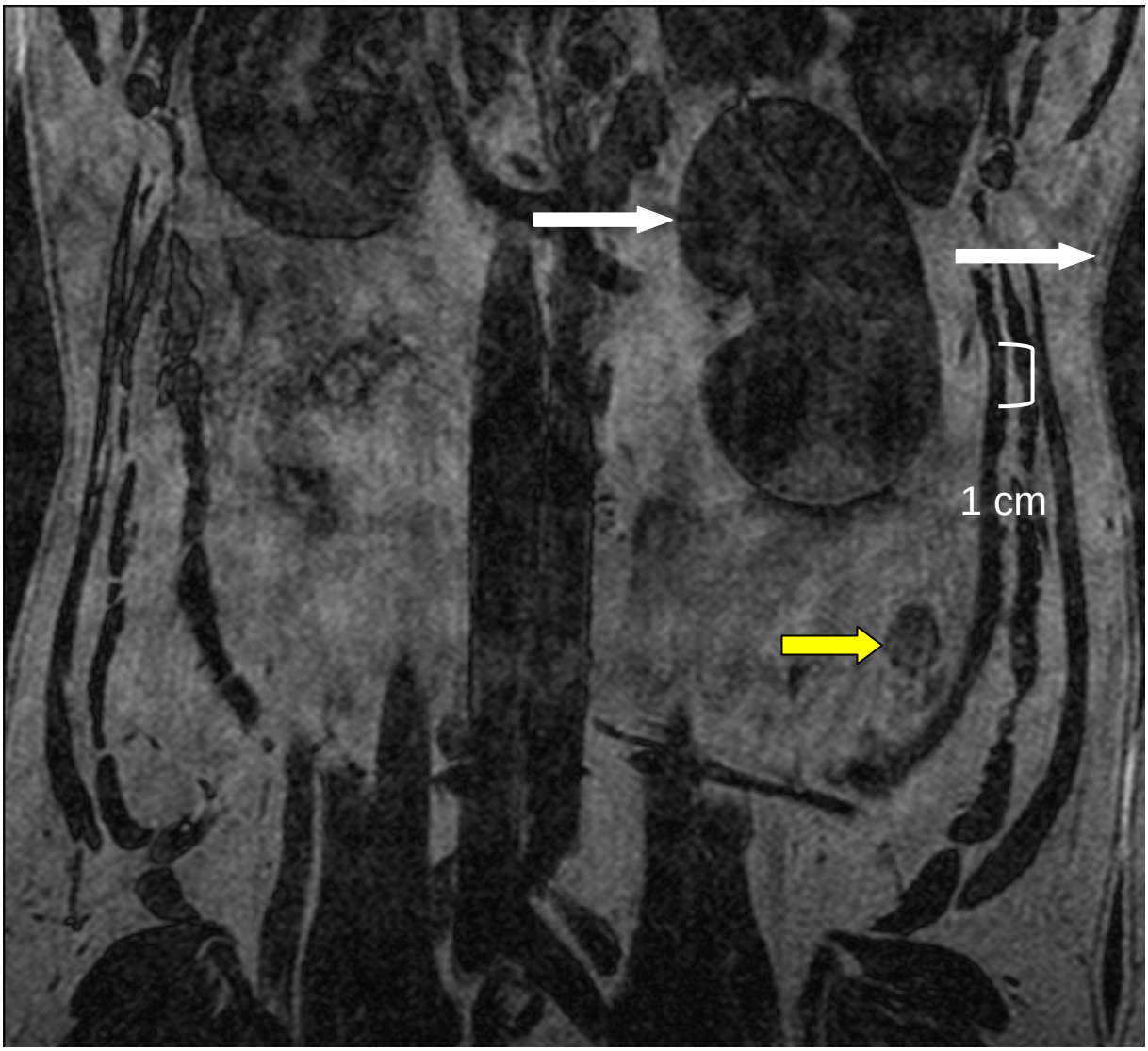

Figure 5: Transverse MR image obtained with the FISP localiser through a transverse plain caudal to the kidneys as indicated in Fig 3. Note that the image is void of detail (blurred) and that no abdominal organs are discernable, particularly in the ventral abdominal area (Yellow arrow). Note that the ghost images (partially brought about by motion) are clearly visible in the dorsal and ventral aspects (White arrows) and almost absent in the lateral aspect of the dog. This is so as most movement, whilst breathing, is believed to have been in this direction.

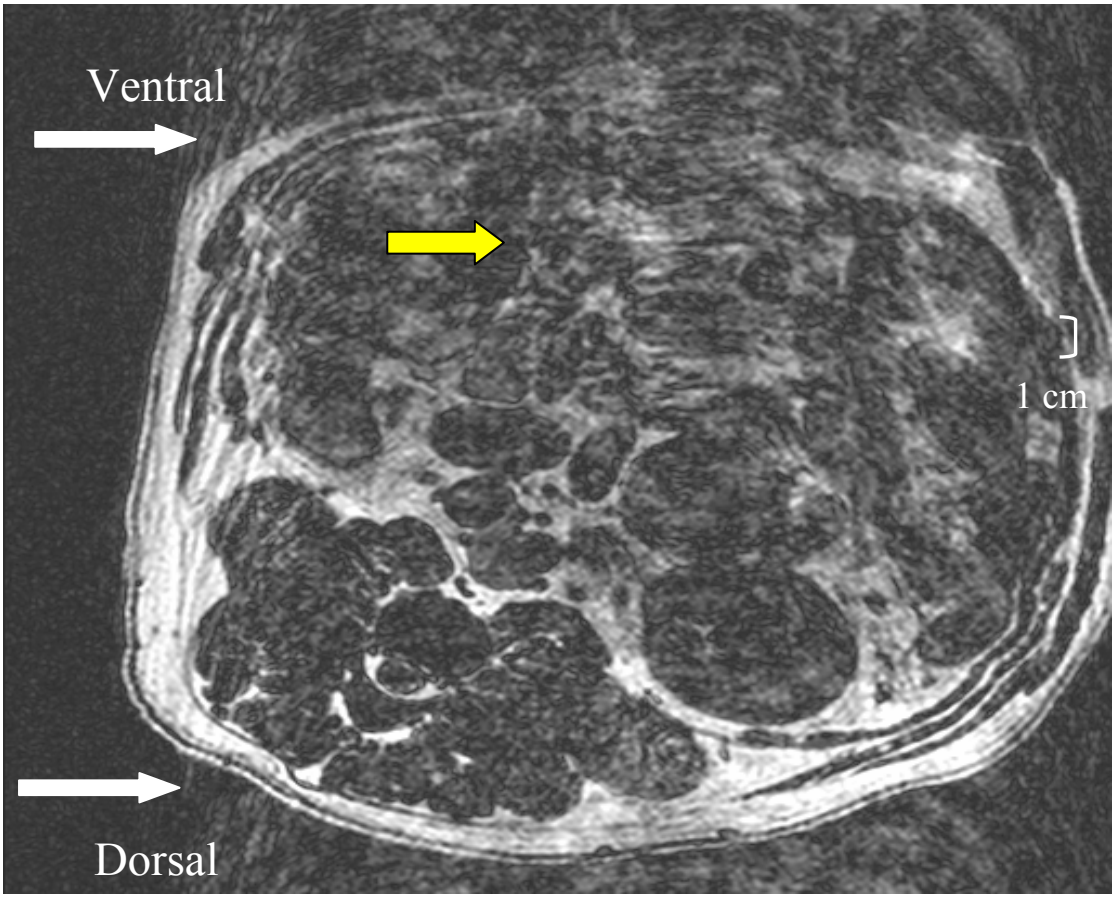

Figure 6: Transverse MR image obtained through a plain caudal to the kidney, as shown in Fig. 3, but zoomed in substantially. This image clearly shows total loss of all detail with no discernable anatomy or structures whatsoever.

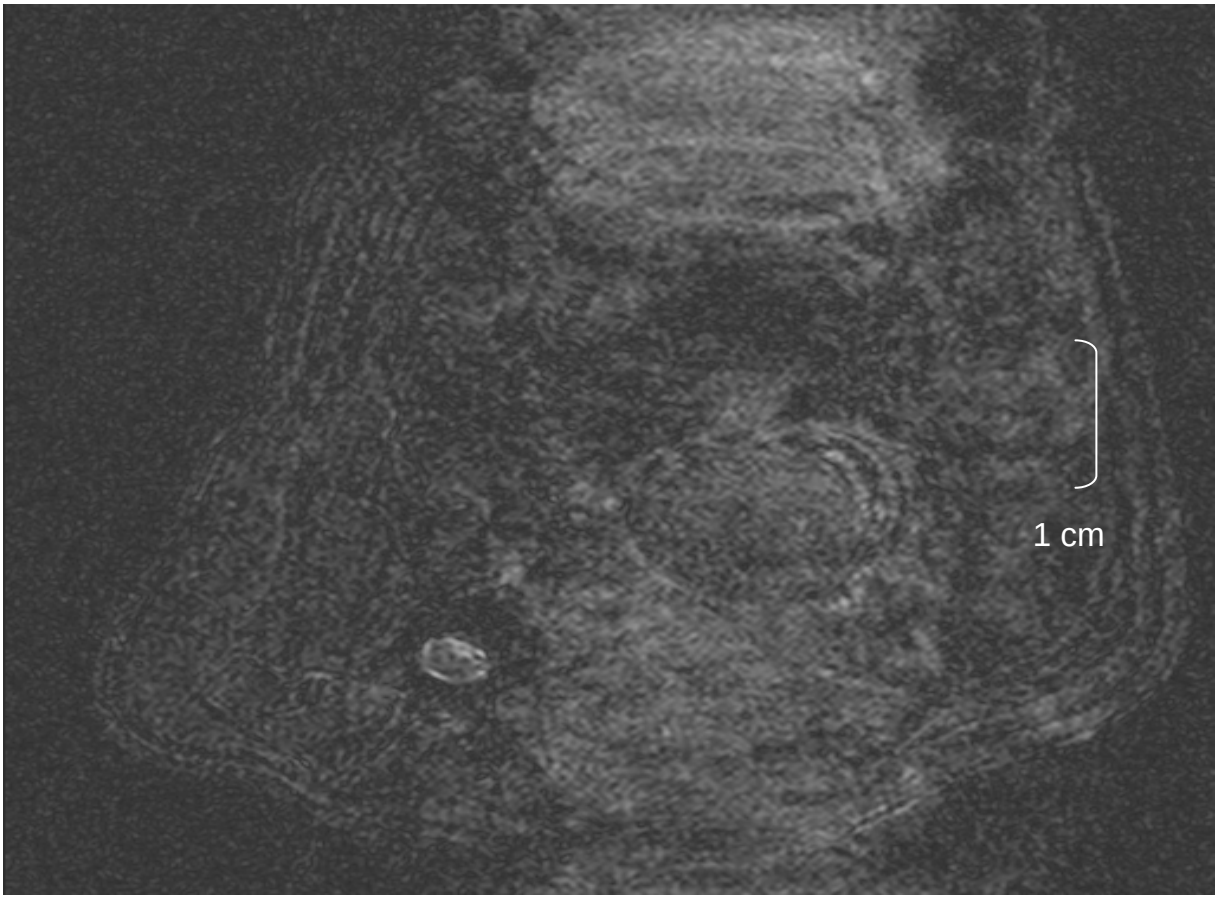

Figure 7: Dissected ovary with three separate corpora lutea, each indicated by a yellow arrow

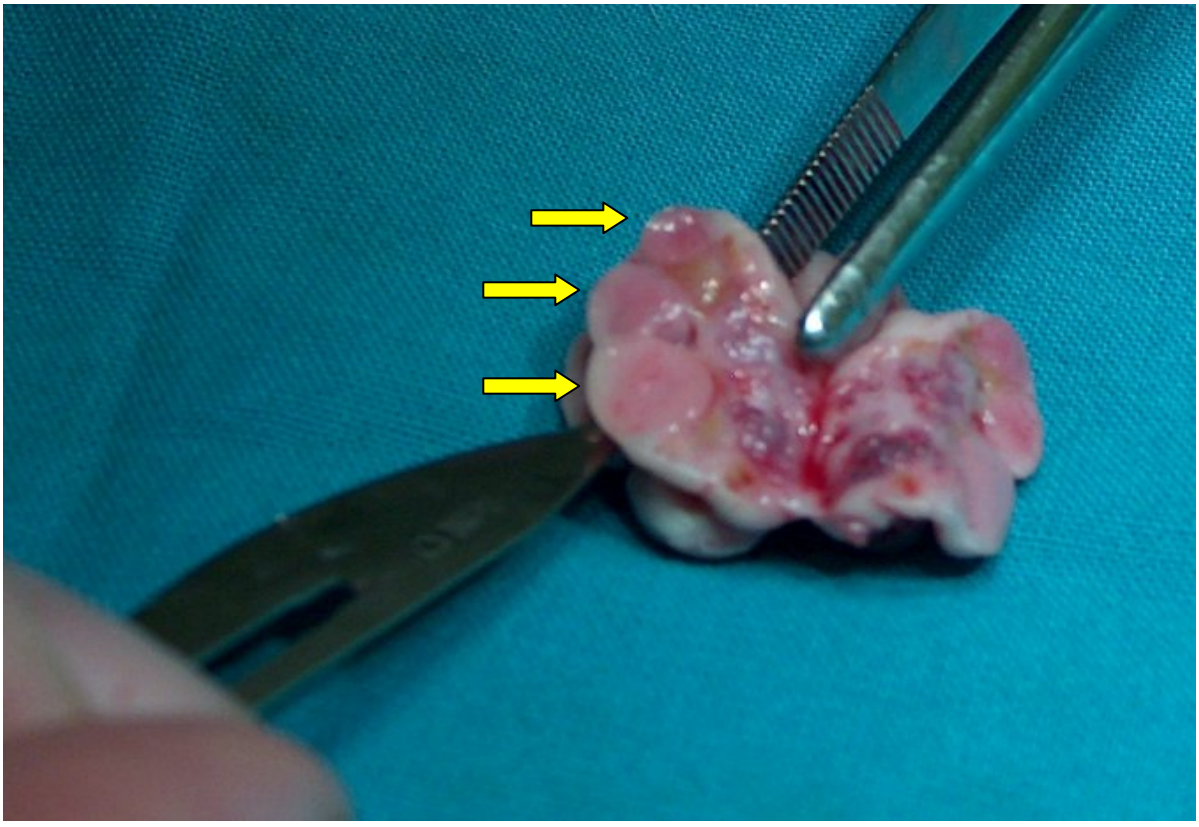

Figure 8: Ovary with thin a walled follicle (periphery indicated by yellow arrows) that collapsed during dissection and which were generally more difficult to count.

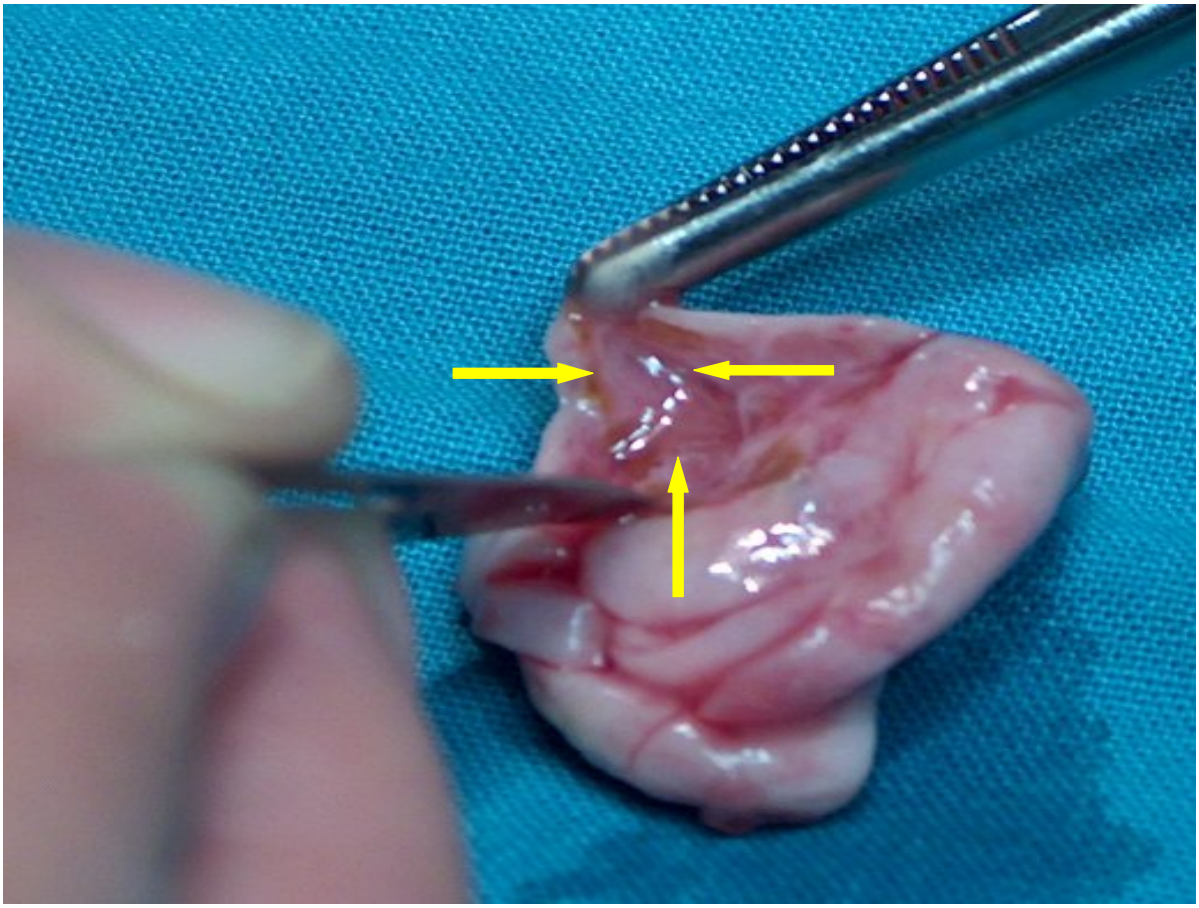

Figure 9: Ovary with partially luteinised and thicker-walled follicles (yellow arrows) that did not totally collapse and were easy to count during dissection.

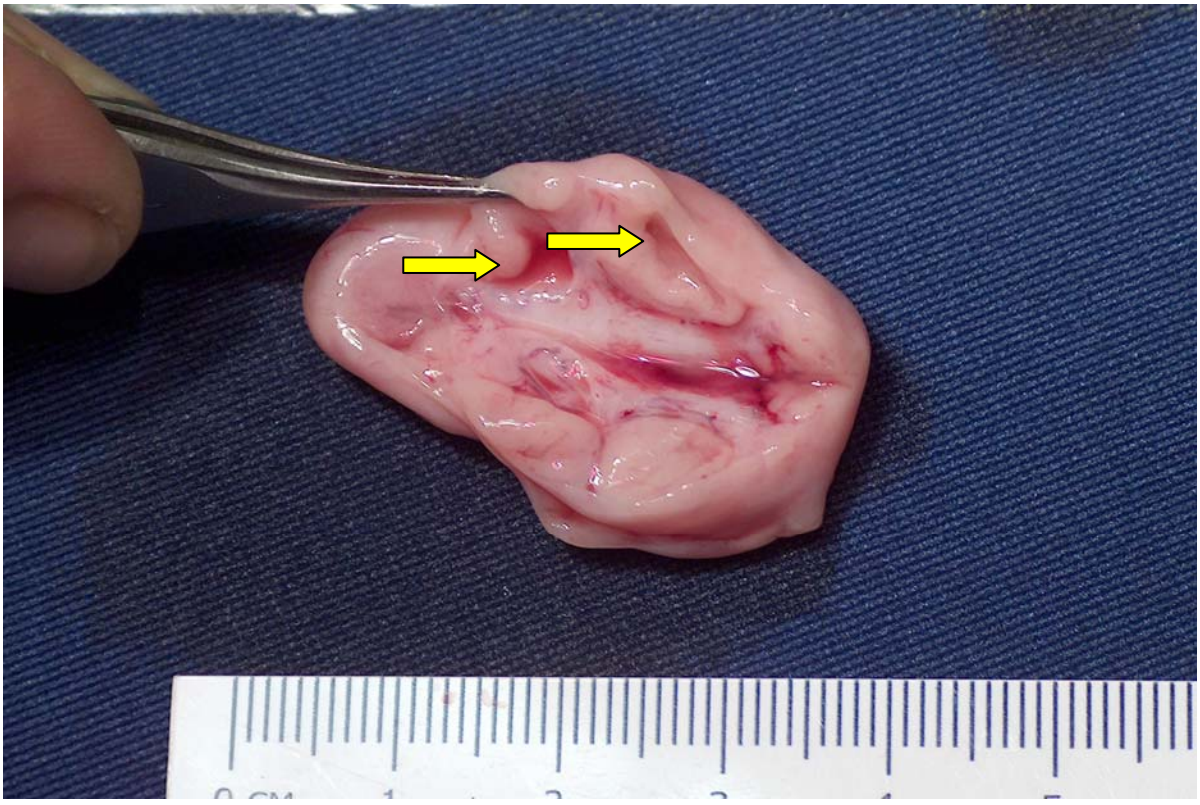

Figure 10: Example of a T_1-weighted MR image of an ovary with follicles. The yellow arrows surround two separate follicles, of which the one is clearer than the other.

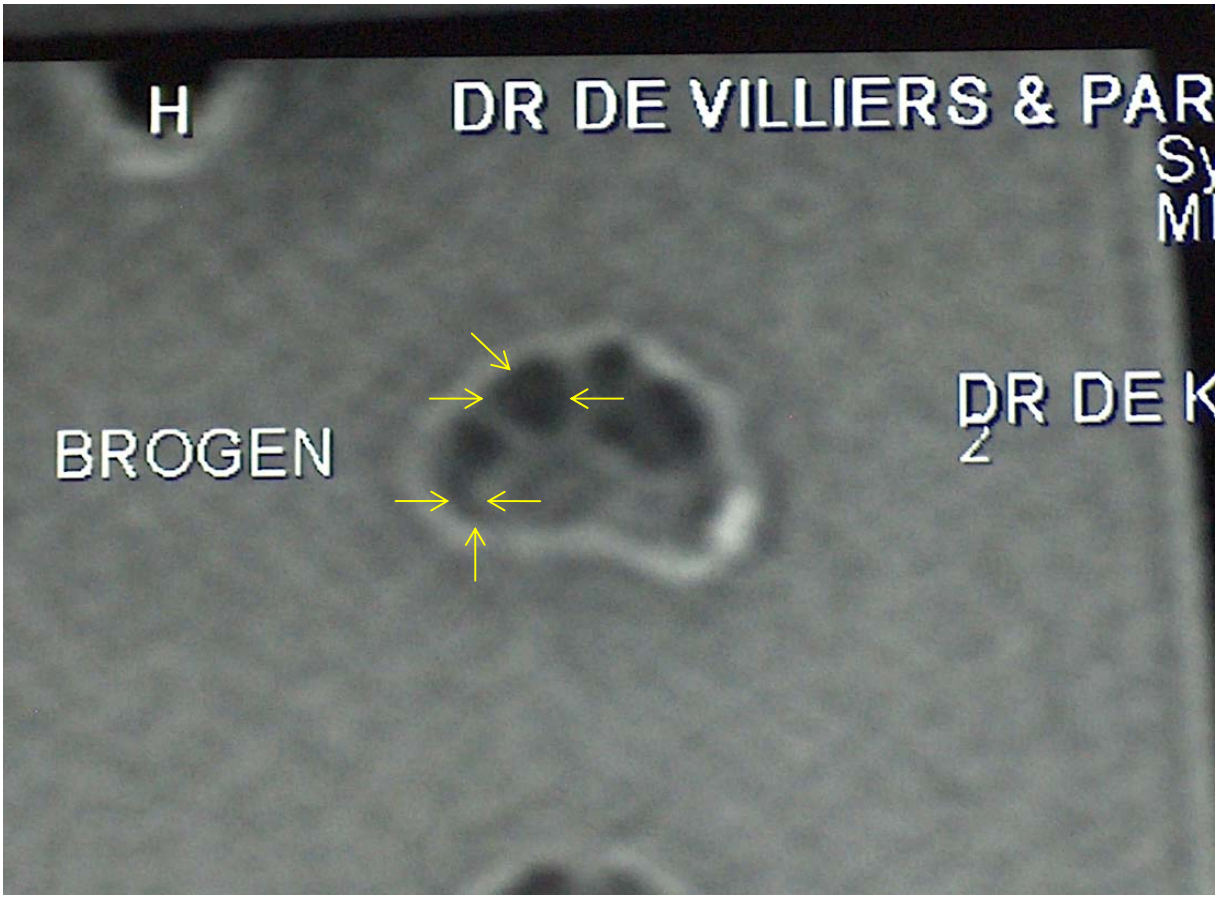

Figure 11: Example of a T_2-weighted MR image of the same ovary as in Fig 10. The yellow arrows surround two separate follicles, of which the one is clearer than the other.

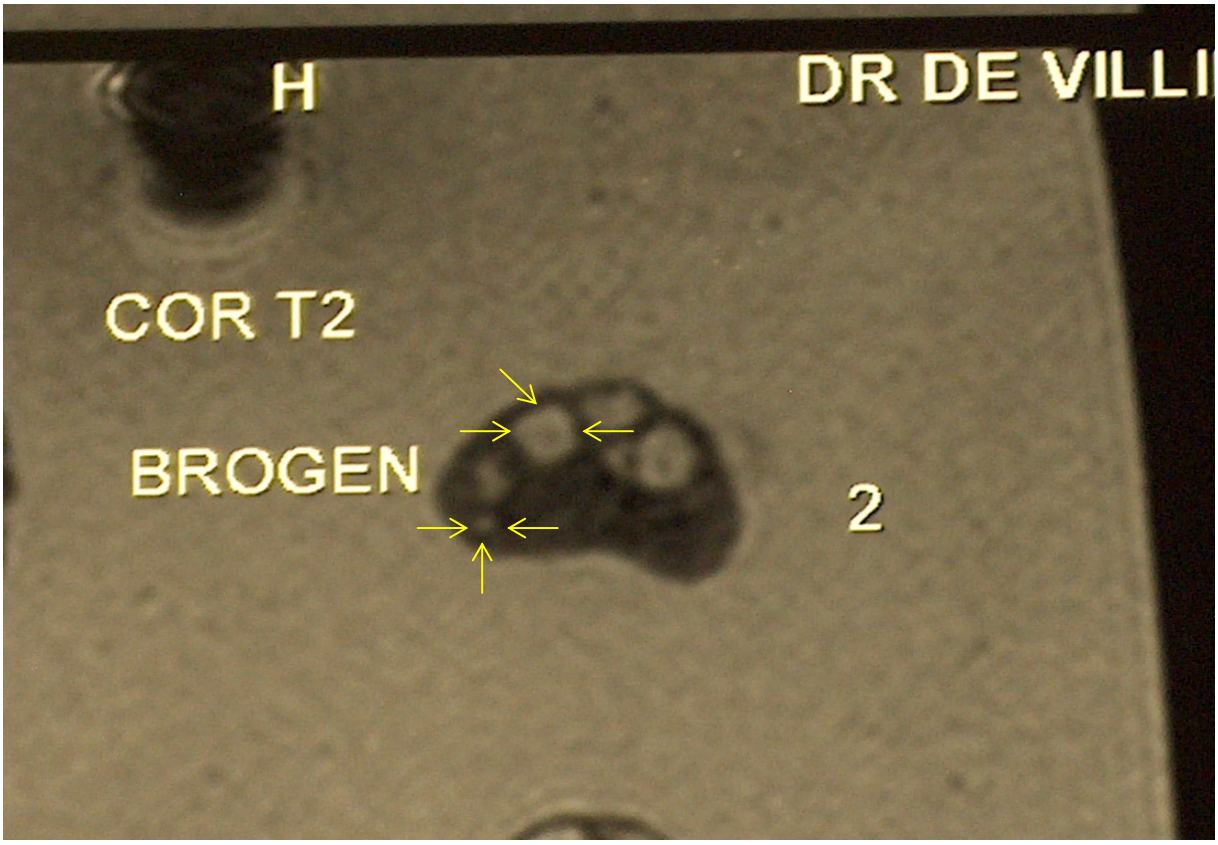

Figure 12: Example of a T_2-weighted MR image where no structures could be identified, but where three corpora lutea were present on dissection

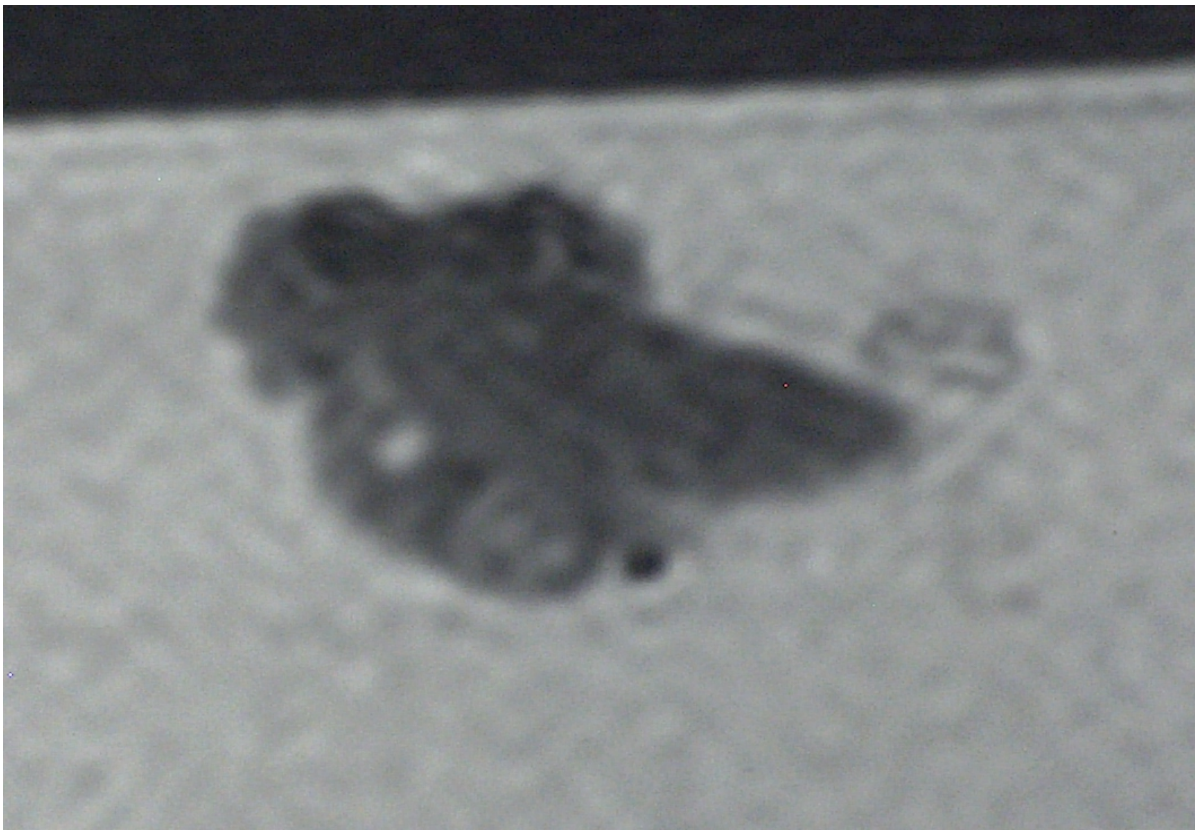

Figure 13: Example of a T2-weighted MR image of an ovary with corpora lutea. (Image obtained with PSIF 3d T_2- time reversed Fast imaging with steady state precession). The yellow arrows surround two separate corpora lutea, of which the one is clearer than the other. The red arrow points at the stromal interface that separates 2 corpora lutea.

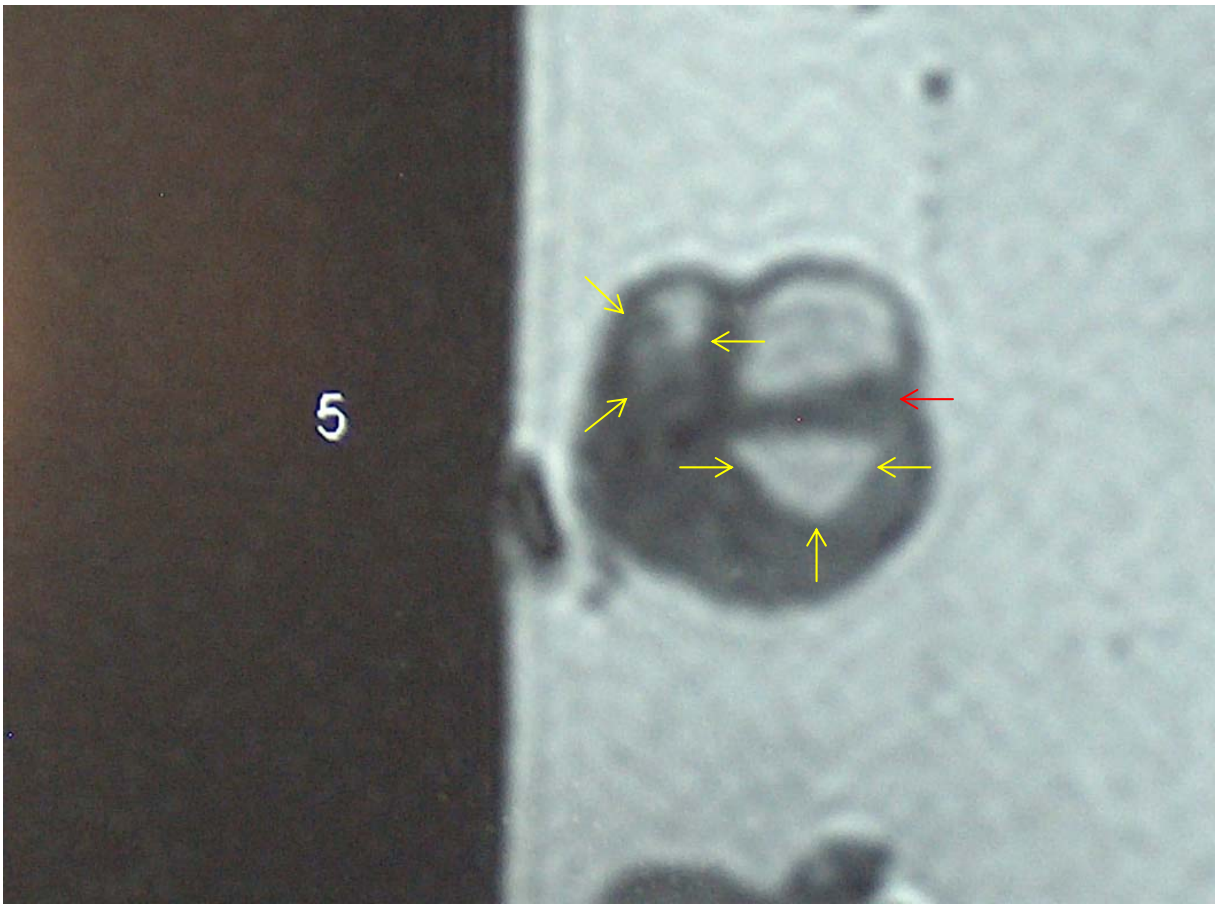

Figure 14: Example of a T_2-weighted MR image of an ovary with follicles. (Image obtained with PSIF 3d T_2 time reversed Fast imaging with steady-state precession). The yellow arrows surround two separate follicles, of which the one is clearer than the other. The red arrow points at the stromal interface that separates 2 follicles.

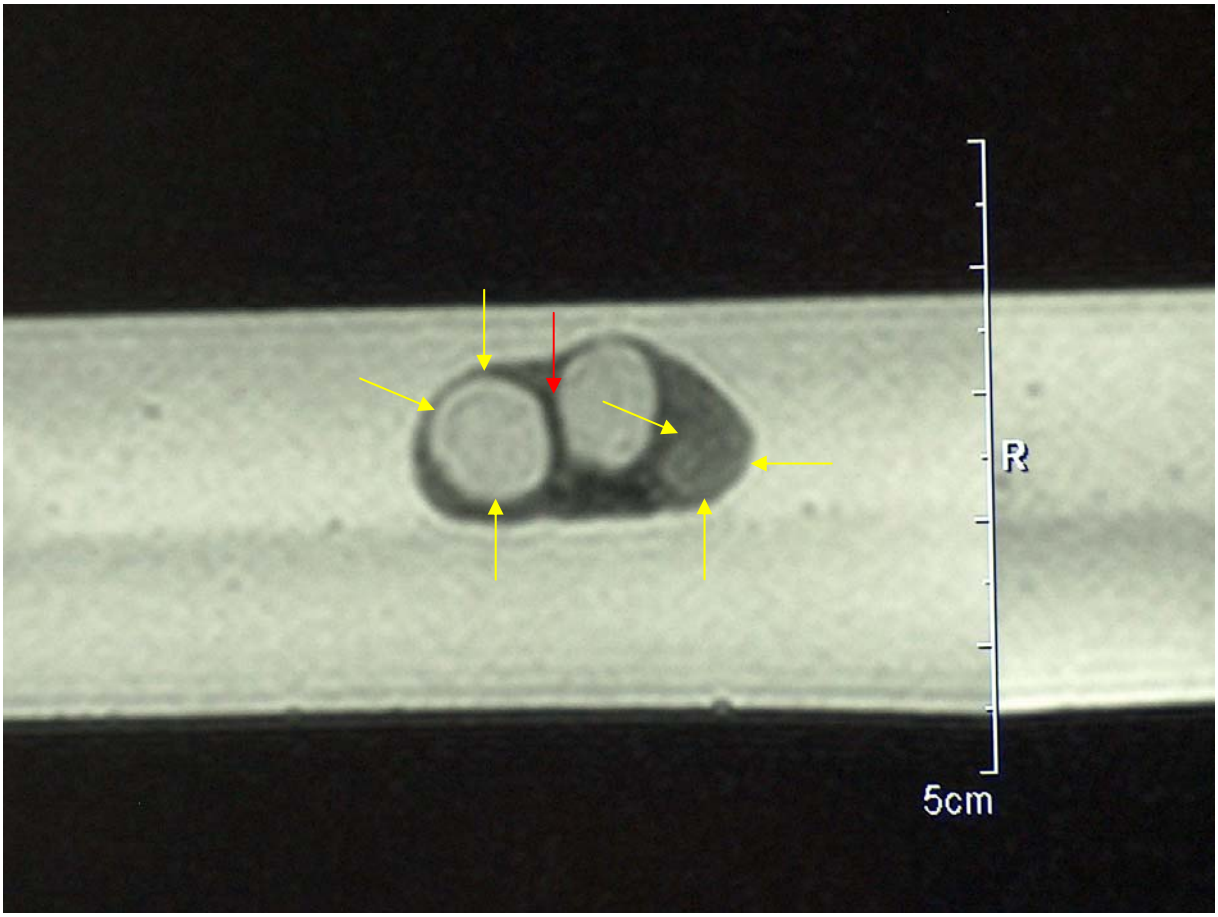

Figure 15: T_2-weighted images of ovaries in a phantom. The yellow arrows surround a follicle (Ovary 2), a late corpus luteum (Ovary 4), an ovarian cyst (Ovary 6) and and early corpus luteum (Ovary 10).

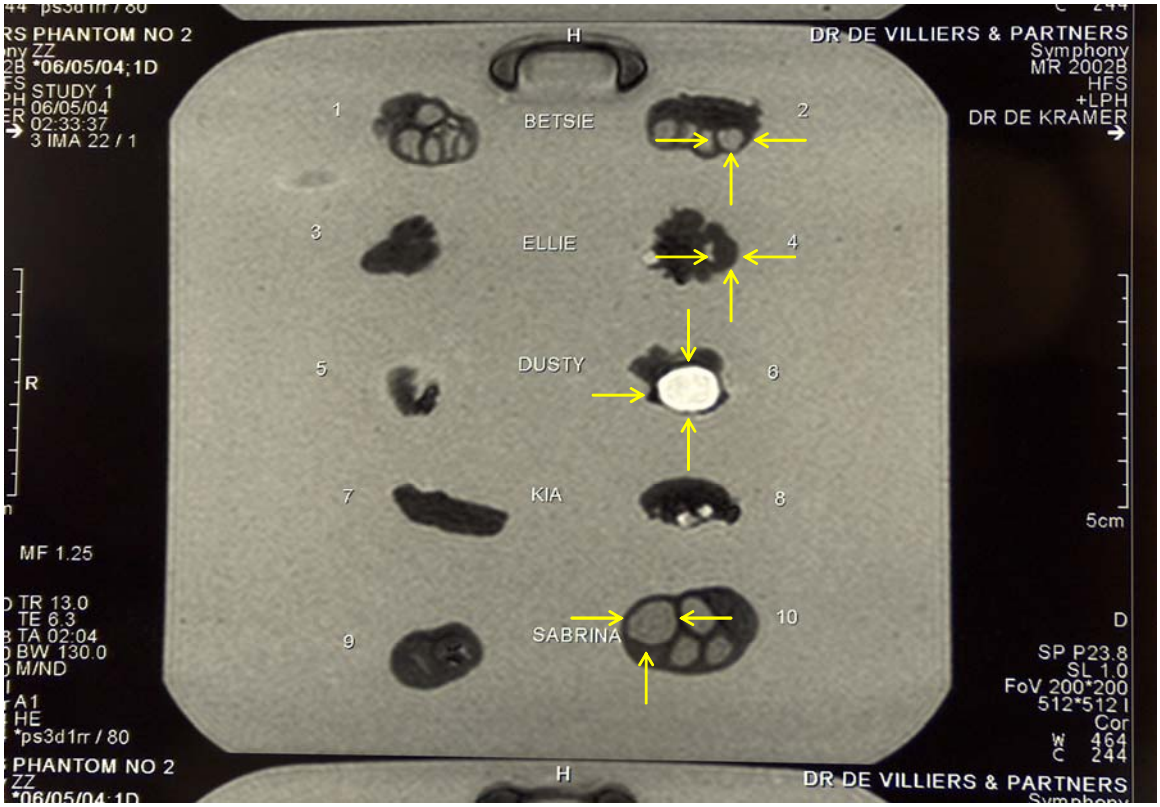

Figure 16: The T_1-weighted MR images of 2 ovaries preserved differently before preparation of the phantom, illustrates clearly the effect (probably dehydration) of the preservation media on the MRI of the ovaries scanned. The ovary on the left was preserved in formalin and the dehydration of the ovary is characterised by the hyperintense appearance of the ovary on MRI, whereas the ovary on the right was preserved in saline and appears hypointense.

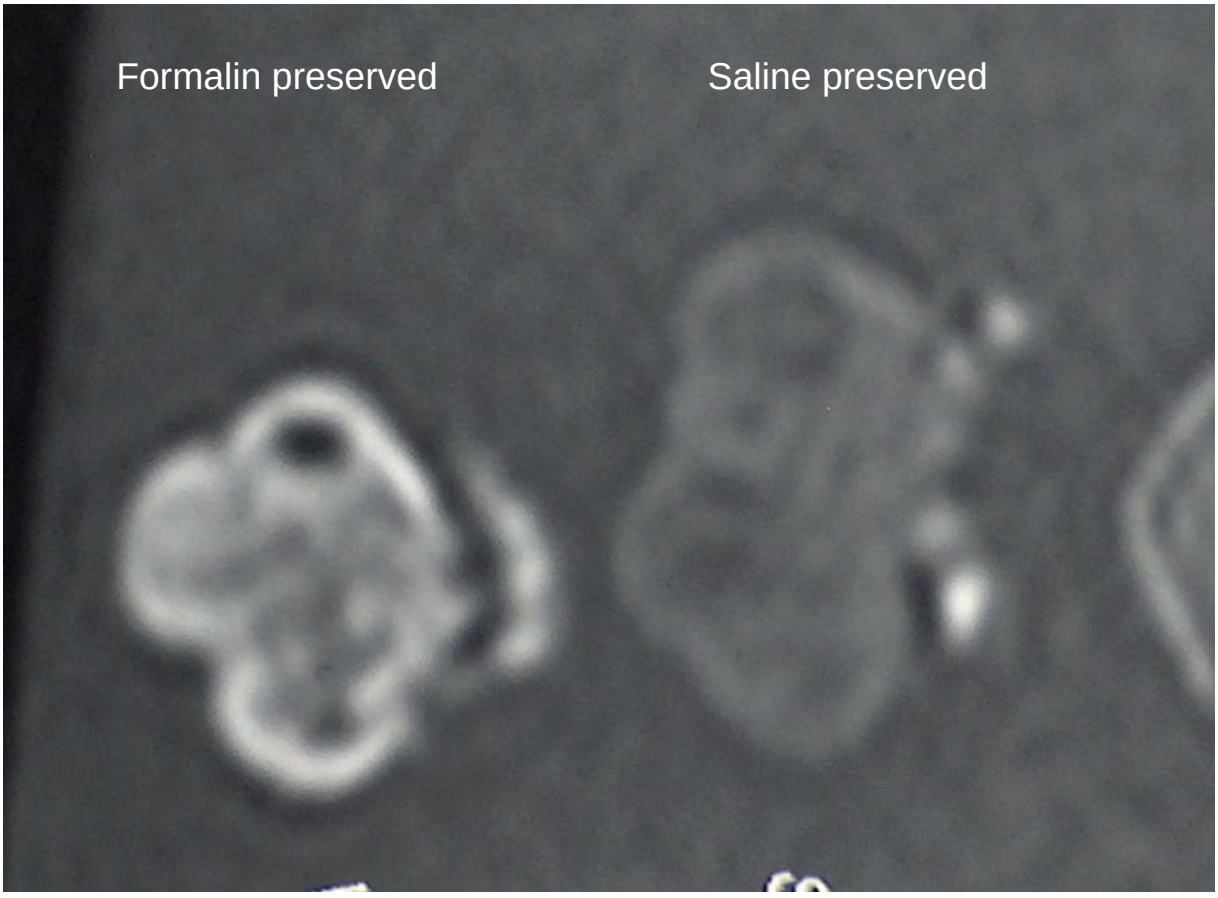

ACKNOWLEDGMENTS

This study was completed under the stressors and rigors of simultaneously having to man and manage two busy animal hospitals, and with less success, fulfil my parenting and family commitments.

During this and other academic journeys in my life, my wife, Zelda and children, Kyle and Mira, were frequently understanding victims of neglect. I owe them lots, and thank them for their gracious response en-route.

To my promoter, Prof. Johan Nöthling, I owe special thanks. I, as do others, admire him for his obvious intellect, perfectionism, and humble-hardworking nature. His response to my frequent interruptions, and at times snail-paced progress, was one of understanding and patience. Throughout, it was clear to me, that he had experience of, and sympathy with, the emotional and physical battle of survival in private practice. Johan, I thank you.

Thanks Freek, Gareth, Glenda, Liza, Cornelia and Celeste at the practice and Vic, Diana and Karen at the Krugersdorp Private Hospital MRI unit, who all have helped me in my efforts to complete this study.

Finally, I owe gratitude to our Creator whom has given me more than most.